(12) INTERNATIONAL APPLICATION PUBLISHED UNDER THE PATENT COOPERATION TREATY (PCT)

(19) World Intellectual Property Organization
International Bureau

(43) International Publication Date
20 June 2013 (20.06.2013)

WIPO | PCT

(10) International Publication Number
WO 2013/090613 Al

(51) **International Patent Classification:**
C12Q 1/68 (2006.01) ***G06F 19/24*** (201 1.01)

(21) **International Application Number:**
PCT/US2012/069561

(22) **International Filing Date:**
13 December 2012 (13. 12.2012)

(25) **Filing Language:** English

(26) **Publication Language:** English

(30) **Priority Data:**
61/570,257 13 December 201 1 (13. 12.201 1) US

(71) **Applicant: RUTGERS, THE STATE UNIVERSITY OF NEW JERSEY** [US/US]; 3 Rutgers Plaza, ASB III, New Brunswick, New Jersey 08901 (US).

(72) **Inventors; and**
(71) **Applicants : TISCHFIELD, Jay** [US/US]; 4 Adams Court, Martinsville, New Jersey 08836 (US). **BROOKS, Andrew** [US/US]; 410 East 57th St. 7A, New York, New York 10022 (US). **FRAHM, Stephanie** [US/US]; 2 Kirkbride Road, Flemington, New Jersey 08822 (US).

(74) **Agent: CASIMIR, David A.;** Casimir Jones, S.C., 2275 Deming Way, Suite 310, Middleton, Wisconsin 53562 (US).

(81) **Designated States** *(unless otherwise indicated, for every kind of national protection available):* AE, AG, AL, AM, AO, AT, AU, AZ, BA, BB, BG, BH, BN, BR, BW, BY, BZ, CA, CH, CL, CN, CO, CR, CU, CZ, DE, DK, DM, DO, DZ, EC, EE, EG, ES, FI, GB, GD, GE, GH, GM, GT, HN, HR, HU, ID, IL, IN, IS, JP, KE, KG, KM, KN, KP, KR, KZ, LA, LC, LK, LR, LS, LT, LU, LY, MA, MD, ME, MG, MK, MN, MW, MX, MY, MZ, NA, NG, NI, NO, NZ, OM, PA, PE, PG, PH, PL, PT, QA, RO, RS, RU, RW, SC, SD, SE, SG, SK, SL, SM, ST, SV, SY, TH, TJ, TM, TN, TR, TT, TZ, UA, UG, US, UZ, VC, VN, ZA, ZM, ZW.

(84) **Designated States** *(unless otherwise indicated, for every kind of regional protection available):* ARIPO (BW, GH, GM, KE, LR, LS, MW, MZ, NA, RW, SD, SL, SZ, TZ, UG, ZM, ZW), Eurasian (AM, AZ, BY, KG, KZ, RU, TJ, TM), European (AL, AT, BE, BG, CH, CY, CZ, DE, DK, EE, ES, FI, FR, GB, GR, HR, HU, IE, IS, IT, LT, LU, LV, MC, MK, MT, NL, NO, PL, PT, RO, RS, SE, SI, SK, SM, TR), OAPI (BF, BJ, CF, CG, CI, CM, GA, GN, GQ, GW, ML, MR, NE, SN, TD, TG).

Published:

— *with international search report (Art. 21(3))*

— *before the expiration of the time limit for amending the claims and to be republished in the event of receipt of amendments (Rule 48.2(h))*

WO 2013/090613 A1

(54) **Title:** COMPOSITIONS AND METHODS FOR FUNCTIONAL QUALITY CONTROL FOR HUMAN BLOOD-BASED GENE EXPRESSION PRODUCTS

(57) **Abstract:** Methods for assessing the integrity of an RNA sample from a given tissue or blood type are disclosed.

Compositions and Methods for Functional Quality Control for Human Blood-Based Gene Expression Products

This application claims priority to United States Provisional Patent Application Serial Number 61/570,257, filed December 13, 2011, the disclosure of which is herein incorporated by reference in its entirety.

Pursuant to 35 U.S.C. §202(c), it is acknowledged that the U.S. Government has rights in the invention described, which was made in part with funds from the National Institutes of Health, Grant Numbers,5U24MH068457 (NIMH); 5U10 AA008401 (NIAAA); SN271200900012C (NIDA) and HHSN276201100016C (NIDDK).

Field of the Invention

This invention relates the fields of molecular biology and quality control maintenance of samples stored in biorepositories. More specifically, the methods of the invention provide a high-throughput, automatable process for assessing and characterizing the integrity of RNA samples utilized in large-scale gene expression studies or biorepositories, significantly limiting sample replicate variability and technical error.

Background of the Invention

Several publications and patent documents are cited throughout the specification in order to describe the state of the art to which this invention pertains. Each of these citations is incorporated by reference herein as though set forth in full.

Gene expression measurements and analytical methods rest upon the assumption that a given messenger RNA sample provides a faithful representation of *in vivo* transcript levels at the time of extraction. In an ideal scenario, fully intact messenger RNA is reverse transcribed to high-quality cDNA for use in gene expression analysis studies, generating reliable and robust data. However, as a labile molecule, the integrity of RNA can be jeopardized at several points prior to, during, and post-extraction, adversely affecting the fidelity of gene expression measurements and hindering data interpretation and discovery. Accurately assessing RNA integrity prior to gene expression analysis on platforms such as microarrays and real-time quantitative PCR proves to be a critical step, requiring a highly sensitive and standardized RNA quality control method [1].

The current industry-standard technique for measuring RNA quality is microcapillary electrophoretic RNA separation, predominantly performed on the Agilent 2100 Bioanalyzer [2, 3]. The 'lab-on-a-chip' microfiuidics technology and data visualization software offers multiple ways to visualize and evaluate RNA integrity, yet these broad-spectrum systems often lack sensitivity on the scale necessitated by RNA samples destined for gene expression analysis. While Bioanalyzer measurements provide a gross analytical assessment of RNA integrity, the proprietary RNA Integrity Number (RIN) scoring algorithm and visualization software has intrinsic limitations preventing in-depth RNA integrity profiles and cannot adequately predict the functional performance of RNA samples intended for gene expression analysis.

Clearly a need exists in the art for improved methods for assessing RNA integrity on a large scale.

Summary of the Invention

In accordance with the present invention, a method for reproducibly assessing the integrity of an RNA sample in a high through put manner is provided. In one embodiment, the method for quantitatively evaluating the extent of RNA degradation in a RNA sample obtained from a tissue or blood specimen entails identifying a candidate gene set specific to said tissue or blood specimen, and determining an arbitrary expression score for each gene present in said set, and sorting said genes into at least two tiers based on said expression score. A plurality of amplification plots and Cx profiles from the set of candidate genes encoding RNAs exposed to differential degradation conditions are then generated, thereby providing a series of differentially weighted Cx profiles correlating to the degradation state of said RNA, said scores corresponding to intact and incrementally degraded RNAs. The test sample is subjected to qPCR, and an amplification plot and a Cx, score generated. The Cx score of the sample is then correlated with those previously determined, thereby providing the degree of degradation of said sample.

In a preferred embodiment the candidate genes are isolated from whole blood. However, any sample type may be used. The term "sample" or "biological sample" as used herein is used in its broadest sense. A sample is derived from a specimen from any source that contains or may contain a molecule of interest (e.g., RNA), including any specimen that is collected from or is associated with a biological or environmental source, or which comprises or contains biological material, whether in whole or in part, and whether living or dead. Samples or biological samples may be plant or animal, including human, fluid (e.g.,

blood or blood fractions, urine, saliva, sputum, cerebral spinal fluid, pleural fluid, milk, lymph, or semen), swabs (e.g., buccal or cervical swabs), solid (e.g., stool), microbial cultures (e.g., plate or liquid cultures of bacteria, fungi, parasites, protozoans, or viruses), or cells or tissue (e.g., fresh or paraffin-embedded tissue sections, hair follicles, mouse tail snips, leaves, or parts of human, animal, plant, microbial, viral, or other cells, tissues, organs or whole organisms, including subcellular fractions or cell extracts), as well as liquid and solid food and feed products and ingredients such as dairy items, vegetables, meat and meat by-products, agricultural materials, and waste. Biological samples may be obtained from all of the various families of domestic plants or animals, as well as wild animals or plants. In some embodiments, the sample comprises or consists of one or more whole cells from a specimen, such as from a fixed or paraffin-embedded formalin-fixed ("FFPE") section, or cells, such as human, animal, plant, or microbial cells grown in culture (e.g., human, animal, or plant cells obtained by fluorescent-activated cell sorting ("FACS"), or replica-plated bacteria or yeast). Environmental samples include environmental material such as surface matter, soil, water, air, or industrial samples, as well as samples obtained from food and dairy processing instruments, apparatus, equipment, utensils, disposable and non-disposable items. These examples are not to be construed as limiting the sample types applicable to the present invention.

In an alternative embodiment the candidate genes are isolated from a tissue selected from the group consisting of breast tissue, colon tissue, lung tissue, kidney tissue, ovarian tissue, liver tissue, muscle tissue, brain tissue, and stomach tissue.

Also provided in accordance with the invention are novel class distinction algorithms which measure RNA quality as a function of the magnitude of deviation from an expected Ct value. This approach enables the researcher to properly weigh or exclude subpar samples from subsequent analysis.

Further provided herein are systems and devices that carry out any of the methods described herein. In some embodiments, such systems or devices employ a computer processor employing a computer memory and/or computer readable medium. As used herein, the terms "processor" and "central processing unit" or "CPU" are used interchangeably and refer to a device that is able to read a program from a computer memory (e.g., ROM or other computer memory) and perform a set of steps according to the program. Devices include, but are not limited to desktop computers, hand-held computers (including pads, phones, and other similar devices), and scientific instruments (e.g., thermocyclers, detection devices, mass spectrometers, etc.). In some embodiments, the systems and devices employ software

configured to carry out the data analysis approaches described herein. In some embodiments, the systems and devices further employ one or more databases or are in communication with such databases that are housed on a separate device or data storage system (e.g., cloud).

For example, in some embodiments, provided herein are methods for quantitatively evaluating the extent of RNA degradation in a sample, comprising; a) identifying a candidate gene set and determining an arbitrary expression score for each gene present in said set, said gene set being specifically expressed in said tissue or said blood specimen and sorting said genes into at least two tiers based on said expression score; b) generating a plurality of amplification plots and C_T profiles from a set of candidate genes encoding RNAs exposed to differential degradation conditions thereby providing a series of differentially weighted C_x profiles correlating to the degradation state of said RNA, said scores corresponding to intact and incrementally degraded RNAs; and c) subjecting RNA in said sample to quantitative amplification, thereby generating an amplification plot and a C_x score; said C_x score being correlated with those determined in step b) said score providing the degree of degradation of said sample. The sample can be of any type including environmental samples, samples obtained from a human, tissue samples, fluid samples, whole blood, and the like.

In some embodiments, the method is coupled with screening or diagnostic techniques for assessing any desired genotype or phenotype, including disease status and progression, general health status, and response to diet, therapeutics, or other stimuli. In some such embodiments, the method further comprises the step of d) analyzing a gene expression profile employing the sample. In some embodiments, the method further comprises the step of e) assessing disease status or progression using the gene expression profile. In some embodiments, the method further comprises the step of d) discarding the sample without conducting a gene expression profile analysis if the degree of degradation is unsuitable (e.g., is of a degree in which a screening or diagnostic test will lack the required or desired level of sensitivity or specificity).

As discussed above, further provided herein are systems and devices that can carry out one or more or all aspects of the methods. For example, in some embodiments, a system or device comprises a computer processor that generates the plurality of amplification plots and C_x profiles. Such systems can include any component useful, necessary, or sufficient for processing the sample, detecting the sample, analyzing the data, and/or using the data. Such components, include, but are not limited to thermocyclers, sample processing components (e.g., that purify or isolate RNA from cells or tissues or other sample types), detection

components (e.g., that mass, optical signals, heat, pH changes, radioactivity, or other detectable signals), and the like.

Brief Description of the Drawings

Figure 1: Mechanisms of messenger RNA degradation by RNases. (a) 5' to 3' exonuclease activity removes the 7-methyl guanosine cap and degrades RNA in a 5' to 3' direction, **(b)** 3' to 5' exonuclease activity removes the poly-A tail and degrades RNA in a 3' to 5' direction, and **(c)** endonucleases attack at specific sites within the molecule and endonucleolytically cleaves the RNA. Modified image from Newbury 2006 **[9].**

Figure 2: Typical qPCR amplification plot, ARn vs. Cycle. A measure of accumulating PCR products, the magnitude of fluorescence (ARn) is plotted against the PCR amplification cycle number (Cycle). The threshold line, in red, is set at the middle of the linear phase of the plot, defining the C_T value for a given qPCR reaction.

Figure 3: Visualizing 28S and 18S ribosomal subunits on gels and electropherograms. The image on the left represents a typical electropherogram: the right peak depicts the 28S ribosomal subunit and the left peak depicts the 18S ribosomal subunit. The image on the right is a corresponding gel image, the top band depicting the 28S subunit and the bottom band depicting the 18S subunit. Image taken from Kuschel 2000 [25].

Figure 4: GeneNote and BioGPS expression data.A representative gene expression data plot generated for numerous experimental tissue vectors. The example shown below represents the GAPDH gene. Image taken from the GeneCards® website (www dot genecards dot org).

Figure 5: Roche UPL ProbeFinder assay design. ProbeFinder software designs UPL assays based on an input target gene; below is one possible assay design for the CD27 gene. ProbeFinder outputs forward and reverse primer sequences flanking the UPL probe of choice, shown in the 'Detailed view' as green and purple text, respectively. Image taken from the ProbeFinder website (www dot roche-applied-science dot com backslash sis backslash rtpcr backslash upl).

Figure 6: Comparison of ideal and poor amplification plots. Figure on left: an ideal, tight amplification plot for the CAPN2 5' assay; limited expression variability exists between

different subjects. Figure on right: a dispersed amplification plot for the TRPM2 3' assay; demonstrates great variability between different subjects.

Detailed Description of the Invention

Sample quality control is central to applied, and clinical genomic analyses. Most sample processing is decentralized, which leads to differential results between laboratories. Thus, in accordance with the present invention, an efficient protocol for QC of each unique sample has been developed and standardized. While QC of RNA from whole blood samples is exemplified herein, the methods described can be applied to a variety of sample sources. The research to develop such a technology is best developed in a biorepository setting where thousands of samples are processed every month. The Rutgers University Cell and DNA Repository currently employs a QC protocol for all human genomic DNA samples that uses a custom-designed SNP genotyping assay panel to determine gender, ethnicity, uniqueness, and sample quality. A similar approach has been developed for RNA given the labile nature of this nucleic acid and the variability associated with extraction and purification thus providing a metric for comparing samples extracted at different sites. This functional QC gene expression panel has commercial applications in terms of qualifying samples for diagnostic and clinical applications.

Real-time quantitative polymerase chain reaction (qPCR) assays offer a more sensitive, modifiable method for quantitatively evaluating the extent of RNA degradation. Fluorescent probe-based assays can be customized to a specific tissue type or field of research by modifying the target genes. Additionally, this method offers a high-throughput, automatable solution for large-scale gene expression studies or biorepositories, significantly limiting sample replicate variability and technical error. By exploiting the regional degradation patterns of RNA, algorithms have been developed to compare gene expression measurements, C_T values, of a test sample to those of an intact RNA control sample and synthetic/empirically degraded RNA samples. Based on the differentially weighted CT profiles for all assays in the panel, an overall quality constant is assigned to a given RNA sample, allowing researchers to properly normalize or exclude any given sample during gene expression data analysis and interpretation.

The following work describes the *de novo* development and validation of a novel functional quality control method for RNA samples extracted from human whole blood, comprised of a custom gene expression assay panel and complementary algorithms.

***RNA Degradation Mechanisms* In Vivo**

While RNA degradation is a hindrance to gene expression research, it is a ubiquitous and controlled activity *in vivo.* Within the cell, active RNA degradation systems are in place to regulate RNA production and decay in order to maintain a steady-state level of RNA messages and their successive proteins. Misfolded or otherwise defective RNA molecules are rapidly degraded by cellular surveillance machinery [4]. In addition, it has been suggested that RNA-degrading enzymes, RNases, can confer protection from viruses by reducing viral replication and protein synthesis *[5,* 6]. Intact cells tightly control the essential activities of RNases, but when cells are disrupted during sample collection and RNA extraction, these endogenous cellular RNases are immediately released and can begin to break down RNA molecules.

Identified by the direction of degradation along an RNA molecule, three major classes of RNases exist in eukaryotes: (1) 5' to 3' exonucleases, (2) 3' to 5' exonucleases, and (3) endonucleases, which cleave RNA internally **[2].** During the transcription process, nascent messenger RNA molecules are modified with protective structures on both ends that serve to maintain stability as mature messenger RNA is translated to protein. As messenger RNA is transcribed, a methylated guanine cap is added to the 5' end of the molecule and a stretch of 150-200 adenine residues is added to the 3' end of the molecule, forming the poly-A tail [8]. Exoribonucleases target the 5' cap or 3' poly-A tail as points of entry, while endoribonucleases can initiate degradation at specific sites within the molecule. Figure 1 depicts three mechanisms of messenger RNA degradation by RNases.

Sources of RNA DegradationEx Vivo

As many gene expression studies are clinically based, subject sample collection and processing pose the challenge of stabilizing and maintaining RNA integrity in an *ex vivo* environment. First and foremost, biospecimen collection methods must be considered when controlling for RNA degradation. Dependent upon tissue type, samples can be collected or stored in a variety of ways, all of which introduce inherent risk of RNA degradation. Formalin-fixed paraffin-embedded (FFPE) tissue samples are routinely used for disease diagnosis and provide a long-term sample storage solution. As archived collections of these samples grow, so does the appeal of extracting RNA for large-scale gene expression studies. However, RNA extracted from fresh, frozen, or archival FFPE specimens is extensively degraded due to the fixation process and length of storage [10]. Alternatively, fresh samples can be collected from tissue biopsies or whole blood drawings for immediate processing,

eliminating the fixation and storage limitations of FFPE tissue samples. However, these samples must be immediately and adequately stabilized by immersion in a proprietary reagent that protects RNA from endogenous ribonuclease degradation and minimizes post-collection gene induction [11].

Regardless of the collection method chosen, variability in RNA extraction techniques and mishandling by technicians further introduces opportunities for RNA degradation. The latency period and conditions between collection and processing, conditions of the extraction process such as time lapse and temperature, and inadvertent contamination with ubiquitous RNases present on lab surfaces, gloves, and skin are common sources of RNA degradation [4, 12]. Post-extraction handling, such as freeze/thaw cycles, heat, and pH fluctuations are also potential sources of RNA degradation [1345]. The first line of defense against RNA degradation is tightly controlling the variables associated with its collection and processing, however, not all samples in a collection will be handled properly and some degree of RNA degradation is inevitable. When paired with the costly venture of biospecimen procurement and storage, it becomes financially and analytically advantageous to include all viable samples in a gene expression study, including data derived from variably degraded RNA [13, 14]. Due to the propensity for RNA degradation, quality control methods become of paramount importance to ensure the reliability and reproducibility of downstream gene expression analysis and data interpretation.

Compounding the issue of RNA degradation is that prior to running an RNA sample on a gene expression platform, it must first be reverse transcribed to stable complementary DNA (cDNA). cDNA is synthesized from a messenger RNA template and serves as the input molecule for gene expression analysis platforms. Demonstrating a ripple-effect, if the messenger RNA template is degraded and of low quality, the cDNA synthesized from it will follow suit, resulting in skewed gene expression data that does not accurately portray the gene expression products present within a given sample at the time of RNA extraction. Numerous platforms exist for measuring gene expression, each with varied applications, multiplexing capability, and throughput. For the purposes of this discussion, the effect of RNA degradation on real-time quantitative PCR data will be considered.

RNA Degradation and Effects on Real-Time Quantitative PCR Measurements

Real-time quantitative PCR (qPCR) is considered a routine, 'gold standard' RNA quantification method. Due to the relatively low cost, speed, and reliability of performing qPCR assays, they are also often used to validate gene expression data generated by other

methods, as is the case with expression microarrays[16, 17]. Designing qPCR assays is a flexible and customizable process, allowing for the design of highly specific assay panels. For high-throughput studies or processes, the reaction set up can be fully automated for more accurate results and more consistent technical replicates. The qPCR workflow consists of three steps: (1) the reverse transcriptase-mediated conversion of labile RNA to stable cDNA, (2) the amplification of cDNA using the polymerase chain reaction (PCR), and (3) the real-time detection and quantification of amplification products [18].

Individual qPCR reactions consist of or comprise the following components: (1) cDNA template, (2) gene expression master mix, (3) forward and reverse primers, (4) a fluorescent probe, and (5) DNase/RNase-free water. Master mix contains the components necessary for the DNA synthesis machinery, primarily thermo-stable DNA polymerase. Primers are short, specific oligonucleotides which hybridize to a DNA template and serve as a start point for DNA synthesis. Forward and reverse primers are used for amplification of both DNA template strands and can be designed to target a specific region for amplification. The probe is a short oligonucleotide labeled with a fluorescent reporter at one end and a fluorescence quencher at the opposite end. The probe hybridizes to the complementary sequence of the DNA template, proximal to and downstream of one of the hybridized primers. Due to the close proximity of the fluorescent moiety and quencher, a fluorescent signal is dampened until the amplification process begins. As the target PCR product is synthesized, the probe is cleaved by the 5' to 3' exonuclease activity of DNA polymerase. Breaking the close proximity of the fluorophore and quencher emits a detectable fluorescent signal upon excitation by a laser within the PCR instrument [19].

During the PCR thermal cycling course, as the target amplicons accumulate, a proportional amount of fluorescent signal accumulates. The magnitude of fluorescence emitted by individual reactions, and thereby the amount of accumulated PCR product, is quantified by a cycle threshold (CT) value. C_T values are determined by a threshold line, which is set at the midpoint of the linear phase of an amplification plot and defines the PCR cycle iteration at which a measurable fluorescence level first surpasses the background fluorescence threshold. C_T values are inversely related to the level of gene expression of the target gene: the greater the amount of target sequence present in the starting cDNA, the earlier the cycle at which fluorescence intensity surpasses the threshold, generating a lower C_T value [18], Once generated, depending upon the application and objectives of the study, CT values are then analyzed with established statistical methods. Figure 2 depicts a typical qPCR amplification plot and threshold line.

qPCR offers sensitive and reliable gene expression quantification, yet it is not without potential drawbacks stemming from lack of standardization at steps within the workflow. Among the variables to consider when planning and executing qPCR assays, RNA sample quality is arguably the most important, followed by assay design efficiency, choice of chemistry, linearity during reverse transcription, and threshold determination [18, 20, 21]. For the purposes of this discussion, assays will henceforth be defined as a primer set/probe pairing. The variables of sample quality and assay design go hand-in-hand when considering the effects of degraded starting material on gene expression quantification. For instance, RNase activity is dictated by a directionally-driven mechanism: RNases move in a 5' to 3' direction, 3' to 5' direction, or attack at specific sequences of a transcript and cleave the molecule at that point. Depending on the entry point of ribonuclease attack and the extent of degradation or fragmentation, a given transcript may no longer contain the region for which an assay was designed, thus under-representing expression level of the target gene. This under-representation corresponds to a higher C_T value, as the amount of starting material is smaller and the threshold takes longer to surpass.

In terms of designing effective assays, the location of the primer and probe sequences is critical. Assays designed proximal to the 3' or 5' ends of the molecule will be at greater risk for failure as they are the entry points for exoribonucleases, whereas assays designed in the middle region are prone to failure due to endoribonuclease degradation activity. Multiple assays per gene should be designed in order to compare regional efficacy. To choose optimal assays from a large candidate pool, a validation study must be conducted to eliminate assays that fail due to poor primer/probe hybridization, large variations in C_T between RNA samples from different subjects, or significant expression level inconsistencies between regional assays of the same target gene. Studies have indicated that a certain threshold of RNA degradation is tolerated without significantly impacting gene expression data, yet beyond which gene expression analysis is adversely impacted by sample degeneration [13, 14, 22, 23]. The hallmark C_T increase for a degraded sample, as compared to an expected C_T value of a control sample, can potentially be used to weight the reliability of gene expression data for a given sample and allow for appropriate inclusion or exclusion of variably degraded RNA samples in a study.

Current RNA Integrity Assessment Methods

Existing RNA integrity assessment tools each have inherent strengths and weaknesses, and each looks at different RNA structural features to determine quality. The

three most common methods used to evaluate RNA integrity will be discussed for comparison: (1) Ratio method: measuring the ratio between the 28S and 18S ribosomal RNA (rRNA) subunit electrophoresis bands, (2) Manual method: subjective evaluation of an electropherogram, and (3) RNA Integrity Number (RIN): objective evaluation of an electropherogram [2]. All of these methods rely on measurements generated by an electrophoretic RNA separation system, such as the Agilent 2100 Bioanalyzer and corresponding RNA 6000 LabChip® kit. The Bioanalyzer combines disposable microfmidic chips, voltage-induced size separation, and laser-induced fluorescence quantification on a small scale, with the capacity to process 12 samples in approximately 30 minutes [24, 25]. Data is visualized within the software as electropherograms and simulated gel electrophoresis images, while RNA concentration, RNA area, and 28S/18S ratios are quantitatively reported.

Traditionally used to evaluate RNA integrity, the 28S/18S rRNA ratio method uses agarose gel electrophoresis stained with ethidium bromide to produce a banding pattern representing the 28S and 18S ribosomal RNA species [3]. More recently, physical gels have been replaced by microfluidics chips. Though the concept remains the same, Bioanalyzer software generates simulated gel images and electropherograms from the data it collects during RNA separation. The intensities of the 28S and 18S bands are used to calculate a ratio reflecting RNA integrity. Band intensity and electropherogram peak amplitude are based on the size of the ribosomal subunit; the larger the molecule, the more intercalating dyes bind to it, hence a stronger intensity displayed by the larger 28S subunit. Figure 3 depicts typical 28S and 18S visualizations on both a gel and an electropherogram. On a gel or gel image, a ratio of 2.0 or greater indicates good to high quality RNA, while an electropherogram peak ratio of $\geq$ 0.65 is considered high quality [2, 3]. The determination of a 28S/18S ratio via physical gel electrophoresis has been largely replaced by microcapillary gel electrophoresis due to the subjectivity involved with determining band intensity ratios. Furthermore, the large amount of input RNA required and the variability associated with electrophoresis conditions make physical gel analysis an unreliable RNA degradation indicator [26]. While Bioanalyzer digital ratio calculation removes subjectivity, it also has drawbacks. Bioanalyzer calculation of the 28S/18S ratio is based on peak area measurements that are heavily dependent on exact definition of the start and end points of the peak, and even accurate determination of this ratio is not sufficient to detect RNA degradation [27].

The manual method of evaluating RNA integrity involves visual inspection of an electropherogram, specifically looking at the 28S and 18S peaks of an electropherogram. A high quality RNA sample is characterized by distinct 28S and 18S peaks and a flat baseline.

With increased degradation, there is a decrease in the 18S to 28S ribosomal band ratio and an increase in the baseline signal between the two ribosomal peaks and the lower marker, while additional peaks begin to appear in the small RNA range as short degradation products accumulate [27, 28]. Much like the 28S/18S ratio used with physical gels, this method is subjective and prone to variability, but may have utility if used in conjunction with a secondary validation method to determine the extent of RNA degradation.

In order to standardize the subjective process of RNA integrity assessment, the RNA Integrity Number (RIN) algorithm was later developed and integrated into the Bioanalyzer software. The RIN algorithm is based on a selection of features that contribute different information about RNA quality, taking into account that a single feature is insufficient to universally evaluate RNA degradation. Specifically, the features incorporated into the RIN algorithm are: (1) the fraction of area beneath the 28S and 18S peaks as compared to total area, reflecting the proportion of large molecules compared to smaller ones, (2) the amplitude of the 28S peak, which correlates with the onset of degradation, (3) the 'fast area' ratio, referring to the degradation peaks observed between the marker and 18S peaks of increasingly degraded RNA, and (4) marker height, an indicator for accumulation of short degradation products [3J. While providing a much more comprehensive evaluation of RNA integrity than the other two methods, the RIN algorithm cannot predict the quality of downstream gene expression data without prior validation work; that is, an RNA sample might be too degraded for use in a microarray study, but might deliver good qPCR data [28, 29]. The inadequate predictive utility of the RIN algorithm, in terms of forecasting sample performance on a range of gene expression platforms, limits its value as an RNA quality control method and creates a niche in the market for a more sensitive quality control analytical tool.

Real-Time Quantitative PCR as a Functional RNA Quality Control Method

While instruments such as the Bioanalyzer offer a comprehensive method of determining RNA quality, to appropriately evaluate the functional potential of a given sample, 'like' must be compared with 'like'. In order to gauge the reliability of a given RNA sample during downstream gene expression analysis, functional performance must be measured as opposed to static evaluation within a system that solely considers structural features of the molecule. Furthermore, the sensitivity of these tools falls off quickly when analyzing RNA samples of increasingly lower quality and yield, sacrificing scoring linearity

at the lower boundary of RNA quality [30, 31]. The limiting threshold of sensitivity inherent to lab-on-a-chip solutions is surpassed by a functional expression assay.

If all variables are controlled for, qPCR assays offer a highly sensitive, reproducible, and customizable quality control method. Already used to confirm and validate gene expression data generated by microarrays, using qPCR as a means to evaluate both RNA integrity and functional potential in one concerted effort is a natural extension of the technology [16, 32]. qPCR assays are highly customizable and assay panels can be specifically designed based on tissue type or area of research based on the target genes chosen. Reaction setup can be automated to eliminate human pipetting error, ensure reproducibility, and allow for high-throughput quality control screening. Additionally, a qPCR quality control method addresses the needs of high-throughput laboratories by eliminating the need for additional costly instruments, consumables, and kits necessitated by other technologies.

With growing incentive to include all samples of a collection in a gene expression study, sample exclusion based on poor RNA integrity can potentially be countered by annotating expression data with sample quality metrics. The generally predictable nature of RNA degradation suggests that correlations may be drawn between transcript integrity and gene expression level for a target gene, as compared to an expected expression baseline. By exploiting the direction and magnitude of C_T shift between a control RNA sample and a test sample, assay-centric class distinction algorithms can be developed and collectively considered to quantify the quality of RNA samples. The following work describes the development of a novel functional quality control method for RNA samples extracted from human whole blood, consisting of a custom gene expression assay panel and complementary class distinction algorithms.

ASSAY DEVELOPMENT

Literature and Database Search for Candidate Genes

A pool of over 1,400 genes expressed in human whole blood was generated from literature and public database searches, primarily genome-wide analysis studies and the Weizmann Institute's GeneCards® online database (www dot genecards dot org) [33-351. Providing a complete summary for each gene, the GeneCards® human gene database acquires and compiles transcriptomic, genetic, proteomic, and functional information from relevant publications and public databases, including Weizmann Institute's own tissue-specific microarray expression data. Candidate genes were selected from the pool based on

adherence to the following criteria: (1) the gene must be measurably expressed in human whole blood cells, (2) the gene must be expressed in a non-disease state, with limited potential for expression variability between whole blood samples from different donors, and (3) the gene must be central to blood cell structure or function (i.e. not an immediate early gene) [36]. For use as a universal RNA quality control method, the final assay panel must be suited to accommodate samples from a broad range of subjects, controlling for disease states, immune challenge, and expression variability between subjects. Taking these variables into account, candidate genes were limited to normal-state, non-transient genes involved in white blood cell structure or function, as indicated by the GeneCards® database.

Expression Profiles for Candidate Genes

Using public microarray data provided by the GeneCards® gene expression database, GeneNote, an arbitrary expression score (0-10,000) was assigned to each gene on the candidate list. GeneNote data was compiled from two sources: Weizmann Institute high-density DNA microarray data and BioGPS, a gene annotation portal (biogps dot gnf dot org) [37-39]. Expression data is presented within GeneNote as a log-scale plot of normalized expression intensity across a range of healthy human tissues, as depicted in Figure 4. Primarily based on Weizmann Institute array experiments performed on the Affymetrix GeneChip® HG-U95 set A-E, consisting of 62,839 probesets representing the full human genome, all expression data was normalized in a tissue-specific manner for comparison on a single plot [37, 38].

GeneNote plots the normalized intensity for each tissue type run in microarray experiments on a scale of 0-10,000 without providing the exact intensity score so approximated expression scores were noted for each gene on the candidate list. Based on the expression score assigned, candidate genes were sorted into six tiers: (la) 150-449, (lb) 450-749, (lc) 750-999, (2) 1000-3332, (3) 3333-6665, and (4) 6666-10,000. As lower-expressing genes can often serve as good class discriminators, genes exhibiting significantly different expression levels between two groups, the low expression group was further stratified for weighted representation in the assay validation experiments [40, 41].

Selection of Genes for Assay Design

A comprehensive master list was compiled of all candidate genes, their functions as provided by the GeneCards®, Entrez Gene, and UniProtKB/Swiss-Prot databases, and expression scores provided by the GeneNote database. The list was ordered by expression

score and a total of 62 genes, 10 from each expression tier and 2 control genes, were chosen for the assay design phase, as presented in **Appendix I.** The decision to include a gene in the design phase was primarily determined by gene function. Genes with a role in cell structure or function were highly preferred over genes with speculative functional roles or genes expressed during periods of immune system challenge or disease, as they are less variably expressed between individuals and are temporally stable.

Assay Design

Based on ease of design and cost effectiveness, Roche Universal ProbeLibrary assays were chosen for the assay validation phase. Within the online Universal ProbeLibrary Assay Design Center, ProbeFinder software (v2.45, human) was used to design region-specific real-time qPCR assays targeting the 62 genes of interest (www dot roche-applied-science dot com backslash sis backslash rtpcr backslashupl). ProbeFinder is a web-based software tool that designs optimal primer set/probe pairings for a user-defined gene of interest. Using 165 proprietary Universal ProbeLibrary (UPL)fluorescent probes, 8- and 9-mer motifs that are highly prevalent in the transcriptome, the software computes all possible primer/probe combinations around the probe hybridization sequences present within the gene of interest. To gauge the efficacy of individual assays, the software performs *in silico* PCR reactions to predict amplicon fidelity and minimize the risk of false assay signals [42]. **Figure 5** depicts an example of a ProbeFinder UPL assay design.

A total of 184 intron-spanning assays were designed with ProbeFinder: three designs per 60 genes of interest and two designs per 2 control genes. For each gene of interest, an optimal assay was designed for the 5', middle, and 3' regions. For control genes, ACTB and GAPDH, optimal assays were designed only for the 5' and 3' regions. Assay designs, consisting of forward and reverse primers and the corresponding UPL probe, were exported from the software and are presented in **Appendix II.** Primers were custom ordered from Sigma according to the following specifications: shipment in a 96-well plate format, purification by standard desalting, and lyophilized forward and reverse primer sets (20 nM each) were to be combined in a single well.

ASSAY VALIDATION

Primer Preparation

The lyophilized primer sets, 20 nM each of both forward and reverse primers per assay design, were reconstituted with 200 μl DNase/RNase-free water for a standard stock solution of 100 μM. From the stock solution, working 1:5 dilutions were prepared on a Biomek FX liquid handling instrument (Beckman Coulter) for use in subsequent qPCR reactions.

Sample Collection and Automated RNA Extraction

Fresh human whole blood samples were collected in PAXgene® Blood RNA tubes (Qiagen/PreAnalytiX), according to manufacturer specifications. PAXgene® Blood RNA tubes contain a proprietary RNA stabilization reagent that protects RNA molecules from RNase degradation during cell lysis and minimizes gene induction post-collection [431. Blood samples were drawn from five healthy donors, totaling two PAXgene® Blood RNA tubes per subject, with 2.5 ml of whole blood drawn per collection tube. Tube sets were labeled A-E to ensure donor anonymity. One set of donor tubes was stored at -20°C for later extraction while the remaining set of tubes was processed immediately.

According to manufacturer specifications, the PAXgene® tubes were incubated for two hours at room temperature then stored overnight at 4°C to adequately lyse the blood cells and stabilize the RNA. Once lysed, total RNA was extracted and purified using the PAXgene® Blood RNA MDx Kit on the BioRobot Universal instrument (Qiagen), according to the manufacturer's protocol. Total RNA yield and purity was assessed using Nanodrop ND-8000 spectrophotometric measurements (Thermo Fisher). Total RNA integrity was assessed with LabChip 90 HT RNA electropherogram and gel electrophoresis images (Caliper Life Sciences). Total RNA quality data is presented in **Appendix III.**

cDNA Synthesis and Amplification

In a two-step process, extracted RNA was reverse transcribed to cDNA, which was then amplified using the Ovation Pico WTA System (NuGEN) on a Biomek FX liquid handling instrument according to the manufacturer's protocol. cDNA yield and purity was assessed using Nanodrop ND-8000 spectrophotometric measurements. cDNA integrity was assessed with LabChip 90 HT RNA electropherogram and gel electrophoresis images. cDNA

quality data is presented in Appendix IV. Working dilutions of 1:200 cDNA were prepared with DNase/RNase-free water for use in subsequent qPCR reactions.

Assay Validation: Real-time Quantitative PCR

Real-time qPCR reactions were run for 184 assays against 4 cDNA samples generated from intact RNA on a 7900HT Real-Time PCR System (Applied Biosystems). Three technical sample replicates and one no template control (NTC) were run for each assay. A general reaction plate map is presented in Appendix V. Single 10 µl reactions consisted of a gene-specific forward/reverse primer set (Sigma), corresponding Universal ProbeLibrary probe (Roche), TaqMan Gene Expression Master Mix (Applied Biosystems), DNase/RNase-free water, and 1:5 dilution cDNA template. To ensure accuracy and produce reliable gene expression data, all qPCR reaction plates were prepared in 384-well PCR plates on a Biomek FX liquid handling instrument.

RESULTS

Assay Performance Analysis and Scoring

For each of the assay validation reactions, RQ Manager version 1.2 software (Applied Biosystems) plotted the magnitude of fluorescence (ARn) against the PCR amplification cycle number. A comprehensive logarithmic amplification plot was generated and a threshold line was manually set at the midpoint of the linear phase of each plot, intersecting to define an individual CT value for each reaction well of a given assay. Individual CT values and amplification plots were exported for qualitative and descriptive statistical analyses.

CT values were grouped by assay then sub-grouped by sample for descriptive statistical analysis. For each assay, the statistical average and standard deviation of triplicate C_T values per sample was calculated. Additionally, for each assay, a statistical average and standard deviation of CT values per all samples was calculated, as presented in Appendix VI. Outlying C_T values below 15 and above 38.5 were excluded from all calculations due to experimental error or assay failure, and NTC C_T values were checked for evidence of contamination. To better evaluate assay performance, the descriptive statistical data was visualized with histogram plots. Histograms were plotted to compare assay performance between individual samples per given assay; all regional assays for a given gene were plotted on the same histogram to reveal local biases, as presented in Appendix VII. To compare performance across all 184 assays, the overall average Rvalue and overall standard deviation

of all four samples per given assay were plotted on a single histogram. Histogram plots were used to determine gene expression consistency across regional assay designs for a given gene.

Three criteria were used to score assay performance: **(1)** expression level consistency across all regional assays of a given gene, (2) amplification plot uniformity and C_T value standard deviation, and (3) conformity to expected expression levels, as determined by GeneNote public microarray data. Expression level consistency among regional assays designed for the same gene served as an indicator that there were no biases stemming from location of the assay design within the gene, important for establishing a reliable baseline for algorithm development and mitigating performance variability. Uniformity among individual reaction amplification plots and corresponding CT value standard deviations served as indicators of how similarly a given assay would perform between samples from different subjects, important for clinical applications and utility as a universal quality control method. Conformity to the expected expression level reported by the GeneNote database served to validate expression data and was indicative of high-quality input RNA, important for assay validation.

Based on these three criteria, two performance lists were generated, one placing emphasis on regional consistency and the other placing emphasis on amplification plot and CT value uniformity among different samples, as presented in **Appendix VIII.** While regional consistency is important for algorithm generation and assay performance predictability, just as important is the consistency between different samples within the same assay. When compared, most of the best-performing assays were found at the top of both lists, so they were combined when choosing the subset of assays for use in the experimental degradation phase of the project.

EXPERIMENTAL RNA DEGRADATIONAND ASSAY PEFORMANCE

MATERIALS AND METHODS

Experimental RNA Degradation Conditions

To determine the best method for experimentally degrading RNA samples, multiple degradation conditions were evaluated [2, 13-15, 44, 45]. Aliquots of native RNA were either subjected to repeat freeze/thaw cycles, heat treatments, or exposure to an endoribonuclease, RNase A. Freeze/thaw cycling consisted of flash-freezing native RNA aliquots on dry ice for 2 minutes, followed by a complete thaw on wet ice for 7.5 minutes. Five 6 µl RNA aliquots were exposed to 3, 6, 9, and 12 freeze/thaw cycles, respectively. RNA integrity was assessed for each aliquot using the RNA 6000 Nano LabChip® kit on a Bioanalyzer 2100 instrument (Agilent); electropherogram and gel electrophoresis images are presented in **Appendix IX.**

Heat treatments consisted of exposing native RNA aliquots to high heat over a time continuum. Five 7 µl RNA aliquots were incubated in a 60°C Mastercycler® Ep thermal cycler heat block (Eppendori) for 30, 60, 90, and 120 minutes, respectively. After each 30-minute time interval, a single aliquot tube was removed from the heat block and frozen immediately on dry ice. RNA integrity was assessed for each aliquot using the RNA 6000 Nano LabChip® kit on a Bioanalyzer 2100 instrument; electropherogram and gel electrophoresis images are presented in **Appendix IX.**

RNase A treatments consisted of exposing native RNA aliquots to an optimal dilution of stock RNase A solution (Qiagen). The enzymatic reaction was stopped at set time points with optimally diluted SUPERase-ln (Ambion), a multiple RNase inhibitor. Several attempts to optimize dilutions and exposure periods resulted in completely degraded RNA before a final RNase A dilution of 1:5,000,000 and SUPERase-ln dilution of 1:2 produced measurable, incrementally degraded RNA [46, 47]. For eight 6 µl RNA aliquots, 1 µl of 1:5,000,000 diluted RNase A was added and tubes were incubated in a 37°C Mastercycler® Ep thermal cycler heat block. At time points 0.5, 1, 2, 4, 8, 16, and 32 minutes, a single tube was taken off the heat block and 1 µl of 1:2 diluted SUPERase-ln was added, thoroughly mixed, and the tube was immediately frozen on dry ice. RNA integrity was assessed for each aliquot using the RNA 6000 Nano LabChip® kit on a Bioanalyzer 2100 instrument; electropherogram and gel electrophoresis images are presented in **Appendix IX.**

Based on the graded degradation patterns produced by the RNase A treatment, this method was chosen for subsequent degradation testing. Since production of RNase inhibitors involves co-purification with RNases which can potentially contaminate stock solutions, a concern arose about reintroducing unwanted RNases during the supposed inactivation step. To address this concern in subsequent RNase experiments, a second RNA purification step was performed after the RNase inactivation step to ensure the degradation process would not continue to fragment the RNA beyond the desired inactivation time point. To stabilize the RNA during the purification step, ten volumes of TRIzol® reagent (Invitrogen) and two volumes of chloroform (Invitrogen) were added to each RNA aliquot in a phase lock gel heavy tube (5 Prime), shaken vigorously, incubated at room temperature for 3 minutes, then centrifuged at 12,000xgand 4°C for 15 minutes. TRIzol® reagent, containing phenol and guanidine isothiocyanate, is often used prior to RNA extraction and purification protocols to maintain RNA integrity during the extraction process [48].The aqueous layer, containing stabilized RNA, was transferred to a fresh microfuge tube and purified with an RNeasy Mini Kit (Qiagen), according to the manufacturer's protocol. The RNeasy Mini Kit is a system for RNA extraction and purification that binds RNA to a silica-membrane spin column, purifying the bound RNA through a series of buffer washes and centrifugation steps [49].

To gauge the amount of RNA yield net loss to be expected as a result of adding an additional purification step, the secondary RNase inactivation step was performed on native RNA. Once satisfied that RNA yield would not be compromised, the RNase A treatment of samples was followed by the secondary RNase inactivation step described previously for all subsequent testing. Nanodrop ND-8000 (Thermo Fisher) and Bioanalyzer 2100 yield and quality data are presented in **Appendix X.**

Manual RNA Extraction and Experimental Degradation

Once the combined RNase A treatment and purification step was defined as the optimal experimental degradation method, RNA was manually extracted from the second set of frozen blood samples using a PAXgene® Blood RNA Kit (Qiagen), according to the manufacturer's protocol. As opposed to the automated method, manually extracting the RNA provided a greater overall yield, necessary for running multiple degradation conditions and subsequent qPCR reactions. RNA yield and purity was assessed using Nanodrop ND-8000 spectrophotometric measurements. RNA integrity was assessed for each sample with electropherogram and gel electrophoresis images on a Bioanalyzer 2100, as presented in **Appendix XI.**

Manually extracted RNA sample 'D' was arbitrarily chosen for experimental degradation by RNase A according to the optimized two-step method previously outlined. Seven 10 µï RNA aliquots were treated and purified according to plan for time points 0, 0.5, 1, 2, **4,** 8, and 16 minutes. RNA yield and purity was assessed using Nanodrop ND-8000 spectrophotometry measurements. RNA integrity was assessed for each aliquot with electropherogram and gel electrophoresis images on a Bioanalyzer 2100, as presented in **Appendix XII.**

cDNA Synthesis and Amplification

In a two-step process, the seven variably-degraded RNA aliquots were reverse transcribed to cDNA, which was then amplified using the Ovation Pico WTA System (NuGEN) on a Biomek FX liquid handling instrument according to the manufacturer's protocol. cDNA yield and purity was assessed using Nanodrop ND-8000 spectrophotometric measurements. cDNA integrity was assessed with LabChip 90 HT RNA electropherogram and gel electrophoresis images (Caliper Life Sciences). cDNA quality data is presented in **Appendix XIII.** Working dilutions of 1:200 cDNA were prepared with DNase/RNase-free water for use in subsequent qPCR reactions.

Incrementally Degraded RNA: Real-time Quantitative PCR

Real-time qPCR reactions were run for 71 of the top-performing assays, as identified by the assay validation phase, against 7 cDNA samples generated from increasingly degraded RNA on a 7900HT Real-Time PCR System (Applied Biosystems). Three technical sample replicates and one no template control (NTC) were run for each assay. A general reaction plate map is presented in **Appendix XIV.** Single 10 µï reactions consisted of a gene-specific forward/reverse primer set (Sigma), corresponding Universal ProbeLibrary probe (Roche), TaqMan Gene Expression Master Mix (Applied Biosystems), DNase/RNase-free water, and 1:5 dilution cDNA template. To ensure accuracy and produce reliable gene expression data, all qPCR reaction plates were prepared in 384-well PCR plates on a Biomek FX liquid handling instrument.

RESULTS

Degraded RNA Assay Performance Analysis

For each of the degradation assays, RQ Manager version 1.2 software (Applied Biosystems) plotted the magnitude of fluorescence (ARn) against the PCR amplification cycle number. A comprehensive logarithmic amplification plot was generated for each assay and a threshold line was manually set at the midpoint of the linear phase of the plot, intersecting to define an individual CT value for each reaction well of a given assay. Individual C_T values and amplification plots were exported for qualitative and descriptive statistical analyses.

C_T values were grouped by assay then sub-grouped by sample for descriptive statistical analysis. For each assay, the statistical average and standard deviation of triplicate C_T values per sample was calculated. Additionally, for each assay, a statistical average and standard deviation of C_T values per all samples was calculated, as presented in **Appendix XV.** Outlying CT values below 15 and above 38.5 were excluded from all calculations due to experimental error or assay failure, and NTC C_T values were checked for evidence of contamination. To better evaluate assay performance, the descriptive statistical data was visualized with histogram plots. Histograms were plotted to compare assay performance between individual samples per given assay; all regional assays for a given gene were plotted on the same histogram to reveal local biases, as presented in **Appendix XVI.** To compare performance across all 71 assays, the overall average CT value and overall standard deviation of all seven samples per given assay were plotted on a single histogram. Comparisons with the initial assay validation phase CT values were also visualized in a single histogram to track general trends in expression level change, confirming that degradation increased overall average C_T values for each assay. To visualize the change in C_T over the course of increasing degradation for each assay, the percent change in CT was plotted using native RNA CT values (To minutes) as the baseline. The relationship between CT value and extent of degradation served as a foundation for deciding algorithm development approaches.

DISCUSSION

Overview

The development of a functional quality control method assessing RNA extracted from human whole blood samples is described herein. Designed to work in concert, the custom gene expression assay panel and set of class distinction algorithms provide an overall RNA quality score capable of predicting future performance on gene expression platforms. Setting it apart from current analytical quality control methodologies, this method relies on dynamic gene expression data rather than static measurements of RNA size, providing a more appropriate assessment of anticipated performance quality.

In summary, a list of candidate genes of variable expressivity in human whole blood cells was compiled, placing emphasis on intransient function and limited variability between subjects. Ultimately 62 genes were selected for Roche Universal Probe Library assay design. For each gene, assays were designed for the 3', middle, and 5' regions of each transcript; assays consisted of forward and reverse primers paired with a specific UPL probe. An assay validation phase consisting of 184 assays was conducted to assess assay performance when reactions were run with high-quality, intact RNA samples. For the top 71 best-performing assays, as determined by validation phase data, qPCR reactions were run with RNA that had been incrementally degraded by RNase A. Data generated by the experimentally degraded RNA reactions will be used to establish an expected baseline C_T value (non-degraded RNA, To) for algorithm development. Additionally, C_T values for incrementally degraded RNA (To.5, Ti, T_2, T_4, T_8, and T_{16} minutes) will serve to extrapolate the relationship between extent of sample degradation and increase in C_T value.

Assay Development

Assays were designed using Roche ProbeFinder software, which provided forward and reverse primer sequences and a corresponding Universal Probe Library (UPL) probe per gene queried. All efforts were made to choose designs located precisely at the 3', middle, and 5' regions of a transcript; however, designs were limited to the regions of the transcript with sequences compatible with one of the 165 possible UPL probes. Additionally, all efforts were made to choose the highest quality assay as determined by the software's *in silico* PCR rating. As was the case with a number of genes, for instance, the 5'-most assay design may be located closer to the middle of the transcript than the 5' end; in these cases, the most optimal assay design available was chosen. While UPL assays were cost-efficient and easy

to design for the considerable number of validation reactions that were run, when finalizing the assay panel Taqman® assays might provide better results. Though more costly, these probe sequences can be custom designed, allowing for the design of assays in more optimal positions along the transcript unlike the pre-fabricated UPL probes.

Assay Validation

During assay validation analysis, assay performance was based on three criteria: (1) consistency across all regional assays of a gene, (2) amplification plot homogeneity, also reflected in standard deviations, and (3) conformity to expected gene expressivity, as established by GeneNote values. For regional assay consistency, a score of 0, 2, or 3 was given to assays designed for the same gene, reflecting the number of assays that expressed at approximately the same level. As the UPL assays were as optimally designed as possible, ideally all regions should express at the same level in intact RNA. However, variations in assay performance are possible and might account for why two assays out of three were consistent, yet the third may have simply been a poorly designed assay.

Amplification plots for individual assays were assessed subjectively, emphasis being placed on tight plots with little variation between samples from different subjects. To be used as a universal quality control method, it was important to limit expression variability between samples taken from different subjects. Assays were scored individually, either presenting tight or dispersed plots. **Figure 6** shows the difference between an ideal plot versus a plot that showed great variability between samples from different subjects.

The last criterion used to score assay performance was correspondence with the expression values provided by GeneNote microarray data. GeneNote data was presented as normalized intensity ranging from 0-10,000 and the data from the validation phase was presented as CT values, so direct correlation between expected and actual data was not possible. Approximated low, middle, and high expressivity ranges were assigned to the expected GeneNote expression score for each gene as well as the CT values generated by the qPCR reactions. Assays were assigned scores of matching expectations, borderline, or not matching expectations.

Once assays were scored by these performance features, they were sorted in two ways. The first list weighted amplification plot scores more heavily while the second list weighted regional assay consistency more heavily. As stated previously, both performance features were rightly influential but due to the possibility of poorly designed assays underperforming, it was unclear which feature should weight most heavily in determining

assay performance. Once both lists were generated, many of the same assays appeared at the tops of both lists so choosing what assays moved on to the experimental RNA degradation phase became less of a challenge.

Experimental RNA Degradation and Assay Performance

Once all assays were assessed using intact, high-quality input RNA, data from reactions using degraded RNA needed to be generated for algorithm development. Based on a literature search, three methods were chosen for testing: (1) freeze/thaw cycles, (2) heating, and (3) RNase treatments. Methods were chosen to mimic conditions that extracted RNA would likely be exposed to following blood samples collection. Small scale experimental conditions were run for each method followed by assessment on a Bioanalyzer. Based on the degradation banding patterns produced by each, RNase A was chosen as the method to move forward with. RNase A was also chosen because it is an extracellular, distributive enzyme produced in abundance on human skin and in blood [4, 50]. RNase A present on gloves, benchtops, and instrument surfaces would be a likely source of degradation in a laboratory setting. As established protocols for purposefully degrading RNA were limited, trial and error testing was run for a number of RNaseA and SUPERase-In dilutions until a final protocol was adopted, as described previously.

Class Prediction Algorithm Development:

We are using a supervised, machine learning approach to discriminate between classes of degradation and ultimately provide a quality grade for each assay in the panel. Data generated by the experimentally degraded RNA reactions can be used to establish an expected baseline CT value (non-degraded RNA, To) for algorithm development. Additionally, C_T values for incrementally degraded RNA ($T_{0.5}$, 11, T_2, T_4, T_8, and T_{16} minutes) will serve to extrapolate the relationship between extent of sample degradation and increase in C_T value. Based on deviation from the expected CT value for a given assay, the sample will be classified as good, moderate, or poor quality. By exploiting the regional degradation patterns of RNA, algorithms have been developed to compare gene expression measurements, CT values, of a test sample to those of an intact RNA control sample and synthetic/empirically degraded RNA samples. Based on the differentially weighted CT profiles for all assays in the panel, an overall quality constant is assigned to a given RNA sample, allowing researchers to properly normalize or exclude any given sample during gene expression data analysis and interpretation. A supervised learning approach is used to create

a class assignment for degraded KNA samples as a function of cDNA transcripts. Assays carry specific weights according to their expression levels (low, medium, high) and their relative position on the transcript (5', middle, 3') with the lowest weighted assay being on the 3' end of the highest expressing genes and the highest weighted assay being on the 5' end of the lowest expressing genes. Weights are assigned to CT values using a principal designed after the following formula:

$$W_2(g) = \frac{\frac{1}{n}\sum_{j=1,n}\left|g_{1j} - \mu_{2,m}(g)\right|}{\sigma_{2,m}(g)} \quad W_2(g) = \frac{\frac{1}{n}\sum_{j=1,n}\left|g_{1j} - \mu_{2,m}(g)\right|}{\sigma_{2,m}(g)}$$

All values are subject to voting once weighted and prior to creation of the class prediction values using the principals in the following formula:

$$V_1(g) = W_2(g) \times \left|S_x - \mu_{2TR,m}(s)\right|$$

$$V_2(g) = W_1(g) \bullet \left|g_x - \mu_{1TR,n}(g)\right|$$

Once weighting and vote assignments are completed votes are counted to create a class prediction set that will be used to measure the continuum of unknown samples on the quality spectrum using an approach related to the following formula:

$$P(x) = \frac{q \bullet \sum_{i=1,p} V_1(g_i) - p \bullet \sum_{i=1,q} V_2(g_i)}{q \bullet \sum_{i=1,p} V_1(g_i) + p \bullet \sum_{i=1,q} V_2(g_i)}$$

The resultant of class prediction analysis is a static, quantitative class prediction matrix that is biologically specific for whole blood RNA samples yielding a value that can be used in conjunction with normalization approaches to directly improve the functional analysis of gene expression measurements as a direct correlative to transcript structure and representation.

The algorithms may be further refined as desired, for example, to reduce bias and decreases sampling variability. For example, in some embodiments, one can count the number of dropouts (defined as either no expression value or a value exceeding a specific selected threshold (e.g., a threshold empirically determined to provide desired results)) overall and/or by region. For example, one can create a 3-level categorized version of the

number of dropouts, using categories of zero, one to three, and more than three dropouts. From this, one can estimate standard deviation across replicates, across regions, and across genes and estimate as well standard deviations for replicates, regions, and genes when restricted to high, medium, and low expressing genes. In some embodiments, standard deviations are estimated under a linear model with the Buckley-James estimator. This estimator allows for censored data (e.g., dropouts). Including dropouts in the estimates of standard deviations reduces bias and decreases sampling variability by including the partial information contained in dropouts.

Model fitting may also be used. In some embodiments, on can fit separate logistic/multinomial regressions to the RNA, cDNA, and microarray quality scores. In some embodiments, to reduce overfitting, one can use the lasso or elastic net methods (or other approaches), which enforce sparse regression models by shrinking all regression coefficients towards zero with a penalty that discourages non-zero coefficients. The result is a small set of predictive variables in a model that is not over-fit. Any desirable variables can be mandated into the models, if desired.

An example of a classification scheme is provided in Table 1, below.

Sample Quality	Gene Panel: High 3'	High M	High 5'	Moderate 3'	Moderate M	Moderate 5'	Low 3'	Low M	Low 5'
Very Good	- No assay dropouts - Tight Ct range across regions (5) - Tight technical replicates			- No assay dropouts - Tight Ct range across regions (5) - Tight technical replicates			- No assay dropouts - Tight Ct range across regions (4) - Tight technical replicates		
Good	- No assay dropouts - Tight Ct range across regions (5) - Tight technical replicates			- No assay dropouts - Tight Ct range across regions (4) - Tight technical replicate			- No assay dropouts - Tight Ct range across regions (4) - Tight technical replicates		
Moderate	- No assay dropouts - Tight Ct range across regions (4) - Tight technical replicates			- No assay dropouts - Tight Ct range across regions (3) - Moderate technical replicates			- Few assay dropouts - Moderate Ct range across regions (3) - Moderate technical replicates		
Poor	- Few assay dropouts - Moderate Ct range across regions (3) - Moderate technical replicates			- Few assay dropouts - Moderate Ct range across regions (3) - Inconsistent technical replicates			- Many assay dropouts, especially in 5' region - Wide Ct range across regions (2) - Very inconsistent technical replicates		
Very Poor	- Few assay dropouts - Wide Ct range across regions (2) - Inconsistent technical replicates			- Many assay dropouts, especially in 5' region - Very wide Ct range across regions (1) - Very inconsistent technical replicates			- Many assay dropouts, especially in 5' region - Very wide Ct range across regions (1) - Very inconsistent technical replicates		

One approach that will utilize this methodology is in the development of clinical diagnostics using gene expression from whole blood for biomarker analysis. The use of gene expression biomarkers for measuring disease progression and treatment efficacy will be the staple of the molecular medical management of large patient populations for a variety of diseases. Given the precision needed in making clinical assessments the ability to measure the sample quality in a functional manner is of paramount importance. The class prediction algorithm will be used in this instance to qualify a sample for diagnostic analysis. If a sample does not meet the established criteria for reproducible and sensitive analysis it will not be used for making a diagnostic measurement. This application is fundamentally different from a research application where samples with varying quality can be used for discovery and normalized to meet performance expectations. In a clinical setting every sample must be qualified at a high level of performance in order to ensure that the conclusions made on gene expression levels are reproducible and accurate.

APPENDIX I

Genes for Validation Phase: Expression Scores

Gene	Accession #	Expression Score	GenBank Definition
ACTB	NM_001101.3	Control	Homo sapiens actin, beta (ACTB), mRNA
ACTR2	NM_001005386.2	2000	Homo sapiens ARP2 actin-related protein 2 homolog (yeast) (ACTR2), transcript variant 1, mRNA
ADAR	NM_001111.3	4500	Homo sapiens adenosine deaminase, RNA-specific (ADAR), transcript variant 1, mRNA
ADD1	NM_001119.3	750	Homo sapiens adducin 1 (alpha) (ADD1), transcript variant 1, mRNA
ADD3	NM_016824.3	1500	Homo sapiens adducin 3 (gamma) (ADD3), transcript variant 1, mRNA
AIM1	NM_001624.2	1000	Homo sapiens absent in melanoma 1 (AIM1), mRNA
ARPC5	NM_005717.2	5500	Homo sapiens actin related protein 2/3 complex, subunit 5, 16kDa (ARPC5), mRNA
BACH2	NM_021813.2	150	Homo sapiens BTB and CNC homology 1, basic leucine zipper transcription factor 2 (BACH2), mRNA
C1orf38	NM_004848.2	3000	Homo sapiens chromosome 1 open reading frame 38 (C1orf38), transcript variant 1, mRNA
CAPN2	NM_001146068.1	750	Homo sapiens calpain 2, (m/II) large subunit (CAPN2), transcript variant 2, mRNA
CD163	NM_004244.4	200	Homo sapiens CD163 molecule (CD163), transcript variant 1, mRNA
CD27	NM_001242.4	650	Homo sapiens CD27 molecule (CD27), mRNA
CD300C	NM_006678.3	500	Homo sapiens CD300c molecule (CD300C), mRNA
CD53	NM_001040033.1	8000	Homo sapiens CD53 molecule (CD53), transcript variant 1, mRNA
CD68	NM_001251.2	250	Homo sapiens CD68 molecule (CD68), transcript variant 1, mRNA
CD83	NM_004233.3	150	Homo sapiens CD83 molecule (CD83), transcript variant 1, mRNA
CDC42SE1	NM_001038707.1	5000	Homo sapiens CDC42 small effector 1 (CDC42SE1), transcript variant 1, mRNA
CSF3R	NM_000760.2	6500	Homo sapiens colony stimulating factor 3 receptor (granulocyte) (CSF3R), transcript variant 1, mRNA
DDX58	NM_014314.3	350	Homo sapiens DEAD (Asp-Glu-Ala-Asp) box polypeptide 58 (DDX58), mRNA
EEF2	NM_001961.3	7000	Homo sapiens eukaryotic translation elongation factor 2 (EEF2), mRNA
F13A1	NM_000129.3	2300	Homo sapiens coagulation factor XIII, A1 polypeptide (F13A1), mRNA
FCN1	NM_002003.2	9000	Homo sapiens ficolin (collagen/fibrinogen domain containing) 1 (FCN1), mRNA
GAPDH	NM_002046.3	Control	Homo sapiens glyceraldehyde-3-phosphate dehydrogenase (GAPDH), mRNA
GZMB	NM_004131.4	1500	Homo sapiens granzyme B (granzyme 2, cytotoxic T-lymphocyte-associated serine esterase 1) (GZMB), mRNA
IL10RB	NM_000628.3	850	Homo sapiens interleukin 10 receptor, beta (IL10RB), mRNA
IL15RA	NM_172200.1	300	Homo sapiens interleukin 15 receptor, alpha (IL15RA), transcript variant 2, mRNA
IL6R	NM_181359.1	500	Homo sapiens interleukin 6 receptor (IL6R), transcript variant 2, mRNA
IL7R	NM_002185.2	3500	Homo sapiens interleukin 7 receptor (IL7R), mRNA
ITGB2	NM_001127491.1	10000	Homo sapiens integrin, beta 2 (complement component 3 receptor 3 and 4 subunit) (ITGB2), transcript variant 2, mRNA

IVNS1ABP	NM_006469.4	750	Homo sapiens influenza virus NS1A binding protein (IVNS1ABP), mRNA
KLRF1	NM_016523.1	650	Homo sapiens killer cell lectin-like receptor subfamily F, member 1 (KLRF1), mRNA
LASP1	NM_006148.2	4500	Homo sapiens LIM and SH3 protein 1 (LASP1), mRNA
LCP1	NM_002298.4	6500	Homo sapiens lymphocyte cytosolic protein 1 (L-plastin) (LCP1), mRNA
LILRA5	NM_021250.2	900	Homo sapiens leukocyte immunoglobulin-like receptor, subfamily A (with TM domain), member 5 (LILRA5), transcript variant 1, mRNA
LPXN	NM_004811.2	1100	Homo sapiens leupaxin (LPXN), transcript variant 2, mRNA
LTF	NM_002343.2	200	Homo sapiens lactotransferrin (LTF), mRNA
LY75	NM_002349.2	800	Homo sapiens lymphocyte antigen 75 (LY75), mRNA
NCF1	NM_000265.4	5500	Homo sapiens neutrophil cytosolic factor 1 (NCF1), mRNA
NCF2	NM_000433.3	8500	Homo sapiens neutrophil cytosolic factor 2 (NCF2), transcript variant 1, mRNA
NCF4	NM_013416.3	4500	Homo sapiens neutrophil cytosolic factor 4, 40kDa (NCF4), transcript variant 2, mRNA
NCL	NM_005381.2	2000	Homo sapiens nucleolin (NCL), mRNA
NC0A1	NM_003743.4	850	Homo sapiens nuclear receptor coactivator 1 (NCOA1), transcript variant 1, mRNA
NLRP1	NM_033004.3	600	Homo sapiens NLR family, pyrin domain containing 1 (NLRP1), transcript variant 1, mRNA
0AS2	NM_002535.2	500	Homo sapiens 2'-5'-oligoadenylate synthetase 2, 69/71kDa (OAS2), transcript variant 2, mRNA
0AS3	NM_006187.2	650	Homo sapiens 2'-5'-oligoadenylate synthetase 3, lOOkDa (OAS3), mRNA
PDLIM1	NM_020992.2	900	Homo sapiens PDZ and LIM domain 1 (PDLIMl), mRNA
PDLIM2	NM_176871.2	950	Homo sapiens PDZ and LIM domain 2 (mystique) (PDLIM2), transcript variant 1, mRNA
RAF1	NM_002880.3	3000	Homo sapiens v-raf-1 murine leukemia viral oncogene homolog 1 (RAF1), mRNA
R0CK2	NM_004850.3	200	Homo sapiens Rho-associated, coiled-coil containing protein kinase 2 (ROCK2), mRNA
SELL	NM_000655.3	8500	Homo sapiens selectin L (SELL), mRNA
SELP	NM_003005.3	700	Homo sapiens selectin P (granule membrane protein 140kDa, antigen CD62) (SELP), mRNA
SERPINA1	NM_000295.4	7500	Homo sapiens serpin peptidase inhibitor, clade A (alpha-1 antiproteinase, antitrypsin), member 1 (SERPINA1), transcript variant 1, mRNA
S0RL1	NM_003105.4	7500	Homo sapiens sortilin-related receptor, L(DLR class) A repeats-containing (SORL1), mRNA
STAT6	NM_003153.3	1000	Homo sapiens signal transducer and activator of transcription 6, interleukin-4 induced (STAT6), mRNA
STX4	NM_004604.3	600	Homo sapiens syntaxin 4 (STX4), mRNA
SYNE2	NM_182910.2	400	Homo sapiens spectrin repeat containing, nuclear envelope 2 (SYNE2), transcript variant 2, mRNA
TES	NM_015641.2	750	Homo sapiens testis derived transcript (3 LIM domains) (TES), transcript variant 1, mRNA
TREM1	NM_018643.2	4500	Homo sapiens triggering receptor expressed on myeloid cells 1 (TREM1), mRNA
TRPM2	NM_003307.3	400	Homo sapiens transient receptor potential cation channel, subfamily M, member 2 (TRPM2), mRNA
TXNIP	NM_006472.3	8000	Homo sapiens thioredoxin interacting protein (TXNIP), mRNA
VIM	NM_003380.3	9500	Homo sapiens vimentin (VIM), mRNA

ZAP70	NM_001079.3	650	Homo sapiens zeta-chain (TCR) associated protein kinase 70kDa (ZAP70), transcript variant 1, mRNA

APPENDIX II

Assay Designs for Validation Phase

* UPL probe sequence orientation may be as listed OR as its reverse complement.

Gene	Accession #	Length	5' Design								
			Probe	Probe Sequence*	Position	Primer	Primer Sequence	Start	End	Tm	GC
ACTB	NM_001101.3	1852	64	cagcctgg	492	Fwd	ccaaccgcgagaagatga	425	442	60	56
						Rvs	ccagaggcgtacagggatag	502	521	59	60
ACTR2	NM_001005386.2	3944	37	ccagggca	224	Fwd	gcggtggctgtaggttgt	167	184	59	61
						Rvs	gcctgcatatccacacttcac	267	287	60	52
ADAR	NM_001111.3	6640	41	cttcagcc	2011	Fwd	tcatcccactattccacagaga	1950	1971	59	45
						Rvs	gctcttcccagaaaagaagga	2022	2042	59	48
ADD1	NM_001119.3	3970	15	tcctgctc	714	Fwd	tggtctcagcttatctacaatcatatc	669	695	59	37
						Rvs	ccaaaagggacaatgaggaa	726	745	59	45
ADD3	NM_016824.3	4454	75	cagcctcc	930	Fwd	tcccagaggcctatcttttttc	901	921	59	48
						Rvs	ttcaaattggtacttccctggt	975	996	59	41
AIM1	NM_001624.2	7553	85	tccaggtc	3546	Fwd	ctggaatgtcattatcagacacaa	3483	3506	59	38
						Rvs	tcagagacgtcgggttcact	3569	3588	60	55
ARPC5	NM_005717.2	2000	51	ctcctgcc	320	Fwd	caagttcgtggacgaagaaga	257	277	60	48
						Rvs	gcagctgtcatgtttccttg	333	352	59	50
BACH2	NM_021813.2	9215	1	cctggagc	563	Fwd	aatgataaagccagaagaaagca	498	520	59	35

						Rvs	cagtgcgaggaagttcttg a	585	604	59	50
Clorf38	NM_004848.2	1650	34	ctgcctct	154	Fwd	ctcgggggtctacttcgag	103	121	59	63
						Rvs	ggacctgggtgaccttgat	176	194	59	58
CAPN2	NM_001146068.1	3270	50	tctggagc	529	Fwd	ctgctctttgtgcattcagc	495	514	59	50
						Rvs	gcttcatagcatccgttgat ct	562	583	60	45
CD163	NM_004244.4	4231	17	aggagctg	274	Fwd	tcagtgcctgttttgtcacc	232	251	59	50
						Rvs	tccactctcccgctacactt	303	322	59	55
CD27	NM_001242.4	1320	72	ttcctggc	343	Fwd	cactactgggctcagggaa a	302	321	60	55
						Rvs	tcacagtccttcacgagga a	353	372	59	50
CD300C	NM_006678.3	1548	6	ttcctctg	429	Fwd	ctctgctcctcctgcttgtc	399	418	60	60
						Rvs	tcatagcgacactgcacac tc	478	498	60	52
CD53	NM_001040033.1	1572	5	tgtggctg	238	Fwd	tcctgtttttcttcaacttgc tc	206	228	59	39
						Rvs	gtagatcccaaagcccaa aa	251	270	59	45
CD68	NM_001251.2	1872	3	cccagcag	222	Fwd	ggctggctgtgcttttct	196	213	59	56
						Rvs	tttttgtgaggacagtcatt cc	253	274	59	41
CD83	NM_004233.3	2478	36	ctggctcc	224	Fwd	ctccagcttctgctcctga	191	209	59	58
						Rvs	ggagcaagccaccttcac	245	262	59	61
CDC42SE1	NM_001038707.1	3193	22	ctccacca	156	Fwd	accagctgtagctgaacgt ct	132	152	59	52
						Rvs	catatctccacgtgtgtcca g	182	202	59	52
CSF3R	NM_000760.2	3003	18	tcctgctg	225	Fwd	gtccaagatcacaaagctg gt	140	160	59	48
						Rvs	ccgcactcctccagacttc	240	258	60	63
DDX58	NM_014314.3	4759	69	cttcctcc	260	Fwd	tggaccctacctacatcct ga	217	237	59	52
						Rvs	ggcccttgttgtttttctca	287	306	60	45

EEF2	NM_001961.3	3163	9	tggtgatg	284	Fwd	tcactgatacccggaaggac	250	269	59	55
						Rvs	ttcaagtcattctccgagagc	323	343	59	48
F13A1	NM_000129.3	3863	78	agctggag	796	Fwd	cctgaatgacatcggggtaa	741	760	60	50
						Rvs	gtccaggatgccatcttca	816	834	59	53
FCN1	NM_002003.2	1292	1	cctggagc	324	Fwd	agaggcaggtgtcattggag	284	303	60	55
						Rvs	ctggtcctgcctttccag	334	351	59	61
GAPDH	NM_002046.3	1310	60	cttcccca	104	Fwd	agccacatcgctcagacac	83	101	60	58
						Rvs	gcccaatacgaccaaatcc	130	148	60	53
GZMB	NM_004131.4	941	18	tcctgctg	98	Fwd	agatgcaaccaatcctgctt	65	84	59	45
						Rvs	catgtcccccgatgatct	125	142	59	56
IL10RB	NM_000628.3	1935	20	ccagccag	120	Fwd	ggtcgtgtgcttggagga	56	73	60	61
						Rvs	ggtaccattcccaatgctga	145	164	60	50
IL15RA	NM_172200.1	1843	47	tccagtgt	343	Fwd	ctcttcgcagtggggaca	312	329	60	61
						Rvs	cccagatgtctgcgtgttc	433	451	60	58
IL6R	NM_181359.1	4082	10	ccacctcc	521	Fwd	gtagccgaggaggaagcat	421	439	59	58
						Rvs	actggtcagcacgcctct	531	548	59	61
IL7R	NM_002185.2	1809	9	tggtgatg	284	Fwd	gcttttgaggacccagatgt	261	280	59	50
						Rvs	aggcactttacctccacgag	318	337	59	55
ITGB2	NM_001127491.1	2932	27	caggcagc	519	Fwd	gctgtccccacaaaaagtg	479	497	59	53
						Rvs	ccggaaggtcacgttgaa	531	548	60	56
IVNS1ABP	NM_006469.4	4205	14	ctgggaga	1241	Fwd	atcaactgggtgcagcgta	1218	1236	60	53
						Rvs	tcagctgagtagtacaaggtttgaa	1282	1306	59	40
KLRF1	NM_016523.1	1242	48	ttcccagt	184	Fwd	tgcccaaacatctcaacttaca	121	142	60	41

						Rvs	aataccattcacggttcca ga	194	214	59	43
LASPl	NM_006148.2	4109	50	tctggagc	568	Fwd	gaaaaccttcgcctcaagc	539	557	59	53
						Rvs	tgaaaccttgcccttgttc	607	626	60	45
LCP1	NM_002298.4	3808	6	ttcctctg	594	Fwd	ttggcacccaacactccta	573	591	60	53
						Rvs	ccagggctttgtttatccag	622	641	59	50
LILRA5	NM_021250.2	1365	80	cctggaga	813	Fwd	agtctgcctgtggcatgg	56	73	60	61
						Rvs	gctgtgcagatggatgaga c	132	151	59	55
LPXN	NM_004811.2	1926	17	aggagctg	219	Fwd	ttggatgtaggacaatgga aga	132	153	59	41
						Rvs	cctttctggaatgctgatcc	235	254	59	50
LTF	NM_002343.2	2390	18	tcctgctg	58	Fwd	gaccgcagacatgaaactt g	29	48	59	50
						Rvs	gccagccagacacagtcc	81	98	60	67
LY75	NM_002349.2	6927	6	ttcctctg	503	Fwd	aatgcatctgatgtctgga aga	472	493	59	41
						Rvs	ccataagagttcccatctct gg	545	566	59	50
NCF1	NM_000265.4	1409	20	ccagccag	129	Fwd	cctgctgggctttgagaa	100	117	60	56
						Rvs	gacaggtcctgccatttca c	158	177	60	55
NCF2	NM_000433.3	2429	38	ctgcttcc	775	Fwd	aaaatcgacaaggcgatg g	747	765	60	47
						Rvs	gggatcaccactggctcat a	789	808	60	55
NCF_4	NM_013416.3	1646	3	cccagcag	195	Fwd	gcgagactctccacctgct	146	164	60	63
						Rvs	catccggaagctgttcaaa g	220	239	60	50
NCL	NM_005381.2	2732	70	ccgccgcc	131	Fwd	ccacttgtccgcttcaca	111	128	59	56
						Rvs	tcttggggtcaccttgattt	168	187	59	45
NC0A1	NM_003743.4	6895	58	ctccatcc	960	Fwd	tcacagccaaaatcaattc a a	937	957	59	33
						Rvs	gccgtgcaatacaaatcag a	984	1003	59	45

NLRP1	NM_033004.3	5623	13	ctctgcct	1008	Fwd	agctgcctgacacatctgg	971	989	59	58
						Rvs	ggagcttggaagagcttggt	1025	1044	60	55
OAS2	NM_002535.2	3647	23	cccagccc	603	Fwd	gagaatctctttcgaggtgctg	548	569	60	50
						Rvs	caaggatcttttgagctctcg	621	641	59	48
OAS3	NM_006187.2	6646	8	ctgccttc	1727	Fwd	tggatggatgttagcctggt	508	527	60	50
						Rvs	cttgtggcttgggtttgac	565	583	59	53
PDLIM1	NM_020992.2	1462	81	ccagggcc	133	Fwd	catgaccacccagcagatag	109	128	59	55
						Rvs	gccttgcttccaggagtg	208	225	59	61
PDLIM2	NM_176871.2	4611	80	cctggaga	267	Fwd	gcccatcatggtgactaagg	209	228	60	55
						Rvs	cgttgatggccacgatta	277	294	59	50
RAF1	NM_002880.3	3291	13	ctctgcct	1175	Fwd	tgtttccaggatgcctgtt	1075	1093	59	47
						Rvs	ggacattaggtgtggatgtcg	1185	1205	60	52
R0CK2	NM_004850.3	6401	17	aggagctg	1552	Fwd	tcagtggcattgggataacat	1520	1540	60	43
						Rvs	tgctgtctatgtcactgctgag	1572	1593	59	50
SELL	NM_000655.3	2448	72	ttcctggc	286	Fwd	ggggtggacaatgctctg	261	278	60	61
						Rvs	taagtccagcagtcggttcc	301	320	60	55
SELP	NM_003005.3	3185	8	ctgccttc	34	Fwd	actgtaagcagtctgggttgg	10	30	59	52
						Rvs	gatggctatttggcagttgg	70	89	60	50
SERPINAl	NM_000295.4	3220	73	tcctcagc	216	Fwd	gettaaataeggacgaggaca	185	205	59	48
						Rvs	acgagacagaagacggcatt	261	280	59	50
S0RL1	NM_003105.4	10924	19	ctccagcc	1444	Fwd	gggaacctgggagtttcttc	1421	1440	59	55

						Rvs	acagccctgggaaagctc	1482	1499	60	61
STAT6	NM_003153.3	3993	54	ctggtctc	287	Fwd	agaagacagcagaggggttg	226	245	59	55
						Rvs	cacttttctgggggcatc	298	316	60	53
STX4	NM_004604.3	1403	62	cagcaggt	417	Fwd	caaactggggaataaagtccag	383	404	59	45
						Rvs	cagctcctgcttcatgctc	455	473	59	58
SYNE2	NM_182910.2	2586	4	cttcctgc	506	Fwd	ggatggtggcaaagaagg	461	478	59	56
						Rvs	catctcccatctgtcgaagg	553	572	60	55
TES	NM_015641.2	2766	85	tccaggtc	185	Fwd	ggacccataggacgcgtta	161	179	60	58
						Rvs	cgtgacctaagcccatcttc	205	224	59	55
TREM1	NM_018643.2	948	66	cagcagcc	87	Fwd	acaggaaggatgaggaagacc	56	76	59	52
						Rvs	ctgcccctctttcagttcata	149	169	59	48
TRPM2	NM_003307.3	5876	14	ctgggaga	534	Fwd	cctgagccagaaggtgaaaa	502	521	60	50
						Rvs	gggtcatgaggtggtagatca	558	578	59	52
TXNIP	NM_006472.3	2953	85	tccaggtc	616	Fwd	cttctggaagaccagccaac	570	589	59	55
						Rvs	gaagctcaaagccgaacttg	638	657	60	50
VIM	NM_003380.3	2151	56	tgctgtcc	252	Fwd	gtttcccctaaaccgctagg	217	236	59	55
						Rvs	agcgagagtggcagagga	267	284	59	61
ZAP70	NM_001079.3	2450	3	cccagcag	92	Fwd	ggagctcagcagacaccag	32	50	59	63
						Rvs	ccaatgccaatggagagc	113	130	60	56

Gene	Accession #	Length	Middle Design								
			Probe	Probe Sequence*	Position	Primer	Primer Sequence	Start	End	Tm	GC
ACTB	NM_001101.3	1852	-	-	-	Fwd	-	-	-	-	-
						Rvs	-	-	-	-	-
ACTR2	NM_001005386.2	3944	61	ctgggcaa	728	Fwd	atgtagccatccaggcagtt	640	659	59	50
						Rvs	gatgagggagagaaaagccttc	741	762	60	50
ADAR	NM_001111.3	6640	39	ctccacct	3208	Fwd	ttcgagaatcccaaacaagg	3174	3193	60	45
						Rvs	ctggattccacagggattgt	3228	3247	59	50
ADD1	NM_001119.3	3970	38	ctgcttcc	1575	Fwd	gacaagatggctgaactctgg	1520	1540	59	52
						Rvs	tgtccatcctctttagtccactt	1599	1621	59	43
ADD3	NM_016824.3	4454	39	ctccacct	1357	Fwd	gcaactagcctgtgagattcag	1315	1336	59	50
						Rvs	cgctgctacagtgtaagtgaaag	1404	1426	59	48
AIM1	NM_001624.2	7553	1	cctggagc	4940	Fwd	tgtctgtctgcaatgggatg	4916	4935	60	50
						Rvs	gaataattgttggttcagaaaattca	4978	5003	59	27
ARPC5	NM_005717.2	2000	27	caggcagc	415	Fwd	caccaagagtcaggcagtga	386	405	60	55
						Rvs	agagatgagcaccttcaagaca	425	446	59	45
BACH2	NM_021813.2	9215	76	tggctgtg	1055	Fwd	aatgatttggtggtcagcttg	1023	1043	59	43
						Rvs	gcttggcagtgtaggcaaac	1085	1104	60	55
C1orf38	NM_004848.2	1650	20	ccagccag	228	Fwd	ccagaaggtggtctgtgagaa	199	219	60	52
						Rvs	catagctctgtggggtgttg	280	299	59	55

CAPN2	NM_001146068.1	3270	82	cagaggag	1312	Fwd	ggctttggcatctatgaggt	1290	1309	59	50
						Rvs	gctgaggtggatgttggtct	1330	1349	60	55
CD163	NM_004244.4	4231	50	tctggagc	1238	Fwd	gaagatgctggcgtgacat	1203	1221	59	53
						Rvs	gctgcctccacctctaagtc	1249	1268	59	60
CD27	NM_001242.4	1320	30	cctcagcc	629	Fwd	tccaaacccttcgctgac	580	597	59	56
						Rvs	tggcctccagcatctcac	657	674	60	61
CD300C	NM_006678.3	1548	19	ctccagcc	778	Fwd	gaggttgaggtgtccgtgtt	737	756	60	55
						Rvs	cttcgtgggaggacctga	806	823	59	61
CD53	NM_001040033.1	1572	58	ctccatcc	579	Fwd	cactcagacaatagcaccaagg	547	568	59	50
						Rvs	cgtgccatttataccacaaca	601	621	59	43
CD68	NM_001251.2	1872	67	tgctggag	882	Fwd	tcagctttggattcatgcag	859	878	59	45
						Rvs	gagccgagaatgtccactgt	950	959	60	55
CD83	NM_004233.3	2478	58	ctccatcc	354	Fwd	acggtctcctgggtcaagt	314	332	59	58
						Rvs	ccctgaggtggtcttcctg	368	386	60	63
CDC42SE1	NM_001038707.1	3193	26	cagcccag	592	Fwd	gggaacatgagtgaattttgg	565	585	59	43
						Rvs	cggtcaatccgtcttctctt	631	650	59	50
CSF3R	NM_000760.2	3003	13	ctctgcct	789	Fwd	tgtaccagaatatgggcatctg	762	783	59	45
						Rvs	ggggctccagtttcacaa	849	856	59	56
DDX58	NM_014314.3	4759	13	ctctgcct	2342	Fwd	atgtgggcaatgtcatcaaa	2308	2327	59	40
						Rvs	aagca cttgcta cctcttgctc	2353	2374	60	50
EEF2	NM_001961.3	3163	25	ctcctcca	1765	Fwd	ctggagatctgcctgaagga	1743	1762	60	55
						Rvs	gagacgaccgggtcagatt	1798	1816	60	58
F13A1	NM_000129.	386	56	tgctgtcc	131	Fwd	ccttcctgttggatttggag	127	129	59	50

	3	3			1			8	7		
						Rvs	ggccacaccgatacatgc	1340	1357	60	61
FCN1	NM_002003.2	1292	38	ctgcttcc	690	Fwd	gctggggaacgacaacat	653	670	59	56
						Rvs	cctcaaagtccaccaggtct	710	729	59	55
GAPDH	NM_002046.3	1310	-	-	-	Fwd	-	-	-	-	-
						Rvs	-	-	-	-	-
GZMB	NM_004131.4	941	78	agctggag	404	Fwd	cttctccaacgacatcatgc	378	397	59	50
						Rvs	acagctctggtccgcttg	420	437	60	61
IL10RB	NM_000628.3	1935	1	cctggagc	639	Fwd	tggaaaaacggtactgatgaaa	574	595	59	36
						Rvs	aaccctcgaacttgaacacaa	660	680	59	43
IL15RA	NM_172200.1	1843	37	ccagggca	606	Fwd	acaacccccagtctcaaatg	574	593	59	50
						Rvs	tgccgtcgttactgtggag	636	654	60	58
IL6R	NM_181359.1	4082	38	ctgcttcc	797	Fwd	ggactgtgcacttgctggt	748	756	59	58
						Rvs	attgctgaggggctctt	807	824	59	56
IL7R	NM_002185.2	1809	12	ctccttcc	509	Fwd	ggagaaaagagtctaacctgcaa	423	445	59	43
						Rvs	gatgtattaaatgtcaccacaaagtca	521	547	60	33
ITGB2	NM_001127491.1	2932	25	ctcctcca	1277	Fwd	cagcaatgtggtccaactca	1235	1254	60	50
						Rvs	gagggcgttgtgatccag	1293	1310	60	61
IVNS1ABP	NM_006469.4	4205	76	tggctgtg	1537	Fwd	cgttgcttcagaaaagactttca	1496	1517	59	41
						Rvs	gaaaaatgacacagaatataccatcc	1547	1572	59	35
KLRF1	NM_016523.1	1242	47	tccagtgt	312	Fwd	tgatctccttgatcctgttgg	228	248	60	48
						Rvs	ttcttcttgtgccattattcactt	327	350	59	33
LASP1	NM_006148.2	4109	3	cccagcag	852	Fwd	accacatcccgaccagtg	816	833	60	61
						Rvs	ccttgtagccaccataggac	872	893	60	55

							tg				
LCPl	NM_002298.4	3808	37	ccagggca	1504	Fwd	aaccctcgagtcaatcatttg	1466	1486	59	43
						Rvs	ttgatcttttcatagagctggaag	1516	1539	59	38
LILRA5	NM_021250.2	1365	1	cctggagc	510	Fwd	gcagggagataccgctgtta	451	470	60	55
						Rvs	tgagagggtgggtttgttgt	536	555	60	50
LPXN	NM_004811.2	1926	77	ccaccacc	389	Fwd	caatatccaggagctcaatgtctac	337	361	60	44
						Rvs	tgagctcatccaactgagca	415	434	60	50
LTF	NM_002343.2	2390	53	ctctgcca	1327	Fwd	tgtgtacactgcaggcaaatg	1289	1309	60	48
						Rvs	ggatcagggtcactgctttg	1350	1369	60	55
LY75	NM_002349.2	6927	53	ctctgcca	2008	Fwd	taagcctgatgacccctgtc	1980	1999	60	55
						Rvs	caattctttctgcatggaatacct	2042	2065	60	38
NCF1	NM_000265.4	1409	33	agctggga	294	Fwd	ccgagatctacgagttccataaa	204	226	59	43
						Rvs	ctgcccgtcaaaccactt	305	322	59	56
NCF2	NM_000433.3	2429	45	ctggggct	1192	Fwd	caactaccttgaaccagttgage	1148	1170	60	48
						Rvs	atgtcggactgcggagag	1208	1225	59	61
NCF4	NM_013416.3	1646	78	agctggag	760	Fwd	gcagctccgagagcagag	695	712	60	67
						Rvs	ccgactgaggaggaagatca	771	790	60	55
NCL	NM_005381.2	2732	80	cctggaga	1218	Fwd	gtggatgtcagaattggtatgact	1156	1179	59	42
						Rvs	caaaccagtgagttccaac***s***	1229	1248	59	50
NC0A1	NM_003743.4	6895	83	cagccacc	3559	Fwd	tgagatcaggcatgcaacag	3527	3546	60	50
						Rvs	gtacagttcccgctgacgtt	3590	3609	60	55

NLRPl	NM_033004.3	5623	45	ctggggct	3421	Fwd	catcctgcctgcaaactca	3397	3415	60	53
						Rvs	cctcagttcctgcctcatct	3452	3471	59	55
OAS2	NM_002535.2	3647	38	ctgcttcc	1280	Fwd	tgttaacatcatccgtacattcct	1247	1270	59	38
						Rvs	ctttggcggttgatcctc	1321	1338	59	56
OAS3	NM_006187.2	6646	43	ctgcccca	1742	Fwd	gacggatgttagcctgctg	1707	1725	59	58
						Rvs	tggggatttggtttggtg	1761	1778	60	50
PDLIM1	NM_020992.2	1462	54	ctggtctc	373	Fwd	aggctgcacagacaacttga	322	341	59	50
						Rvs	atggatgacgcttcccttc	395	413	60	53
PDLIM2	NMJL76871.2	4611	30	cctcagcc	884	Fwd	ccagctcctttcggctct	850	857	60	61
						Rvs	gtgagctgggcaagaagg	910	927	59	61
RAF1	NM_002880.3	3291	56	tgctgtcc	1464	Fwd	tgggaaatagaagccagtgaa	1439	1459	59	43
						Rvs	cctttaggatctttactgcaacatc	1526	1550	59	40
R0CK2	NM_004850.3	6401	84	tctgctgc	3140	Fwd	tgaagaaaagaccaaacttggtaaa	3110	3134	60	32
						Rvs	agttgggcagccaaagagt	3175	3193	59	53
SELL	NM_000655.3	2448	57	ctggggcc	801	Fwd	gccccagtgtcagtttgtg	762	780	60	58
						Rvs	ccaaagggtgagtacagtcca	821	841	60	52
SELF	NM_003005.3	3185	23	cccagccc	1007	Fwd	ttagttggaccggaagtggt	957	976	59	50
						Rvs	caggtgctgacactgcaca	1028	1046	60	58
SERPINAl	NM_000295.4	3220	9	tggtgatg	1146	Fwd	gcacctggaaaatgaactcac	1116	1136	59	48
						Rvs	gggtaaatgtaagctggcaga	1180	1200	59	48
S0RL1	NM_O031O5.4	10924	85	tccaggtc	3432	Fwd	tggagacatgagcgatgaga	3389	3408	60	50

						Rvs	gactcctggcaacgaaactg	3444	3463	60	55
STAT6	NM_003153.3	3993	3	cccagcag	1790	Fwd	ggtcgcagttcaacaagga	1767	1785	59	53
						Rvs	gtccaggacaccatcaaacc	1821	1840	60	55
STX4	NM_004604.3	1403	69	cttcctcc	548	Fwd	tgcagctgaaggccataga	520	538	60	53
						Rvs	cgaattgctgggacagga	610	627	60	56
SYNE2	NM_182910.2	2586	17	aggagctg	1135	Fwd	gtgtcggagggaactaatgc	1106	1125	59	55
						Rvs	tcca cttgaggttga cgttct	1145	1165	59	48
TES	NM_015641.2	2766	63	ctcctcct	522	Fwd	tgtctccatcaatacagttacctatga	490	516	60	37
						Rvs	tccttgggtagcatctgcat	560	579	60	50
TREM1	NM_018643.2	948	75	cagcctcc	413	Fwd	tctggactgtatcagtgtggatct	386	410	60	44
						Rvs	ccaggggtccctgaaaaa	472	489	60	56
TRPM2	NM_003307.3	5876	24	cagctccc	2004	Fwd	accttctcatttgggccatt	1971	1990	60	45
						Rvs	cgatgcagtcctggctct	2031	2048	60	61
TXNIP	NM_006472.3	2953	26	cagcccag	1134	Fwd	ttcgggttcagaagatcagg	1105	1124	60	50
						Rvs	ggatccaggaacgctaacat	1177	1196	59	50
VIM	NM_003380.3	2151	39	ctccacct	928	Fwd	gaccagctaaccaacgacaaa	897	917	60	48
						Rvs	gaagcatctcctcctgcaat	977	996	59	50
ZAP70	NM_001079.3	2450	1	cctggagc	618	Fwd	gtga eta cgtgcgccaga c	578	596	60	63
						Rvs	cgtagcaatgagcttctccac	652	672	60	52

Gene	Accession #	Length	3' Design								
			Probe	Probe Sequence*	Position	Primer	Primer Sequence	Start	End	Tm	GC
ACTB	NM_001101.3	1852	11	cttccagc	867	Fwd	attggcaatgagcggttc	832	849	59	50
						Rvs	tgaaggtagtttcgtggatgc	902	922	60	48
ACTR2	NM_001005386.2	3944	27	caggcagc	1089	Fwd	ttggtgttgctgaattgctt	1057	1076	59	40
						Rvs	accctccagaaagcacaatg	1130	1149	60	50
ADAR	NM_001111.3	6640	53	ctctgccca	3518	Fwd	tttattgtcaaccaccccaag	3495	3515	59	43
						Rvs	ccttagtcttcccggattgc	3548	3567	60	55
ADD1	NM_001119.3	3970	69	cttcctcc	2042	Fwd	cccagcactcccatcaag	2022	2039	60	61
						Rvs	gtggcagcatcactgtcatc	2076	2095	60	55
ADD3	NM_016824.3	4454	15	tcctgctc	2114	Fwd	ggacaatcgaacgtaaacaaca	2076	2097	59	41
						Rvs	tgaatttgtgaaacagatgaagc	2138	2160	59	35
AIM1	NM_001624.2	7553	27	caggcagc	5415	Fwd	gaaggatgtatcaaatgcagga	5381	5402	59	41
						Rvs	cttggagccagatgttaccag	5438	5458	59	52
ARPC5	NM_005717.2	2000	25	ctcctcca	596	Fwd	ctgcaatggcatgaaaagg	567	585	60	47
						Rvs	tgcagtcaagacacgaacaa	613	632	59	45
BACH2	NM_021813.2	9215	79	ccaggagg	2639	Fwd	cagtgagtcgtgtcctgtgc	2609	2628	60	60
						Rvs	tgtgatttgatctacaggaaaagg	2655	2678	59	38
C1orf38	NM_004848.2	1650	44	tgggcagc	710	Fwd	gatccaagccatcatgcac	655	673	60	53
						Rvs	tgatgaactctggcaaggtct	730	750	59	48
CAPN2	NM_001146068.1	3270	45	ctgggggct	1776	Fwd	caaaattatggttgacatgctagatt	1733	1758	59	31

						Rvs	tcgtccagagaatgtagaactcc	1787	1809	59	48
CD163	NM_004244.4	4231	85	tccaggtc	3635	Fwd	aatgggaatttataacccagtgag	3585	3608	59	38
						Rvs	ggtgaatttctgctccattca	3647	3667	60	43
CD27	NM_001242.4	1320	43	ctgcccca	916	Fwd	catcaacgaaggaaatagatcaaac	845	871	60	33
						Rvs	ctcctggatggggatggt	941	958	60	61
CD300C	NM_006678.3	1548	23	cccagccc	872	Fwd	agcgtgaccagaaaggaca	845	863	59	53
						Rvs	gaagcggacattgctgaac	895	913	59	53
CD53	NM_001040033.1	1572	9	tggtgatg	732	Fwd	tggtttcattccaatttcctg	700	720	59	38
						Rvs	aggacatccccaacacctc	757	775	59	58
CD68	NM_001251.2	1872	1	cctggagc	1079	Fwd	gtccacctcgacctgctct	1053	1071	60	63
						Rvs	cactggggcaggagaaact	1122	1140	60	58
CD83	NM_004233.3	2478	21	tggctctg	624	Fwd	acagagcggagattgtcctg	600	619	60	55
						Rvs	ctctgtagccgtgcaaacttac	666	687	59	50
CDC42SEl	NM_001038707.1	3193	26	cagcccag	859	Fwd	tctaggggcttatagctccaataat	796	820	59	40
						Rvs	ctggtaggggcagcatttc	869	887	60	58
CSF3R	NM_000760.2	3003	88	catcctcc	2215	Fwd	ctgggtgcccacaatcat	2194	2211	60	56
						Rvs	gcactgtgagcttggtgatg	2254	2273	60	55
DDX58	NM_014314.3	4759	29	cttctgcc	4673	Fwd	ccatgtaagacttgcctgctt	4649	4669	59	48
						Rvs	gaggcttaatagattcacagttcca	4716	4740	60	40
EEF2	NM_001961.3	3163	47	tccagtgt	2329	Fwd	gagcccatctaccttgtgga	2307	2326	60	55
						Rvs	cctgttcaaaaccccgtaga	2359	2378	59	50
F13A1	NM_000129.	386	81	ccaggg	221	Fwd	tggagtaacaagaccaatga	213	215	60	38

	3	3		cc	3		agaa	6	9		
						Rvs	tggctatcagcttccgatg	2230	2248	59	53
FCNl	NM_002003.2	1292	13	ctctgcct	775	Fwd	tgctaagtacaaatcattcaaggtg	743	767	59	36
						Rvs	ggcccgttagagaattaccc	824	843	59	55
GAPDH	NM_002046.3	1310	45	ctgggg ct	425	Fwd	gagtccactggcgtcttcac	391	410	60	60
						Rvs	ttcacacccatgacgaacat	490	509	59	45
GZMB	NM_004131.4	941	37	ccaggg ca	705	Fwd	gggggacccagagattaaaa	633	652	60	50
						Rvs	ccattgtttcgtccataggag	717	737	59	48
IL10RB	NM_000628.3	1935	7	cttctcc c	864	Fwd	gctgtggtgcgtttacaaga	831	850	59	50
						Rvs	gaggatggcccaaaaactct	900	919	60	50
IL15RA	NM_172200.1	1843	18	tcctgct g	953	Fwd	gtggctatctcca cgtcca c	931	950	60	60
						Rvs	catggcttccatttcaacg	1029	1047	60	47
IL6R	NM_181359.1	4082	67	tgctgg ag	1254	Fwd	cggtcaaagacattcacaac a	1218	1238	59	43
						Rvs	gcgtcgtggatgacacagt	1264	1282	60	58
IL7R	NM_002185.2	1809	72	ttcctgg c	598	Fwd	aaagttttaa tgca cgatgta gctt	570	594	59	32
						Rvs	tgtgctggata aattca catg c	626	647	60	41
ITGB2	NM_001127491.1	2932	18	tcctgct g	2220	Fwd	gggactcagagggctgct	2182	2199	60	67
						Rvs	ggcctgccacacactctc	2266	2283	60	67
IVNS1ABP	NM_006469.4	4205	17	aggagc tg	2273	Fwd	ggactttaattgcacccatga	2239	2259	59	43
						Rvs	aaccatcaaagccaccacat	2312	2331	60	45
KLRF1	NM_016523.1	1242	78	agctgg ag	464	Fwd	cgagatctgcagaccagaca	378	397	60	55
						Rvs	gagattttctttccaaacaat acaca	481	506	59	31
LASP1	NM_006148.	410	77	ccacca	932	Fwd	cagccccagtctccatacag	900	919	60	60

	2	9		cc		Rvs	ggcggcgctgtagtcata	962	979	60	61
LCPl	NM_002298.4	3808	49	tggtggcc	1771	Fwd	gccttgatttggcagctaat	1715	1734	59	45
						Rvs	tttcattcacccagttgacaat	1799	1820	59	36
LILRA5	NM_021250.2	1365	68	aggagcag	831	Fwd	tggtcagaacccagtgacct	793	812	60	55
						Rvs	tgttttgtgacggactgagg	846	865	59	50
LPXN	NM_004811.2	1926	83	cagccacc	956	Fwd	ggagaggtgtttggtgcag	866	884	59	58
						Rvs	gaaaggtagttttccaacactgg	971	993	59	43
LTF	NM_002343.2	2390	79	ccaggagg	2138	Fwd	ctaatctgaaaaagtgctcaacctc	2110	2134	59	40
						Rvs	gccatcttcttcggttttacttc	2165	2187	60	43
LY75	NM_002349.2	6927	26	cagcccag	3627	Fwd	tggatcggactcttcagtca	3553	3572	59	50
						Rvs	cagtcttcgagttgcccatta	3639	3659	60	48
NCF1	NM_000265.4	1409	10	ccacctcc	406	Fwd	ctgcccaccaagatctcc	380	397	59	61
						Rvs	ttgggcatcaagtatgtctctg	477	498	60	45
NCF2	NM_000433.3	2429	11	cttccagc	1757	Fwd	ggaaggggatataatcctggtg	1712	1733	60	50
						Rvs	ccaccttccctttgcactc	1767	1785	60	58
NCF4	NM_013416.3	1646	69	cttcctcc	1200	Fwd	gtcacccccttagggacatc	1175	1194	60	60
						Rvs	gagctatgtcctctctggaact	1259	1282	59	50
NCL	NM_005381.2	2732	19	ctccagcc	1802	Fwd	gaaattgagggcagagcaat	1780	1799	59	45
						Rvs	tgacaaacagagttttggatgg	1849	1870	60	41
NC0A1	NM_003743.4	6895	3	cccagcag	4409	Fwd	gcaaccagctctcatccact	4361	4380	60	55
						Rvs	gacgtcagcaaacacctgaa	4427	4446	59	50

NLRPl	NM_033004.3	5623	89	cagcatcc	4448	Fwd	cactgtgtctgggtctggttc	4425	4445	60	57
						Rvs	tcttctccagggcttcgata	4486	4505	59	50
OAS2	NM_002535.2	3647	36	ctggctcc	1621	Fwd	cctgcctttaatgcactgg	1590	1608	59	53
						Rvs	atgagccctgcataaacctc	1641	1660	59	50
OAS3	NM_006187.2	6646	1	cctggagc	2792	Fwd	gtgctgccagcctttgac	2752	2769	60	61
						Rvs	ggtcgacgtagacttgagagc	2804	2824	59	57
PDLIM1	NM_020992.2	1462	74	ctgctgcc	609	Fwd	aacaatgccctggagtcaaa	587	606	60	45
						Rvs	aggctgagcatggtctaagg	642	661	59	55
PDLIM2	NM_176871.2	4611	22	ctccacca	1171	Fwd	gggctgaacctgaagatgc	1083	1101	60	58
						Rvs	cctggtcttcctcctgtcc	1193	1211	59	63
RAF1	NM_002880.3	3291	57	ctggggcc	1951	Fwd	ggttgaacaacctactggctct	1918	1939	59	50
						Rvs	gggttgttatcctgcattcg	1967	1986	60	50
R0CK2	NM_004850.3	6401	8	ctgccttc	4617	Fwd	acagcttgccccaaacaa	4589	4606	60	50
						Rvs	tggaagaatacgatcaccttga	4643	4664	59	41
SELL	NM_000655.3	2448	59	cagtggca	1208	Fwd	tcaaatcctagtccaatatgtcaaaa	1126	1151	60	31
						Rvs	cccagagaatgcagtaaccat	1219	1239	59	48
SELF	NM_003005.3	3185	76	tggctgtg	2499	Fwd	caaaaagatgatgggaaatgc	2466	2486	59	38
						Rvs	catgggtgtttatggaaaacctt	2557	2578	59	41
SERPINAl	NM_000295.4	3220	82	cagaggag	1298	Fwd	aatggggctgacctctcc	1273	1290	60	61
						Rvs	gtcagcacagccttatgcac	1330	1349	59	55

S0RL1	NM_003105.4	10924	77	ccaccacc	5325	Fwd	cgattctaaatccattaccacca	5285	5307	60	39
						Rvs	caccatagctgtcaatgtgga	5338	5358	59	48
STAT6	NM_003153.3	3993	64	cagcctgg	2452	Fwd	tcaacgtgttgtcagccttc	2406	2425	59	50
						Rvs	gggtgaggctggtcaaag	2476	2493	59	61
STX4	NM_004604.3	1403	51	ctcctgcc	988	Fwd	ttttctggctaccgaagtgg	899	918	60	50
						Rvs	gttctccagggccgtctt	1002	1019	60	61
SYNE2	NM_182910.2	2586	75	cagcctcc	1365	Fwd	taatggccttgcagggaac	1294	1312	60	53
						Rvs	tctcactgctctga actttgct	1397	1418	59	45
TES	NM_015641.2	2766	3	cccagcag	826	Fwd	ttcctggaggggatagaagc	804	823	60	55
						Rvs	atactcagtttgcagcaatagca	887	909	59	39
TREM1	NM_018643.2	948	20	ccagccag	692	Fwd	ttacaaatgtgacagatatcatcagg	639	664	59	35
						Rvs	aagaccaggctcttactcagga	705	726	59	50
TRPM2	NM_003307.3	5876	85	tccaggtc	3587	Fwd	cgaggacatcagcaataaggt	3544	3564	59	48
						Rvs	atggagcccgacctcttc	3601	3618	60	61
TXNIP	NM_006472.3	2953	77	ccaccacc	1461	Fwd	atgcccctgagttcaagttc	1438	1457	59	50
						Rvs	actgcacattgttgttgagga	1495	1515	59	43
VIM	NM_003380.3	2151	13	ctctgcct	1648	Fwd	tacaggaagctgctggaagg	1611	1630	60	55
						Rvs	accagagggagtgaatccag	1695	1714	59	55
ZAP70	NM_001079.3	2450	52	ctcctccc	1496	Fwd	gctgcacaagttcctggtc	1470	1488	59	58
						Rvs	tcatccccatggacacct	1538	1555	59	56

APPENDIX III

Assay Validation Phase: RNA Extraction Quality Control Data

Nanodrop ND-8000 RNA Yield Data:

Sample ID	ng/µl	A260	mm	260/280	260/230	Constant	Yield (µg)
A	30.48	0.762	0.315	2.42	0.18	40	3.66
B	6.99	0.175	0.038	4.59	0.05	40	0.84
C	28.46	0.712	0.303	2.35	0.12	40	3.42
D	28.08	0.702	0.29	2.42	0.19	40	3.37
E	65.4	1.635	0.711	2.3	0.32	40	7.85

LabChip 90 **HT** Microcapillary Electrophoresis RNAQuality Data :

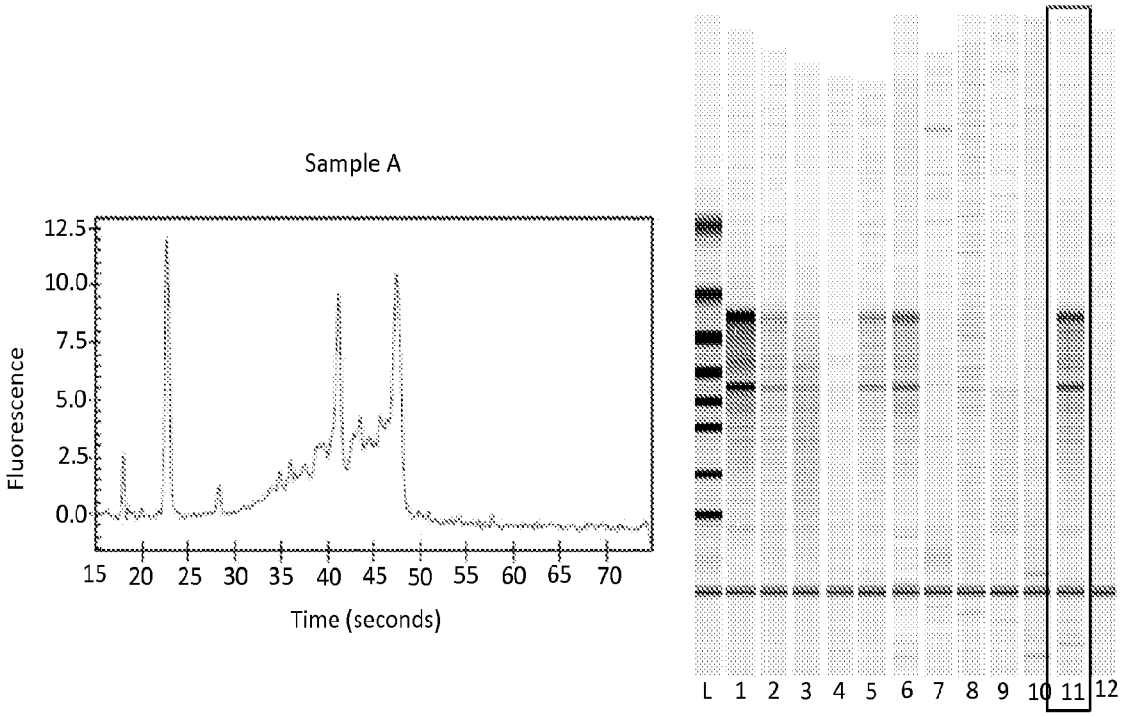

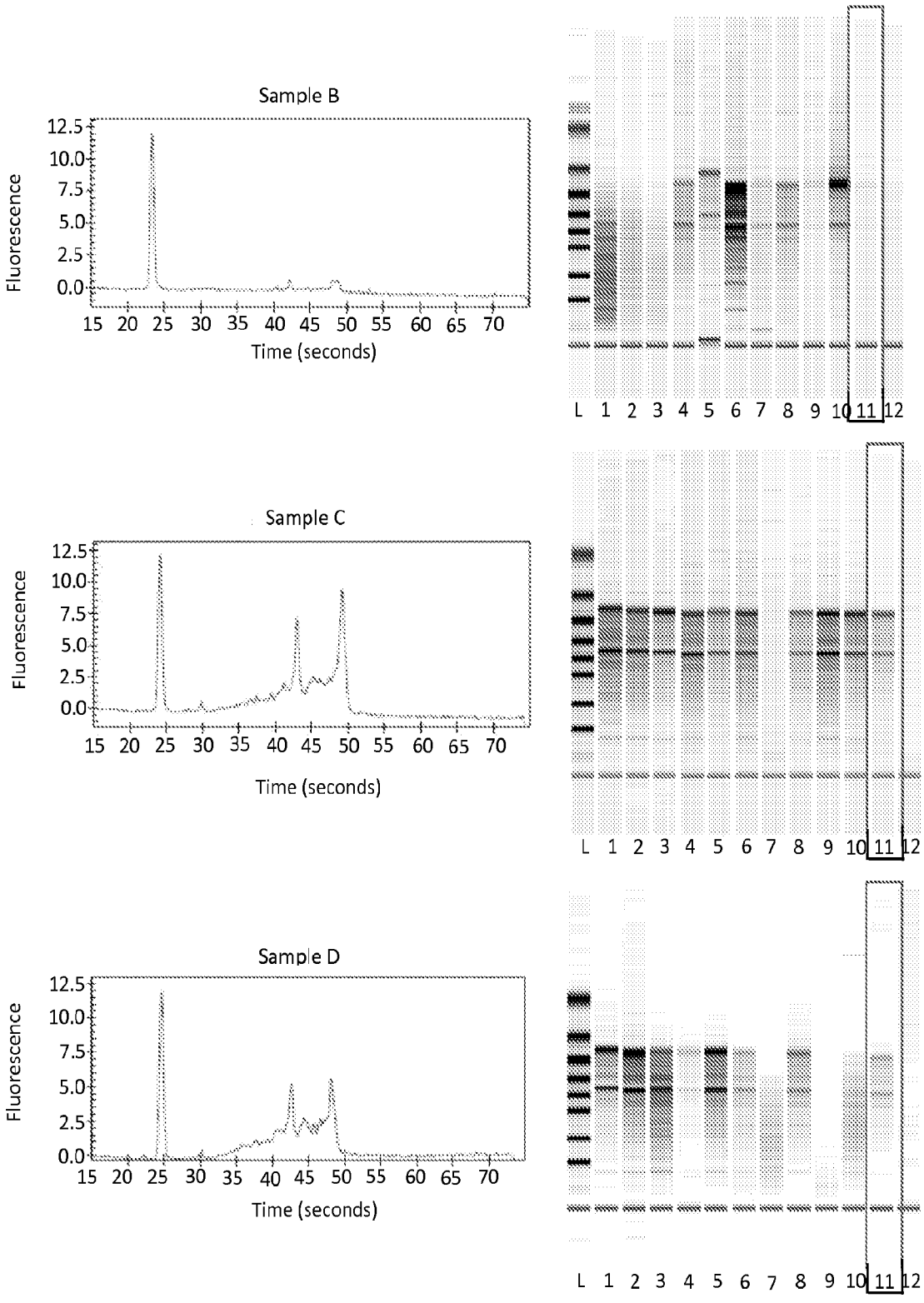
Sample B
Fluorescence
12.5
10.0
7.5
5.0
2.5
0.0
15 20 25 30 35 40 45 50 55 60 65 70
Time (seconds)
L 1 2 3 4 5 6 7 8 9 10 11 12
Sample C
Fluorescence
12.5
10.0
7.5
5.0
2.5
0.0
15 20 25 30 35 40 45 50 55 60 65 70
Time (seconds)
L 1 2 3 4 5 6 7 8 9 10 11 12
Sample D
Fluorescence
12.5
10.0
7.5
5.0
2.5
0.0
15 20 25 30 35 40 45 50 55 60 65 70
Time (seconds)
L 1 2 3 4 5 6 7 8 9 10 11 12

LabChip 90 HT Microcapillary Electrophoresis RNA Quality Data (continued):

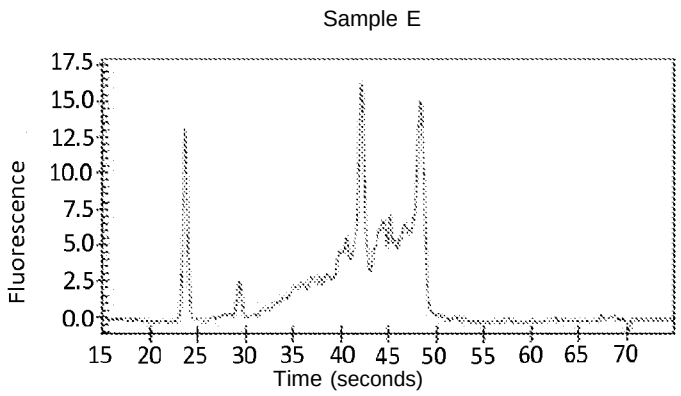

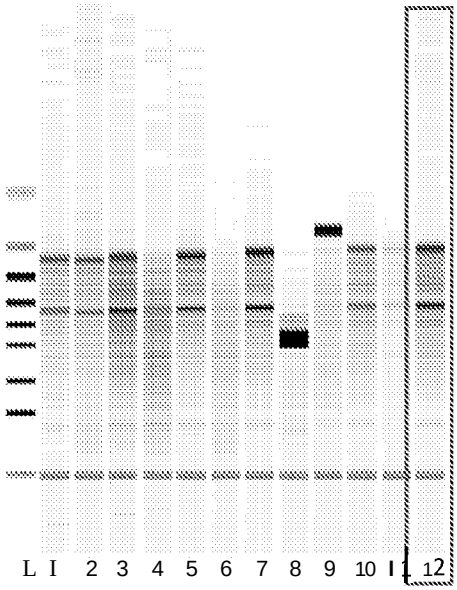

Assay Validation Phase: cDNA Synthesis and Amplification Quality

Nanodrop ND-8000 cDNA Yield Data:

Sample ID	ng/µl	A260	A280	260/280	260/230	Constant	Yield (µg)
A	199.21	6.037	3.115	1.94	1.94	33	5.98
B	161.39	4.891	2.516	1.94	1.88	33	4.84
C	214.14	6.489	3.368	1.93	1.91	33	6.42
D	225.02	6.819	3.535	1.93	1.91	33	6.75
E	210.83	6.389	3.303	1.93	1.91	33	6.32

LabChip 90 HT Microcapillary Electrophoresis cDNAQuality Data:

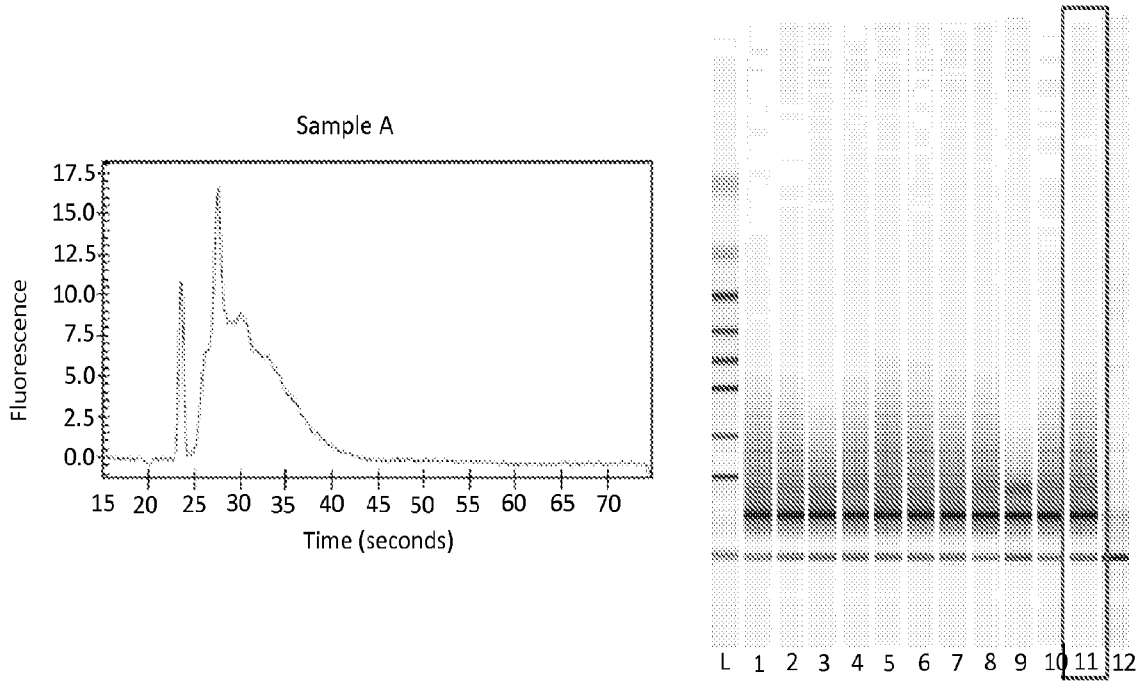

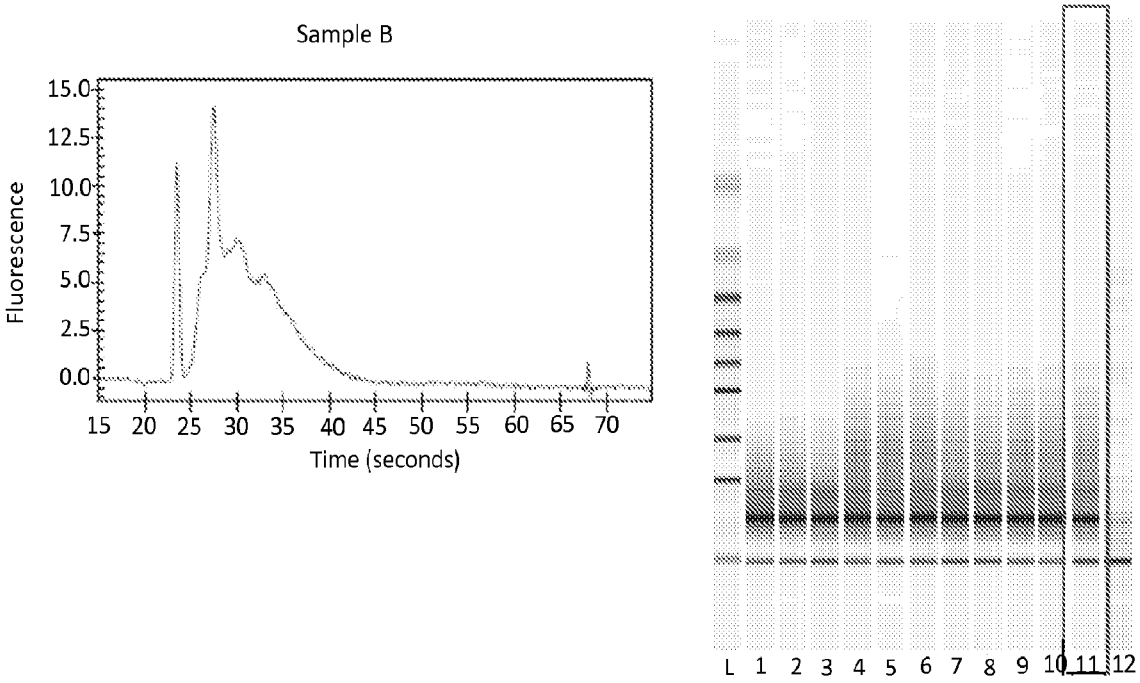

5

LabChip 90 HT Microcapillary Electrophoresis cDNAQuality Data (continued):

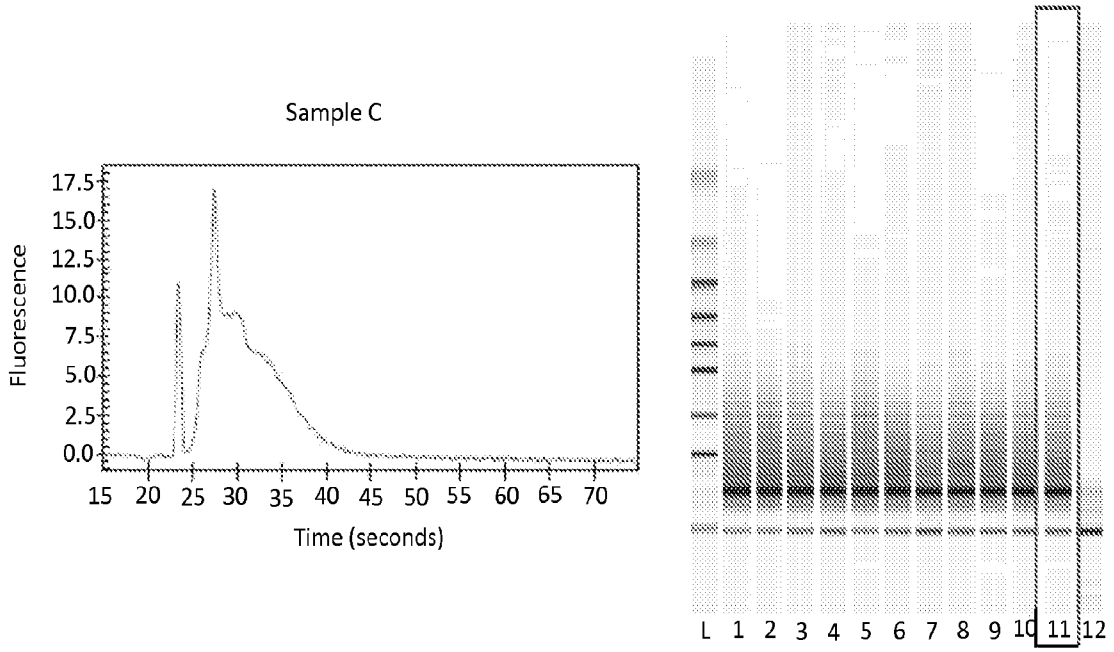

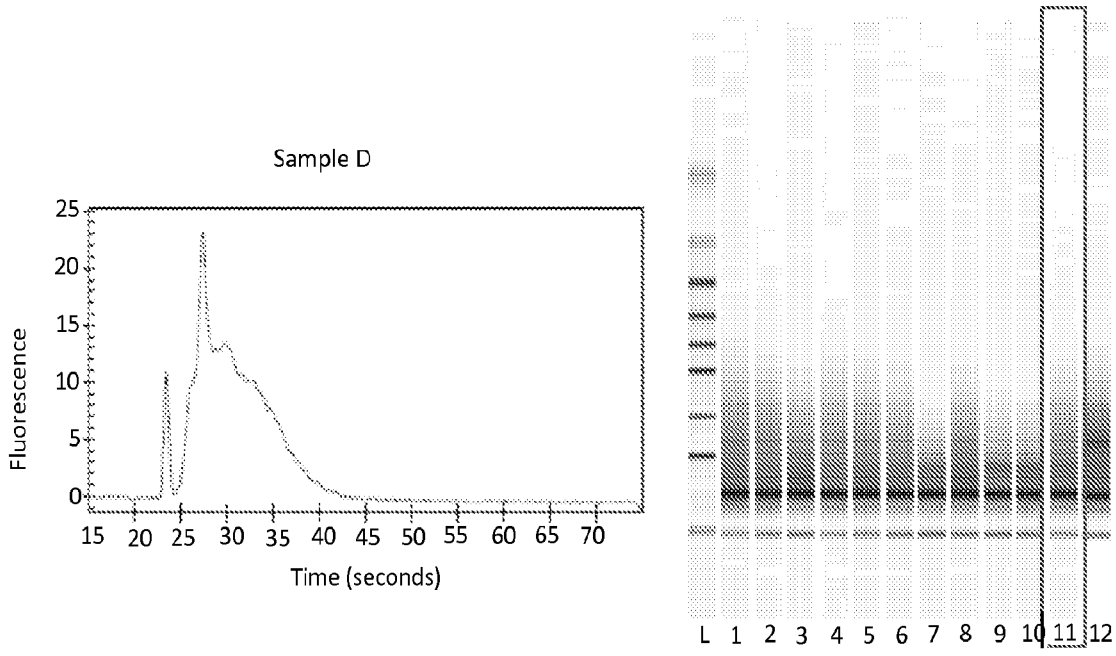

5

LabChip 90 HT Microcapillary Electrophoresis cDNAQuality Data (continued):

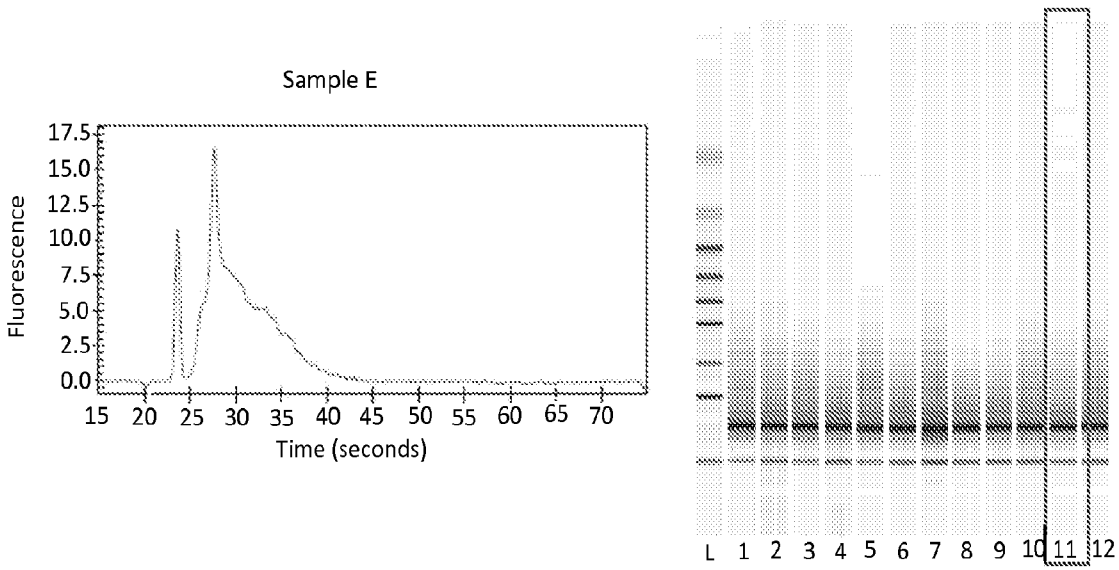

5

APPENDIX V

Assay Validation Phase: qPCR 384-well General Plate Map for Assay Validation qPCR Reactions

- Numbers refer to unique assays
- 'NTC stands for No Template Control; these wells contain only assay master mix but no cDNA sample

	1	2	3	4	5	6	7	8	9	10	11	12	13	14	15	16	17	18	19	20	21	22	23	24
A	1	1	2	2	3	3	4	4	5	5	6	6	7	7	8	8	9	9	10	10	11	11	12	12
B	1	NTC	2	NTC	3	NTC	4	NTC	5	NTC	6	NTC	7	NTC	8	NTC	9	NTC	10	NTC	11	NTC	12	NTC
C	1	1	2	2	3	3	4	4	5	5	6	6	7	7	8	8	9	9	10	10	11	11	12	12
D	1	NTC	2	NTC	3	NTC	4	NTC	5	NTC	6	NTC	7	NTC	8	NTC	9	NTC	10	NTC	11	NTC	12	NTC
E	1	1	2	2	3	3	4	4	5	5	6	6	7	7	8	8	9	9	10	10	11	11	12	12
F	1	NTC	2	NTC	3	NTC	4	NTC	5	NTC	6	NTC	7	NTC	8	NTC	9	NTC	10	NTC	11	NTC	12	NTC
G	1	1	2	2	3	3	4	4	5	5	6	6	7	7	8	8	9	9	10	10	11	11	12	12
H	1	NTC	2	NTC	3	NTC	4	NTC	5	NTC	6	NTC	7	NTC	8	NTC	9	NTC	10	NTC	11	NTC	12	NTC
I	13	13	14	14	15	15	16	16	17	17	18	18	19	19	20	20	21	21	22	22	23	23	24	24
J	13	NTC	14	NTC	15	NTC	16	NTC	17	NTC	18	NTC	19	NTC	20	NTC	21	NTC	22	NTC	23	NTC	24	NTC
K	13	13	14	14	15	15	16	16	17	17	18	18	19	19	20	20	21	21	22	22	23	23	24	24
L	13	NTC	14	NTC	15	NTC	16	NTC	17	NTC	18	NTC	19	NTC	20	NTC	21	NTC	22	NTC	23	NTC	24	NTC
M	13	13	14	14	15	15	16	16	17	17	18	18	19	19	20	20	21	21	22	22	23	23	24	24
N	13	NTC	14	NTC	15	NTC	16	NTC	17	NTC	18	NTC	19	NTC	20	NTC	21	NTC	22	NTC	23	NTC	24	NTC
O	13	13	14	14	15	15	16	16	17	17	18	18	19	19	20	20	21	21	22	22	23	23	24	24
P	13	NTC	14	NTC	15	NTC	16	NTC	17	NTC	18	NTC	19	NTC	20	NTC	21	NTC	22	NTC	23	NTC	24	NTC

APPENDIX VI

Assay Validation Phase: Expression Data and Descriptive Statistics

- Average C_T is the average of three technical replicates
- Overall Average C_T is the average of three technical replicates of all four samples
- 'Undet.' indicates that the C_T value was undetermined for that sample

Detector	Threshold	Avg C_T A	StDev A	Avg C_T E	StDev E	Avg C_T C	StDev C	Avg C_T D	StDev D	Overall Avg C_T	Overall StDev
ACTB_L	0.042	24	0.2	23.9	0.16	24.24	0.43	23.63	0.21	23.94	0.33
ACTB_R	0.062	21.18	0.17	21.22	0.07	20.91	0.1	20.91	0.07	21.05	0.18
ACTR2_L	0.091	22.72	0.16	22.68	0.1	22.76	0.23	22.72	0.34	22.72	0.19
ACTR2_M	0.082	25.84	0.14	25.63	0.07	25.52	0.14	25.4	0.14	25.6	0.2
ACTR2_R	0.066	23.27	0.23	22.99	0.06	23.13	0.08	23.28	0.15	23.17	0.17
ADAR_L	0.042	25.42	0.62	25.5	0.1	25.56	0.26	25.94	0.1	25.6	0.36
ADAR_M	0.042	24.38	0.24	24.9	0.04	23.81	0.17	24.57	0.1	24.41	0.43
ADAR_R	0.03	25.84	0.31	26.21	0.09	26.09	0.22	26.08	0.11	26.06	0.22
ADD1_L	0.035	29.52	0.22	29.72	0.18	29.18	0.48	29.31	0.15	29.43	0.33
ADD1_M	0.044	27.05	0.03	26.3	0.11	26.71	0.1	27.1	0.05	26.79	0.34
ADD1_R	0.09	26.18	0.21	25.05	0.17	25.12	0.19	25.35	0.26	25.43	0.51
ADD3_L	0.056	28.41	0.2	28.94	0.1	28.36	0.12	28.38	0.12	28.52	0.28
ADD3_M	0.088	27.49	0.14	27.92	0.13	27.23	0.11	27.45	0.21	27.52	0.29
ADD3_R	0.047	24.2	0.14	24.06	0.05	24.15	0.03	24.28	0.18	24.17	0.13
AIM1_L	0.043	30.55	0.3	29.47	0.17	30.39	0.07	30.93	0.06	30.33	0.58
AIM1_M	0.091	30.69	0.14	30.25	0.22	30.15	0.24	30.7	0.23	30.45	0.32
AIM1_R	0.132	26.05	0.08	25.74	0.18	25.76	0.08	25.91	0.21	25.87	0.18
ARPC5_L	0.063	22.06	0.54	22.2	0.16	21.85	0.11	21.86	0.05	21.99	0.29
ARPC5_M	0.077	21.25	0.1	21.2	0.02	20.74	0.1	20.62	0.16	20.95	0.3
ARPC5_R	0.057	22.39	0.41	22.17	0.16	21.7	0.15	21.57	0.17	21.96	0.41
BACH2_L	0.091	36.88	0.88	34.1	0.21	33.06	0.25	33.75	0.47	34.45	1.58
BACH2_M	0.035	Undet.	Undet.	27.64	0.17	27.54	0.28	26.92	0.2	27.36	0.39
BACH2_R	0.053	31.36	0.25	30.01	0.14	31.82	0.16	30.5	0.53	30.93	0.79

Clorf38_L	0.067	27.51	0.4	27.46	0.16	27.22	0.02	27.76	0.16	27.49	0.28
Clorf38_M	0.071	28.85	0.06	27.89	0.13	28.02	0.05	28.69	0.19	28.36	0.44
Clorf38_R	0.08	35.5	1.08	31.88	0.44	32	0.4	31.9	0.1	32.82	1.7
CAPN2_L	0.086	28.17	0.07	27.95	0.1	28.69	0.19	27.34	0.05	28.04	0.51
CAPN2_M	0.088	24.1	0.19	23.74	0.1	23.77	0.12	23.89	0.16	23.88	0.19
CAPN2_R	0.093	25.12	0.1	25.06	0.14	25.11	0.08	25.32	0.13	25.15	0.14
CD163_L	0.019	30.25	0.49	30.01	0.07	30.2	0.19	30.19	0.16	30.16	0.26
CD163_M	0.046	28.2	0.61	28.91	0.87	28.64	0.35	28.06	0.09	28.45	0.6
CD163_R	0.082	27.76	0.05	27.71	0.1	27.97	0.02	27.86	0.08	27.83	0.12
CD27_L	0.032	28.74	0.17	28.73	0.21	30.11	0.11	29.14	0.25	29.18	0.61
CD27_M	0.028	31.83	0.06	32.55	0.26	31.96	0.27	32.81	0.07	32.29	0.45
CD27_R	0.05	30.1	0.13	30.03	0.37	30.66	0.33	30.72	0.12	30.38	0.4
CD300CJ.	0.031	32.8	0.26	32.61	0.13	34.07	0.39	31.06	0.21	32.63	1.14
CD300C_M	0.083	30.52	0.2	29.52	0.11	31.47	0.26	30.09	0.25	30.4	0.77
CD300C_R	0.066	30	0.39	30.03	0.33	31.18	0.34	29.69	0.11	30.23	0.65
CD53_L	0.022	23.2	0.28	23.35	0.59	23.6	0.65	23.27	0.3	23.36	0.44
CD53_M	0.061	24.94	0.21	24.71	0.12	24.85	0.22	24.69	0.13	24.8	0.19
CD53_R	0.023	26.16	0.21	25.93	0.41	25.88	0.25	25.63	0.29	25.9	0.33
CD68_L	0.04	22.1	0.09	21.45	0.04	21.89	0.18	21.58	0.08	21.75	0.28
CD68_M	0.059	27.48	0.2	27.34	0.69	27.15	0.23	28.61	0.23	27.65	0.69
CD68_R	0.132	26.55	0.08	25.54	0.07	26.09	0.12	25.95	0.2	26.03	0.39
CD83_L	0.036	Undet.	Undet.	36.28	0.41	37.07	Undet.	36.94	1.05	36.63	0.66
CD83_M	0.061	33.21	0.22	34.6	0.97	36.34	2.97	37.32	Undet.	34.82	1.92
CD83_R	0.095	30.81	0.34	29.83	0.15	30.34	0.17	31.5	0.17	30.62	0.67
CDC42SE1J.	0.04	29.85	0.19	30.36	0.16	31.55	0.47	31.67	0.49	30.86	0.86
CDC42SE1_M	0.076	24.79	0.12	24.95	0.3	24.42	0.22	24.68	0.16	24.71	0.27
CDC42SE1_R	0.058	24.34	0.05	24.09	0.3	23.97	0.09	23.51	0.18	23.98	0.35
CSF3R_L	0.028	26.03	0.18	26.58	0.51	25.76	0.63	25.92	0.31	26.1	0.47

CSF3R_M	0.06	28.29	0.08	28.59	0.15	27.67	0.13	28.03	0.09	28.15	0.37
CSF3R_R	0.056	24.39	0.23	24.65	0.31	24.38	0.24	24.51	0.17	24.48	0.24
DDX58_L	0.062	27.34	0.58	28.48	0.2	27.41	0.07	27.82	0.18	27.76	0.55
DDX58_M	0.04	26.45	0.9	26.3	0.09	25.88	0.32	26.28	0.25	26.23	0.48
DDX58_R	0.056	27.79	0.1	27.63	0.08	27.4	0.19	28.35	0.33	27.8	0.41
EEF2_L	0.01	28.23	0.84	27.96	Undet.	28.62	0.08	28.59	0.28	28.43	0.43
EEF2_M	0.062	24.29	0.1	24.13	0.14	24.15	0.34	24.28	0.07	24.21	0.18
EEF2_R	0.026	25.61	0.14	25.73	0.34	25.25	0.23	25.9	0.28	25.62	0.33
F13A1_L	0.06	27.91	0.11	27.31	0.14	26.29	0.09	26.96	0.12	27.12	0.62
F13A1_M	0.077	26.95	0.26	26.47	0.09	25.29	0.08	26.42	0.12	26.28	0.65
F13A1_R	0.085	27.85	0.15	26.89	0.16	26.01	0.11	27.52	0.23	27.07	0.75
FCN1_L	0.134	25.52	0.13	24.63	0.26	25.01	0.4	25.33	0.09	25.12	0.41
FCN1_M	0.054	29.98	0.33	23.7	0.42	23.81	0.49	24.68	0.14	25.54	2.72
FCN1_R	0.051	25.08	0.07	24.47	0.11	24.67	0.11	25.03	0.07	24.81	0.28
GAPDH_L	0.08	24.43	0.12	24.55	0.13	25.37	0.09	25.07	0.18	24.86	0.42
GAPDH_R	0.122	27.22	0.19	26.7	0.2	26.81	0.22	27.16	0.23	26.97	0.29
GZMB_L	0.006	28.71	Undet.	30.31	0.53	29.97	Undet.	29.06	0.24	29.68	0.77
GZMB_M	0.06	33.12	0.92	26.79	0.14	25.95	0.24	26.24	0.13	28.02	3.11
GZMB_R	0.06	26.7	0.1	25.74	0.22	26.19	0.2	25.73	0.04	26.09	0.44
IL10RB_L	0.056	30.73	0.07	30.23	0.17	29.77	0.17	30.35	0.07	30.27	0.37
IL10RB_M	0.055	31.71	0.43	30.91	0.26	31.04	0.11	30.57	0.3	31.06	0.5
IL10RB_R	0.053	29.69	0.15	29.33	0.09	29.18	0.11	28.96	0.09	29.29	0.29
IL15RA_L	0.031	37.37	Undet.	34.24	0.12	35.93	0.86	34.67	0.26	35.19	1.13
IL15RA_M	0.104	30.26	0.13	28.23	0.18	29.76	0.24	29.29	0.31	29.39	0.81
IL15RA_R	0.01	35.18	0.53	36.73	1.36	36.08	0.37	34.81	0.48	35.75	1.06
IL6R_L	0.066	33.22	0.29	34.2	0.22	33.69	0.38	33.91	0.33	33.75	0.46
IL6R_M	0.041	28.03	0.42	28.57	0.17	28.34	0.02	27.54	0.28	28.1	0.48
IL6R_R	0.076	25.43	0.19	25.48	0.09	25.42	0.02	25.58	0.22	25.48	0.15

IL7R_L	0.022	26.88	0.16	Undet.	Undet.	27.26	0.2	Undet.	Undet.	27.07	0.26
IL7R_M	0.06	28.11	1.02	28.96	0.11	28.82	0.13	28.92	0.08	28.7	0.57
IL7R_R	0.033	25.03	0.23	26.06	0.07	25.62	0.4	26.28	0.03	25.75	0.54
ITGB2_L	0.061	25.49	0.22	25.25	0.11	25.48	0.09	25.3	0.11	25.38	0.17
ITGB2_M	0.042	25.97	0.45	25.81	0.32	26.18	0.29	26.25	0.3	26.05	0.35
ITGB2_R	0.018	26.96	0.35	26.6	0.28	26.86	0.27	27.34	0.57	26.94	0.43
IVNS1ABP_L	0.069	27.76	0.19	27.56	0.29	26.79	0.07	27.15	0.19	27.32	0.43
IVNS1ABP_M	0.029	27.82	0.62	27.43	0.66	28.16	0.23	27.58	0	27.75	0.49
IVNS1ABP_R	0.035	27.12	0.13	27.55	0.1	26.72	0.32	26.75	0.18	27.04	0.39
KLRF1_L	0.03	34.22	0.29	32.9	0.18	32.51	0.23	32.89	0.24	33.13	0.71
KLRF1_M	0.021	34.32	0.51	34.07	0.62	35.22	2.32	34.41	0.3	34.44	0.92
KLRF1_R	0.05	33.06	0.28	33.5	0.37	33.64	0.06	34.94	0.45	33.78	0.79
LASP1_L	0.062	25.45	0.23	24.98	0.08	25.45	0.08	24.91	0.15	25.2	0.29
LASP1_M	0.059	25.62	0.26	25.31	0.15	24.89	0.15	24.82	0.09	25.16	0.37
LASP1_R	0.067	27.69	0.22	27.22	0.09	26.85	0.04	26.97	0.04	27.18	0.36
LCP1_L	0.015	21.57	0.33	21.54	0.37	21.63	0.16	21.17	0.36	21.5	0.32
LCP1_M	0.0S8	20.78	0.22	20.32	0.17	20.94	0.05	20.52	0.13	20.64	0.28
LCP1_R	0.033	25.34	0.21	25.06	0.24	25.1	0.57	25.08	0.11	25.14	0.3
LILRA5_L	0.025	31.01	0.24	30.99	0.08	32.35	0.25	30.95	0.07	31.33	0.64
LILRA5_M	0.112	29.65	0.29	29.39	0.25	31.21	0.11	30.2	0.33	30.11	0.76
LILRA5_R	0.067	28.1	0.05	27.59	0.2	29.03	0.19	27.68	0.17	28.1	0.61
LPXN_L	0.038	31.96	0.17	31.18	0.3	31.89	0.36	31.51	0.27	31.64	0.4
LPXN_M	0.08	29.41	0.14	29.76	0.2	29.76	0.07	29.57	0.06	29.63	0.19
LPXN_R	0.068	32.11	0.15	32.09	0.25	32.48	0.22	31.69	0.44	32.09	0.38
LTF_L	0.022	36.81	0.62	37.05	0.47	35.13	0.2	34.3	0.23	35.73	1.26
LTF_M	0.037	28.75	0.09	27.63	0.03	27.73	0.11	29.08	0.07	28.3	0.66
LTF_R	0.08	27.4	0.15	25.74	0.09	26.25	0.06	26.95	0.11	26.59	0.67
LY75_L	0.024	31.12	0.22	31.33	0.29	32.26	0.33	30.8	0.21	31.38	0.61
LY75_M	0.029	29.13	0.09	29.32	0.18	28.7	0.58	28.87	0.17	29.01	0.37

LY75_R	**0.069**	**29.27**	**0.29**	**30.01**	**0.3**	**29.29**	**0.23**	**28.64**	**0.19**	**29.3**	**0.55**
NCF1_L	**0.061**	**24.76**	**0.51**	**24.93**	**0.13**	**24.38**	**0.06**	**24.39**	**0.19**	**24.62**	**0.35**
NCF1_M	**0.063**	**26.14**	**0.02**	**26.2**	**0.26**	**25.21**	**0.28**	**25.44**	**0.17**	**25.75**	**0.48**
NCF1_R	**0.064**	**23.91**	**0.04**	**24.06**	**0.15**	**23.69**	**0.24**	**23.74**	**0.22**	**23.85**	**0.22**
NCF2_L	**0.059**	**24.44**	**0.1**	**24.81**	**0.15**	**24.4**	**0.1**	**24.24**	**0.12**	**24.47**	**0.24**
NCF2_M	**0.093**	**23.09**	**0.17**	**23.54**	**0.19**	**23.45**	**0.1**	**23.27**	**0.17**	**23.34**	**0.23**
NCF2_R	**0.042**	**24.63**	**0.1**	**24.88**	**0.08**	**24.66**	**0.04**	**24.52**	**0.22**	**24.67**	**0.17**
NCF4J.	**0.052**	**27.47**	**0.38**	**28.01**	**0.1**	**27.61**	**0.04**	**27.35**	**0.13**	**27.61**	**0.31**
NCF4_M	**0.075**	**26.74**	**0.2**	**26.76**	**0.11**	**27.05**	**0.16**	**27.02**	**0.2**	**26.89**	**0.21**
NCF4_R	**0.147**	**31.07**	**0.18**	**31.03**	**0.26**	**32.49**	**0.37**	**31.71**	**0.08**	**31.58**	**0.65**
NCL_L	**0.057**	**25.74**	**0.15**	**25.55**	**0.19**	**25.82**	**0.15**	**26.23**	**0.08**	**25.84**	**0.29**
NCL_M	**0.03**	**24.31**	**0.11**	**23.83**	**0.2**	**24.39**	**0.22**	**24.41**	**0.12**	**24.24**	**0.29**
NCL_R	**0.059**	**23.42**	**0.16**	**23.46**	**0.21**	**23.19**	**0.11**	**23.47**	**0.01**	**23.39**	**0.17**
NCOAl_L	**0.049**	**25.09**	**0.35**	**24.7**	**0.14**	**24.37**	**0.22**	**24.64**	**0.15**	**24.7**	**0.33**
NCOAl_M	**0.058**	**24.79**	**0.16**	**25.08**	**0.09**	**24.61**	**0.1**	**24.49**	**0.14**	**24.74**	**0.26**
NCOAl_R	**0.096**	**27.8**	**0.2**	**28.47**	**0.06**	**28.04**	**0.11**	**27.9**	**0.1**	**28.05**	**0.29**
NLRP1_L	**0.06**	**26.98**	**0.13**	**27.55**	**0.23**	**27.16**	**0.33**	**27.05**	**0.09**	**27.19**	**0.3**
NLRP1_M	**0.129**	**28.39**	**0.21**	**28.58**	**0.23**	**28.25**	**0.11**	**28.5**	**0.18**	**28.43**	**0.21**
NLRP1_R	**0.032**	**28.86**	**0.11**	**29.05**	**0.21**	**28.96**	**0.25**	**28.57**	**0.23**	**28.86**	**0.26**
OAS2_L	**0.132**	**29.98**	**0.09**	**30.12**	**0.13**	**30.02**	**0.09**	**29.76**	**0.15**	**29.97**	**0.17**
OAS2_M	**0.051**	**27.4**	**0.14**	**26.76**	**0.08**	**27.4**	**0.1**	**27.34**	**0.15**	**27.23**	**0.3**
OAS2_R	**0.096**	**27.06**	**0.14**	**26.86**	**0.11**	**27.24**	**0.16**	**27.14**	**0.24**	**27.08**	**0.2**
OAS3_L	**0.068**	**29.73**	**0.2**	**31.92**	**0.14**	**34.05**	**0.87**	**31.36**	**0.1**	**31.77**	**1.66**
OAS3_M	**0.059**	**29.46**	**0.17**	**28.16**	**0.04**	**29.42**	**0.2**	**28.41**	**0.2**	**28.86**	**0.63**
OAS3_R	**0.08**	**28.09**	**0.22**	**29.69**	**0.22**	**29.04**	**0.13**	**28.94**	**0.06**	**28.94**	**0.61**
PDLIM1_L	**0.079**	**33.66**	**0.42**	**32.15**	**0.16**	**31.19**	**0.21**	**30.83**	**0.26**	**31.95**	**1.17**
PDLIM1_M	**0.093**	**28.86**	**0.33**	**28.01**	**0.19**	**27.86**	**0.06**	**28.06**	**0.15**	**28.2**	**0.45**
PDLIM1_R	**0.037**	**27.9**	**0.16**	**28.97**	**0.29**	**28.1**	**0.18**	**29.01**	**0.19**	**28.5**	**0.55**
PDLIM2_L	**0.041**	**30.35**	**0.07**	**31.38**	**0.62**	**30.44**	**0.24**	**30.85**	**0.2**	**30.75**	**0.52**
PDLIM2_M	**0.034**	**32.18**	**0.17**	**31.72**	**0.11**	**32.13**	**0.19**	**32.47**	**0.36**	**32.12**	**0.34**

PDLIM2_R	0.012	Undet.	Undet.	Undet.	Undet.	38.02	Undet.	Undet.	Undet.	38.02	Undet.
RAF1_L	0.047	30.25	0.11	29.6	0.2	29.67	0.15	29.62	0.23	29.79	0.32
RAF1_M	0.067	30.28	0.16	30.76	0.11	30.62	0.39	30.23	0.03	30.47	0.3
RAF1_R	0.082	27.46	0.04	27.02	0.07	26.97	0.11	26.69	0.1	27.03	0.29
ROCK2_L	0.038	23.79	0.1	23.8	0.2	23.88	0.28	23.77	0.12	23.81	0.17
ROCK2_M	0.013	31.41	0.25	30.43	0.09	30.37	0.46	31.01	0.18	30.81	0.51
ROCK2_R	0.083	30.54	0.15	29.61	0.1	30.95	0.11	30.98	0.25	30.52	0.59
SELL_L	0.045	23.28	0.2	24.06	0.11	23.8	0.12	22.65	0.26	23.45	0.59
SELL_M	0.17	24.4	0.16	24.58	0.27	24.99	0.14	23.96	0.08	24.48	0.41
SELL_R	0.039	26.91	0.14	27.37	0.17	27.33	0.39	26.68	0.1	27.05	0.36
SELP_L	0.104	35.34	0.55	30.57	0.07	28.75	0.03	30.61	0.15	31.32	2.56
SELP_M	0.072	33.18	0.3	30.78	0.23	31.87	0.17	32.78	0.9	32.15	1.05
SELP_R	0.027	Undet.	Undet.	35.1	0.38	33.06	0.43	37.31	0.07	35.16	1.86
SERPINA1_L	0.064	25.82	0.25	24.34	0.02	23.83	0.15	24.52	0.16	24.63	0.78
SERPINA1_M	0.03	26.43	0.49	24.44	0.22	24.66	0.2	25.34	0.23	25.22	0.85
SERPINA1_R	0.112	22.34	0.05	21.23	1.08	21.97	0.16	22.58	0.16	22.03	0.71
S0RL1_L	0.093	24.57	0.15	24.68	0.12	24.96	0.07	24.48	0.16	24.67	0.22
S0RL1_M	0.075	26.1	0.22	26.36	0.02	25.87	0.19	25.93	0.19	26.09	0.24
S0RL1_R	0.086	23.63	0.17	23.59	0.07	23.68	0.2	23.44	0.19	23.58	0.17
STAT6_L	0.08	24.4	0.04	24.27	0.25	24.39	0.29	24.2	0.1	24.32	0.19
STAT6_M	0.082	25.79	0.16	25.68	0.14	25.43	0.11	25.38	0.15	25.57	0.21
STAT6_R	0.05	27.44	0.06	28.55	0.43	27.94	0.28	27.98	0.21	27.98	0.47
STX4_L	0.072	25.77	0.25	25.22	0.11	25.69	0.08	25.71	0.21	25.6	0.28
STX4_M	0.076	29.93	0.18	29.66	0.38	32.2	0.46	29.9	0.22	30.42	1.12
STX4_R	0.082	29.09	0.16	28.54	0.21	28.76	0.08	28.55	0.12	28.74	0.26
SYNE2_L	0.06	28.25	0.36	28.18	0.22	28.98	0.13	27.76	0.1	28.29	0.5
SYNE2_M	0.057	25.26	0.27	25.63	0.12	25.57	0.17	25.5	0.09	25.49	0.21
SYNE2_R	0.062	33.43	1.08	32.01	0.08	31.27	0.09	33.01	0.34	32.43	1.01

TES_L	0.098	24.37	0.12	24.81	0.17	23.76	0.2	23.97	0.21	24.23	0.45
TES_M	0.095	28.53	0.06	28.77	0.17	28.96	0.02	28.19	0.05	28.61	0.31
TES_R	0.041	28.15	0.07	28.32	0.14	28.33	0.22	27.97	0.18	28.19	0.21
TREM1_L	0.053	29.88	0.1	29.54	0.03	29.54	0.16	29.57	0.24	29.63	0.2
TREM1_M	0.076	27.95	0.24	26.87	0.06	27.35	0.16	28.22	0.12	27.6	0.56
TREM1_R	0.05	26.72	0.01	26.38	0.12	26.72	0.13	27.21	0.18	26.76	0.33
TRPM2_L	0.069	30.54	0.16	35.71	0.59	35.65	0.98	31.57	0.3	33.37	2.5
TRPM2_M	0.075	34.13	0.92	32.99	0.51	33.32	0.14	34.05	0.69	33.62	0.74
TRPM2_R	0.091	35.71	Undet.	37.02	1.16	33.16	0.49	33.83	0.31	34.77	1.82
TXNIP_L	0.086	20.51	0.07	20.32	0.1	20.15	0.2	19.81	0.12	20.2	0.29
TXNIP_M	0.057	21.78	0.04	21.78	0.23	21.63	0.21	21.37	0.21	21.64	0.24
TXNIP_R	0.11	23.83	0.15	23.94	0.13	23.62	0.13	23.59	0.18	23.75	0.2
VIM_L	0.057	35.4	0.28	37.37	0.98	35.47	0.21	37.63	0.84	36.39	1.17
VIM_M	0.051	25.59	0.12	25.56	0.19	25.88	0.36	25.96	0.12	25.75	0.26
VIM_R	0.056	23.23	0.12	23.03	0.02	23.28	0.15	23.45	0.16	23.24	0.19
ZAP70_L	0.054	37.11	1.17	36.46	0.94	36.35	0.1	36.41	0.89	36.56	0.76
ZAP70_M	0.106	31.13	0.11	31.28	0.24	31.43	0.18	31.48	0.01	31.33	0.2
ZAP70_R	0.091	30.35	0.05	30.92	0.3	29.93	0.33	30.51	0.25	30.42	0.43

APPENDIX VII

Assay Validation Histograms: Sample Average and Overall Average C_T Values of Regional Assays

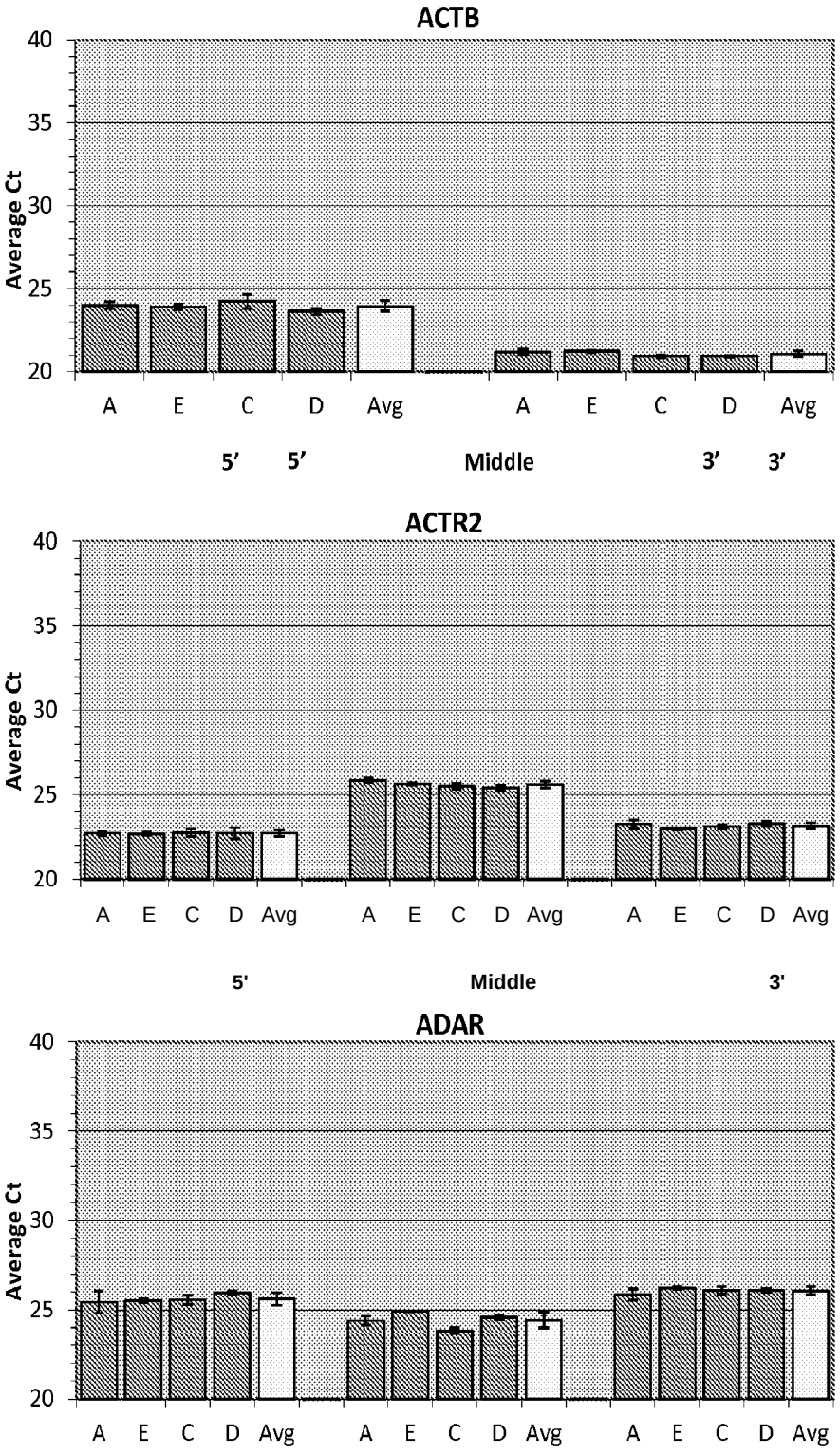

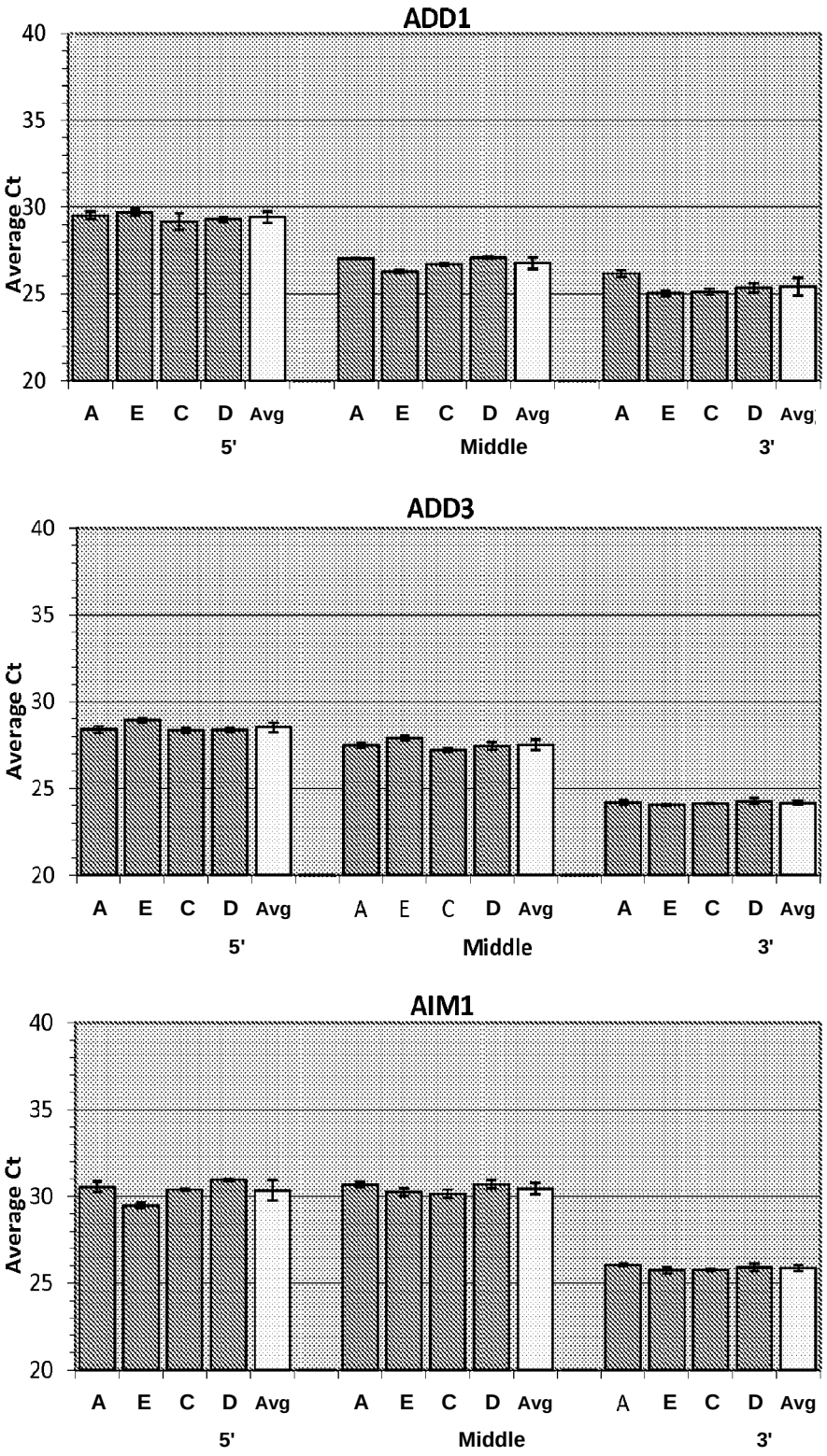
ADD1
Average Ct
40
35
30
25
20
A E C D Avg A E C D Avg A E C D Avg
5' Middle 3'
ADD3
Average Ct
40
35
30
25
20
A E C D Avg A E C D Avg A E C D Avg
5' Middle 3'
AIM1
Average Ct
40
35
30
25
20
A E C D Avg A E C D Avg A E C D Avg
5' Middle 3'

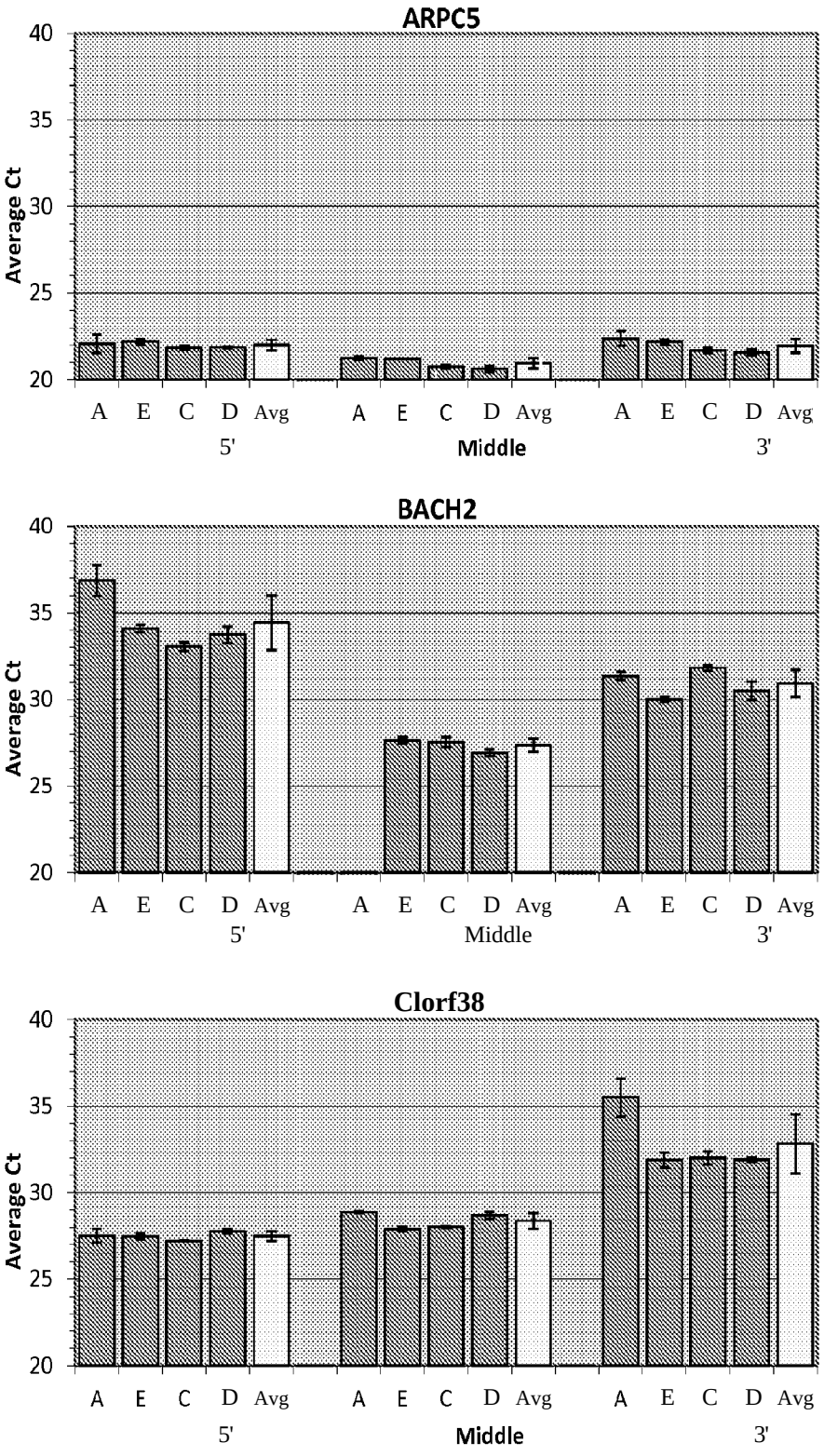
ARPC5
Average Ct
40
35
30
25
20
A E C D Avg A E C D Avg A E C D Avg
5' Middle 3'
BACH2
Average Ct
40
35
30
25
20
A E C D Avg A E C D Avg A E C D Avg
5' Middle 3'
Clorf38
Average Ct
40
35
30
25
20
A E C D Avg A E C D Avg A E C D Avg
5' Middle 3'

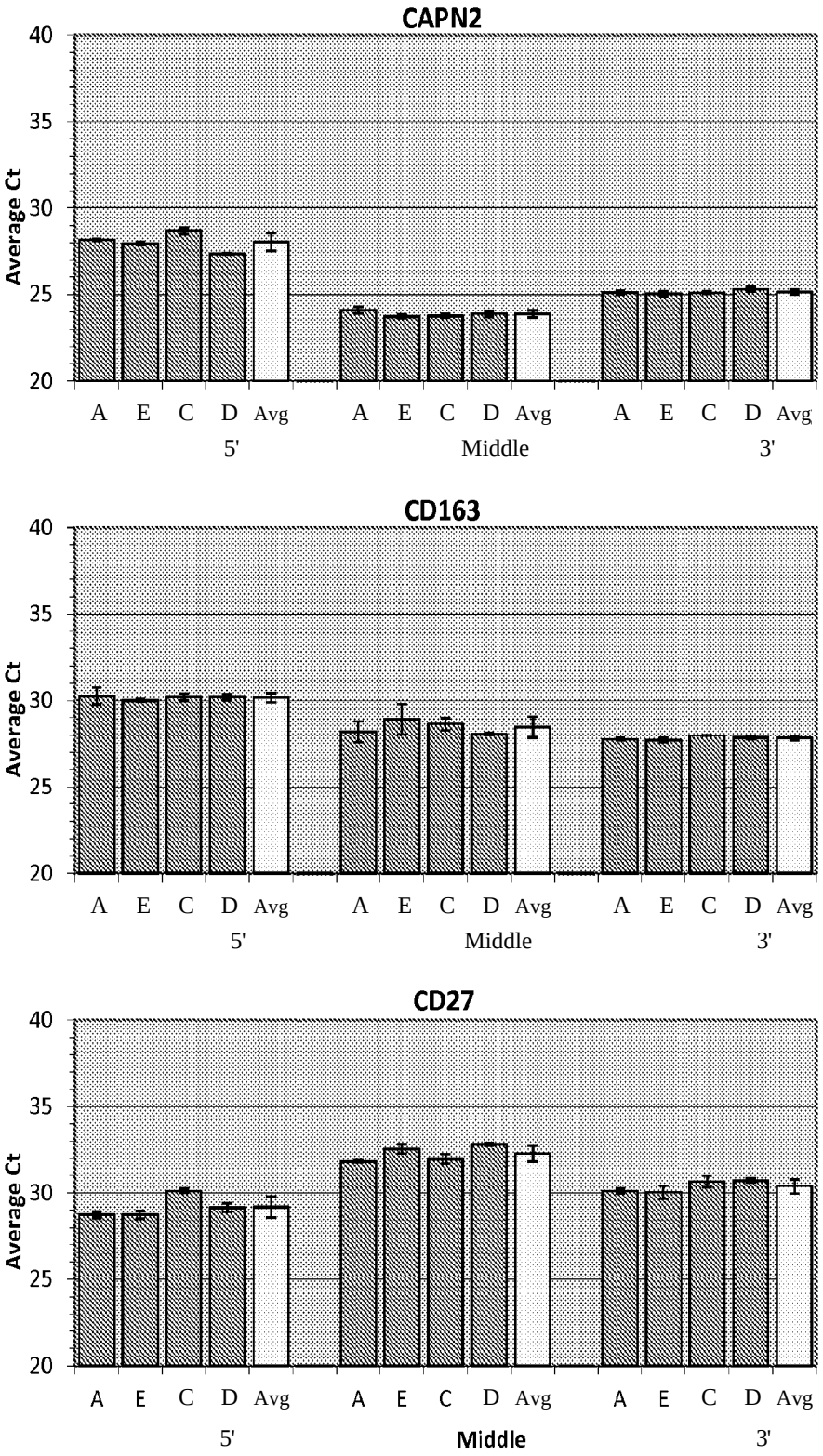
CAPN2
Average Ct
40
35
30
25
20
A E C D Avg A E C D Avg A E C D Avg
5' Middle 3'
CD163
Average Ct
40
35
30
25
20
A E C D Avg A E C D Avg A E C D Avg
5' Middle 3'
CD27
Average Ct
40
35
30
25
20
A E C D Avg A E C D Avg A E C D Avg
5' Middle 3'

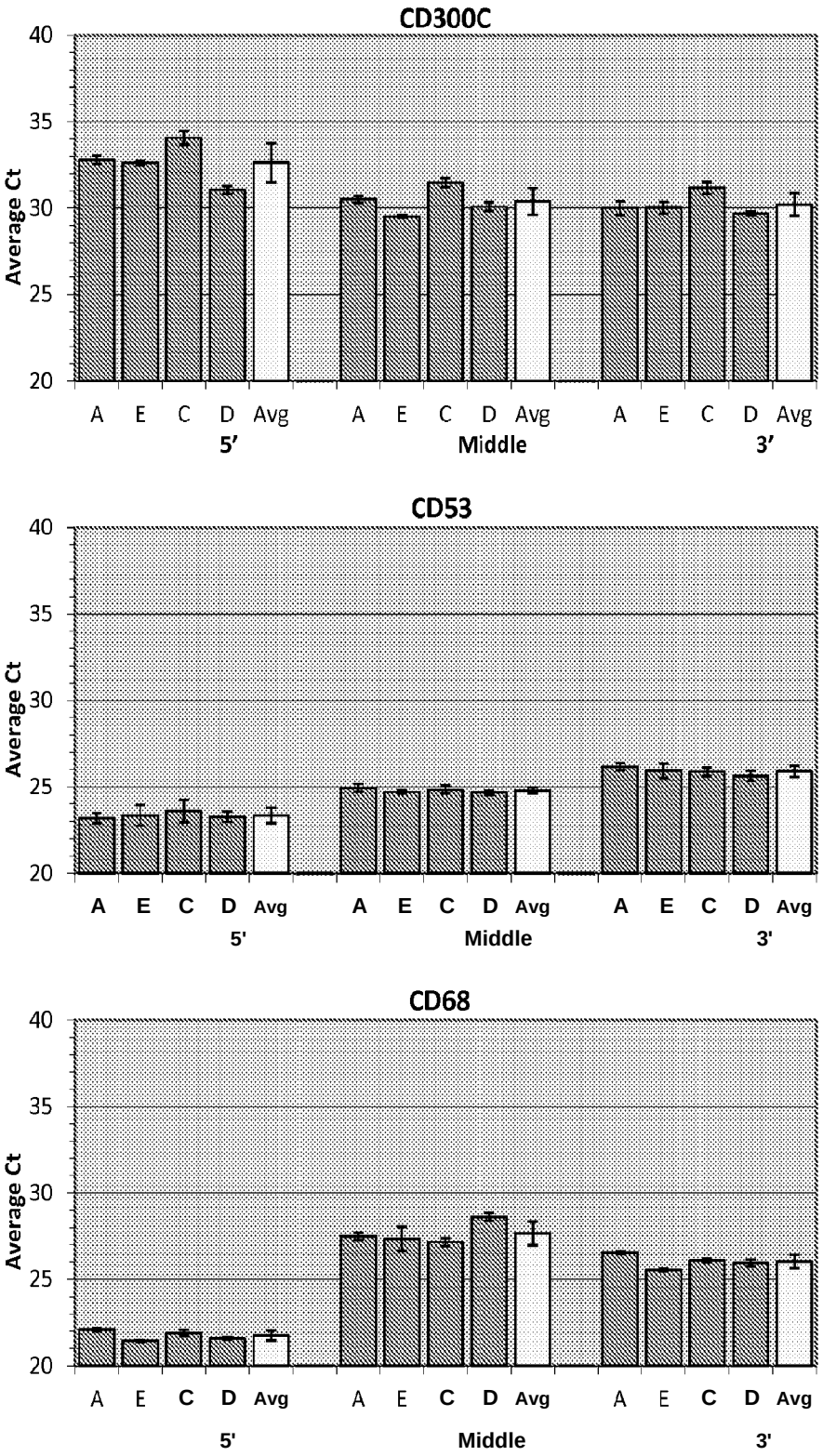
CD300C
Average Ct
40
35
30
25
20
A E C D Avg A E C D Avg A E C D Avg
5′
Middle
3′
CD53
Average Ct
40
35
30
25
20
A E C D Avg A E C D Avg A E C D Avg
5'
Middle
3'
CD68
Average Ct
40
35
30
25
20
A E C D Avg A E C D Avg A E C D Avg
5'
Middle
3'

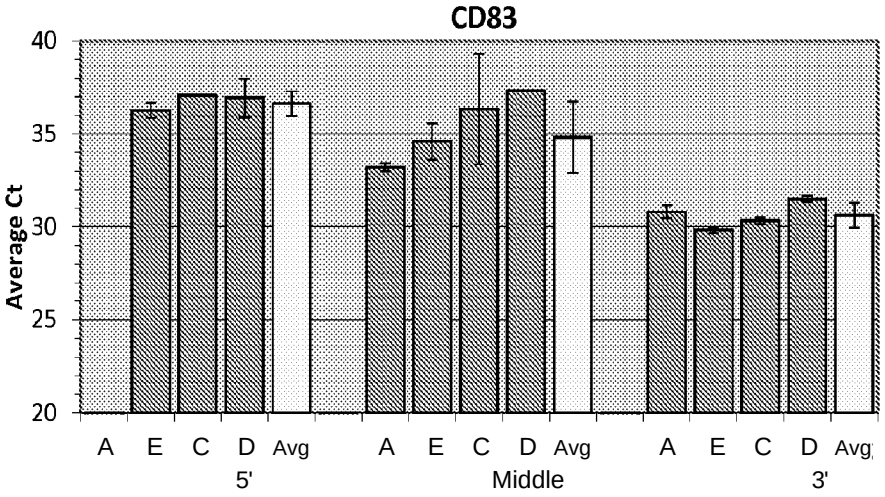
CD83
Average Ct
40
35
30
25
20
A E C D Avg A E C D Avg A E C D Avg
5' Middle 3'

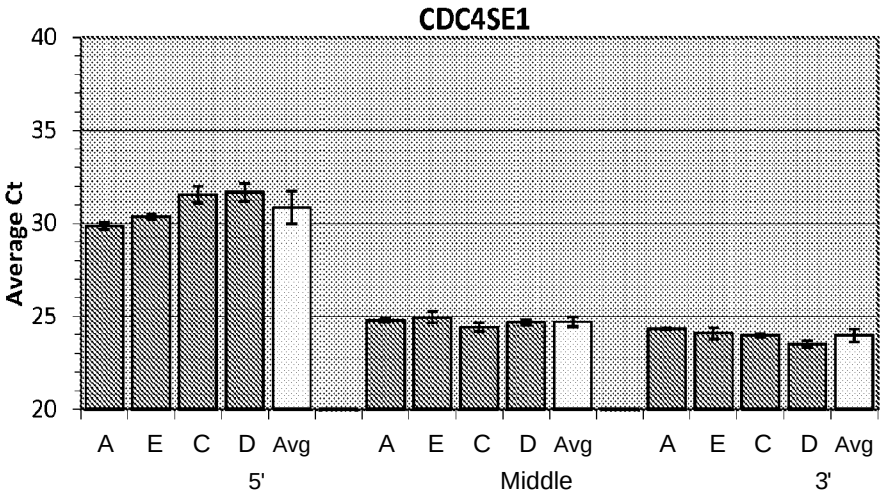
CDC4SE1
Average Ct
40
35
30
25
20
A E C D Avg A E C D Avg A E C D Avg
5' Middle 3'

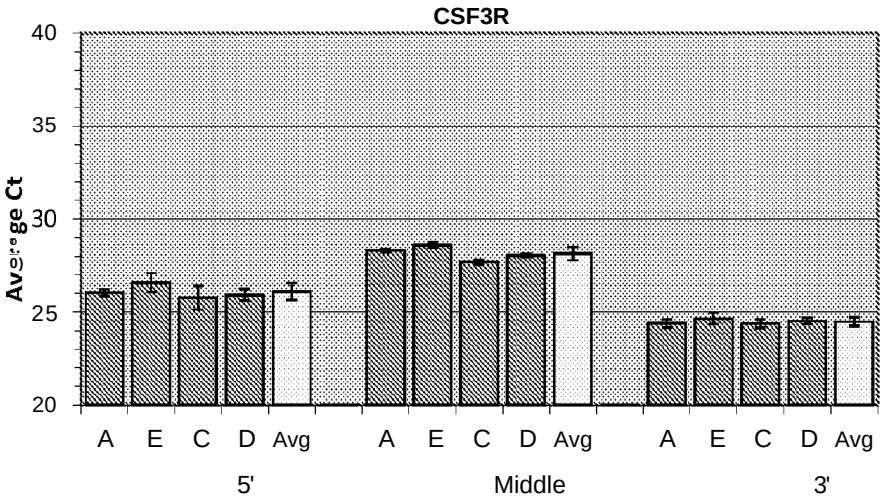
CSF3R
Average Ct
40
35
30
25
20
A E C D Avg A E C D Avg A E C D Avg
5' Middle 3'

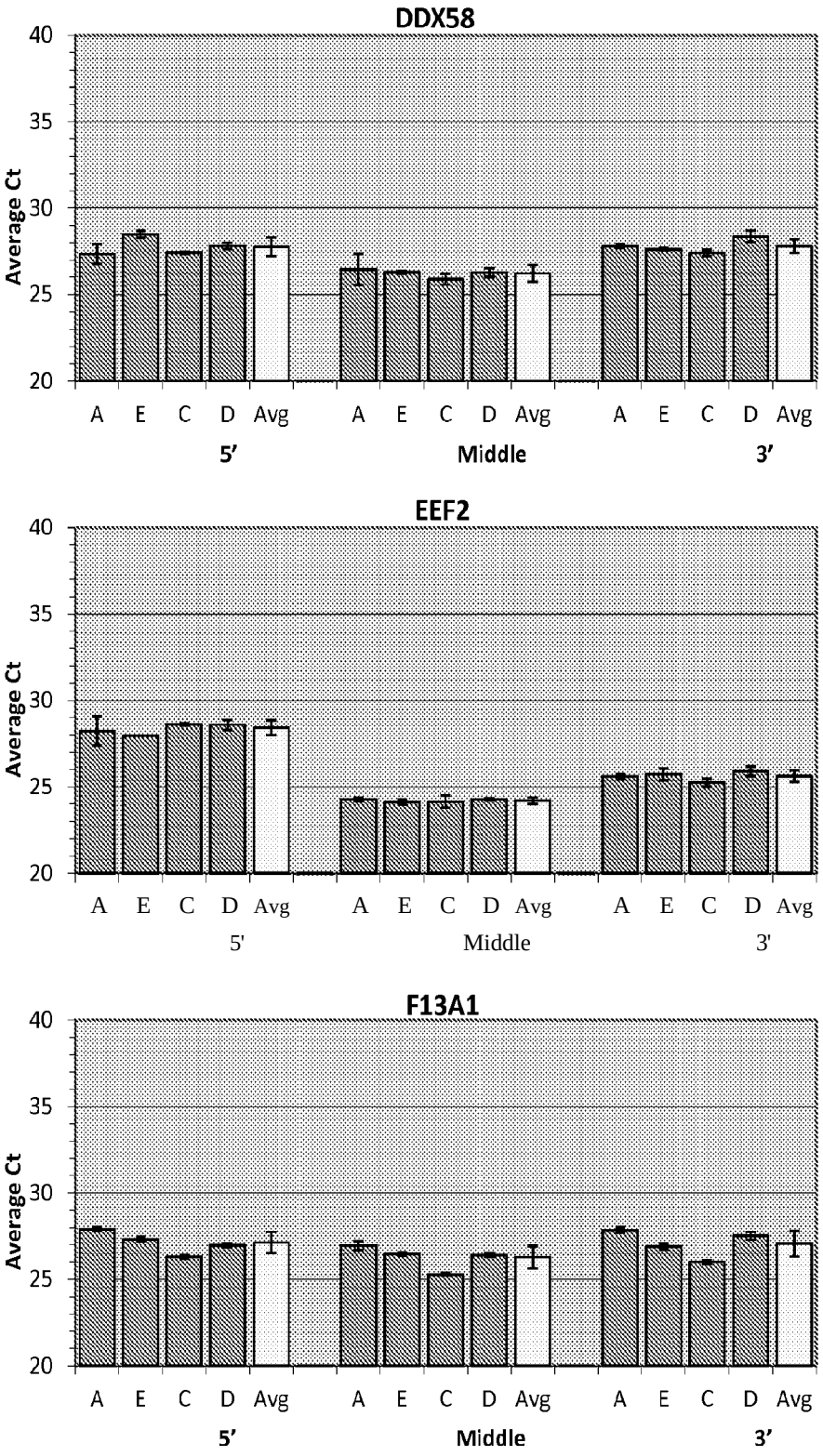
DDX58
Average Ct
40
35
30
25
20
A E C D Avg A E C D Avg A E C D Avg
5′
Middle
3′
EEF2
Average Ct
40
35
30
25
20
A E C D Avg A E C D Avg A E C D Avg
5'
Middle
3'
F13A1
Average Ct
40
35
30
25
20
A E C D Avg A E C D Avg A E C D Avg
5′
Middle
3′

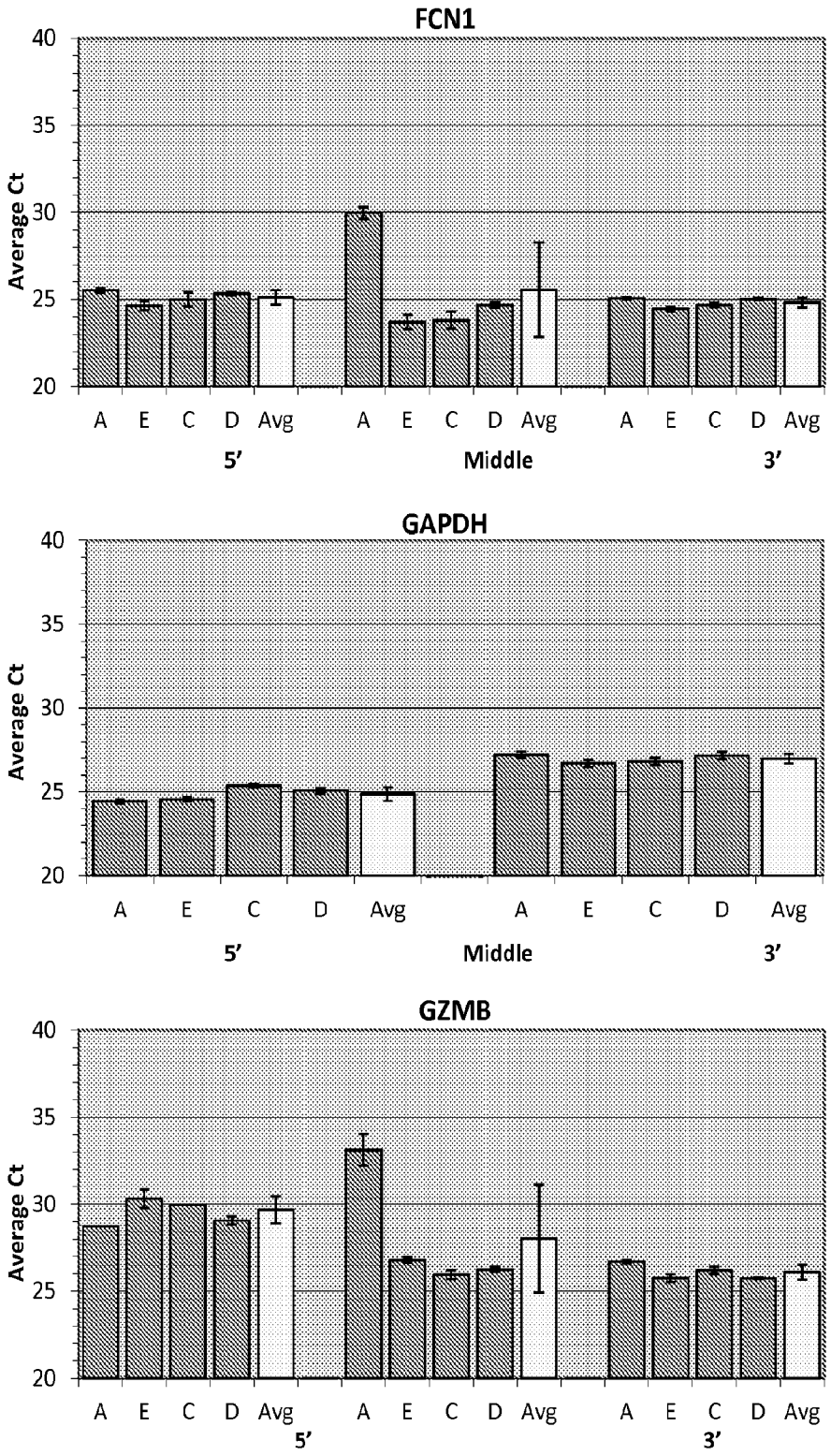
FCN1
Average Ct
40
35
30
25
20
A E C D Avg A E C D Avg A E C D Avg
5'
Middle
3'
GAPDH
Average Ct
40
35
30
25
20
A E C D Avg A E C D Avg
5'
Middle
3'
GZMB
Average Ct
40
35
30
25
20
A E C D Avg A E C D Avg A E C D Avg
5'
3'

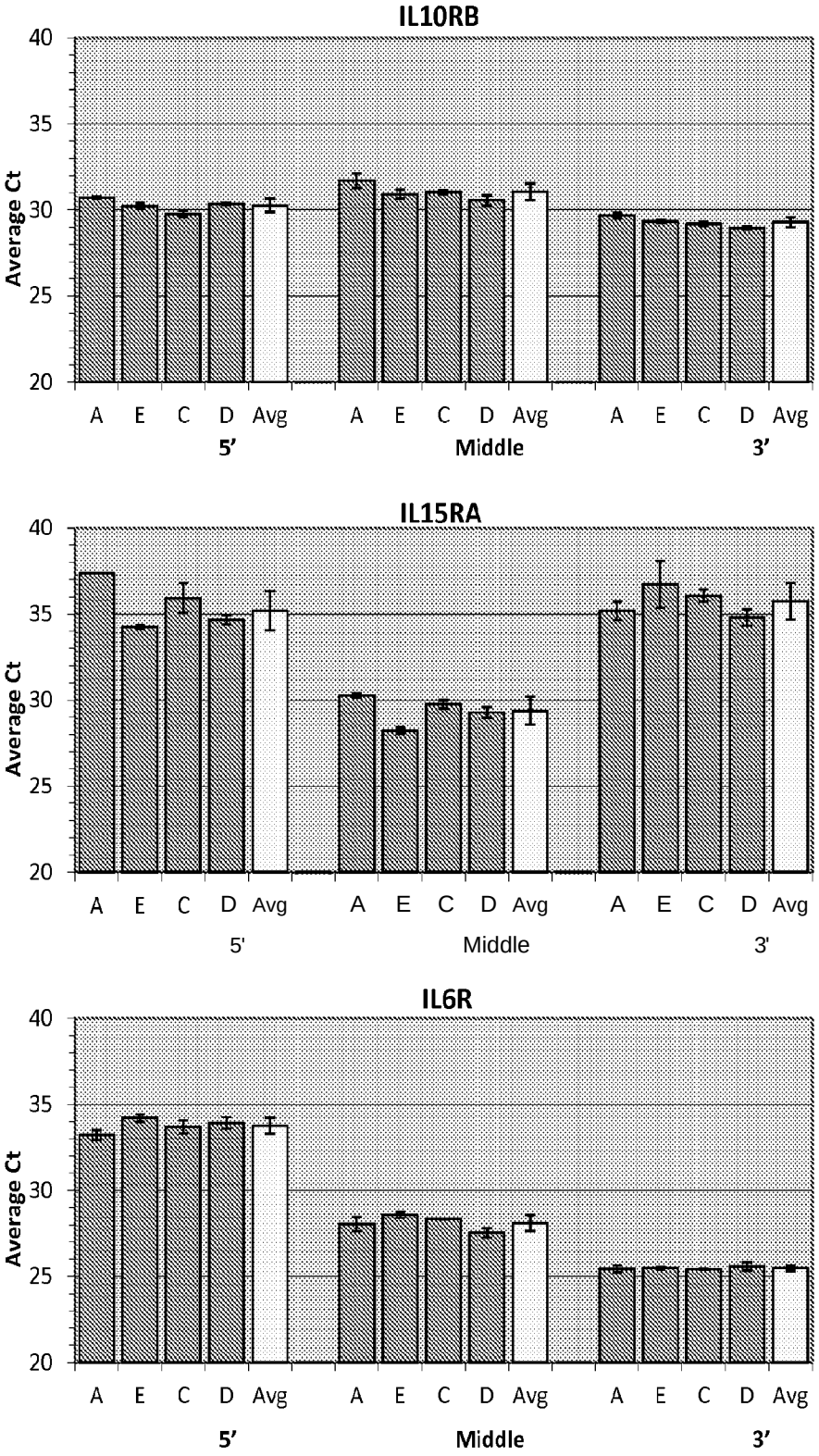
IL10RB
Average Ct
40
35
30
25
20
A E C D Avg A E C D Avg A E C D Avg
5'
Middle
3'
IL15RA
Average Ct
40
35
30
25
20
A E C D Avg A E C D Avg A E C D Avg
5'
Middle
3'
IL6R
Average Ct
40
35
30
25
20
A E C D Avg A E C D Avg A E C D Avg
5'
Middle
3'

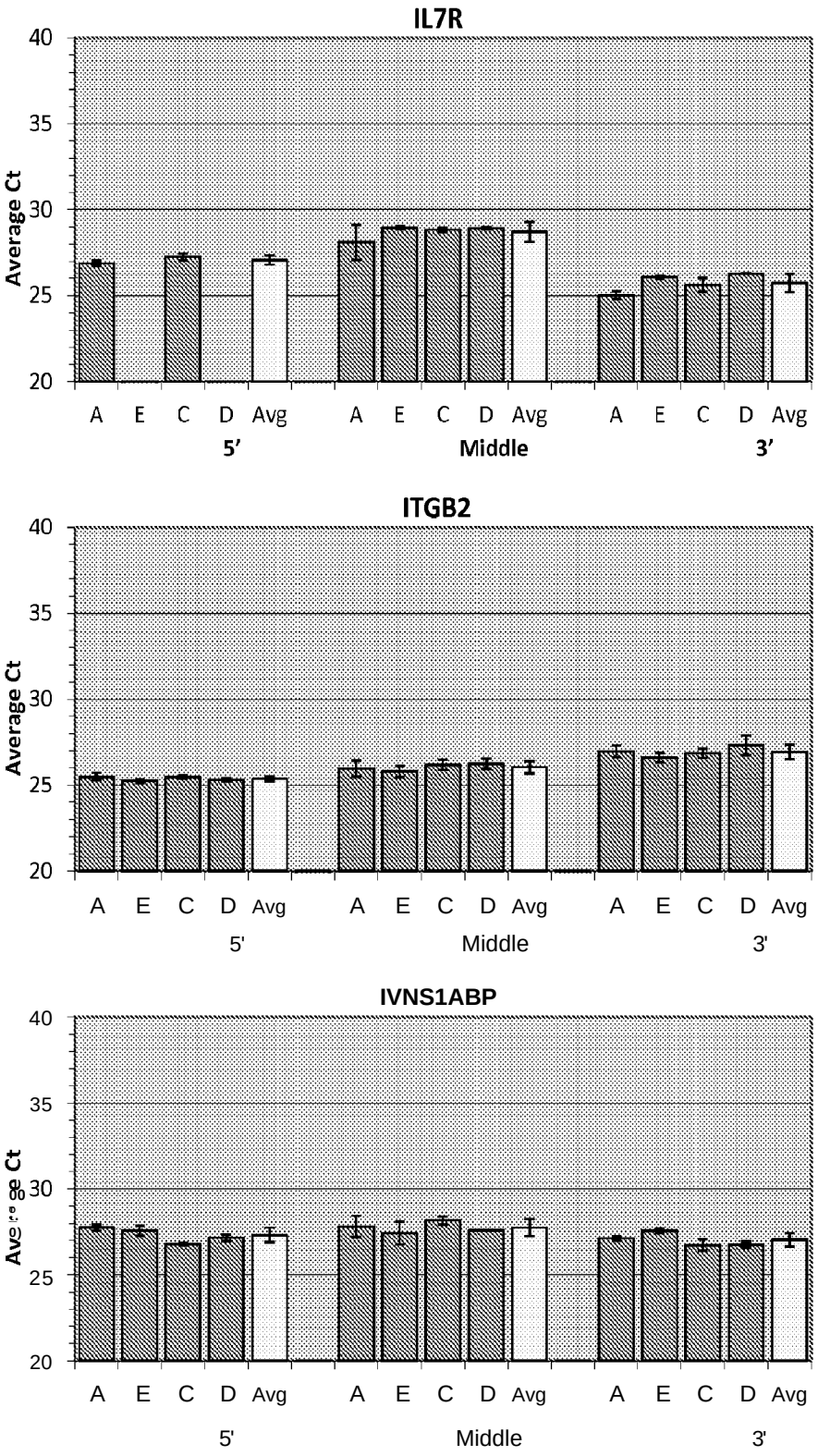
IL7R
Average Ct
40
35
30
25
20
A E C D Avg A E C D Avg A E C D Avg
5'
Middle
3'
ITGB2
Average Ct
40
35
30
25
20
A E C D Avg A E C D Avg A E C D Avg
5'
Middle
3'
IVNS1ABP
Average Ct
40
35
30
25
20
A E C D Avg A E C D Avg A E C D Avg
5'
Middle
3'

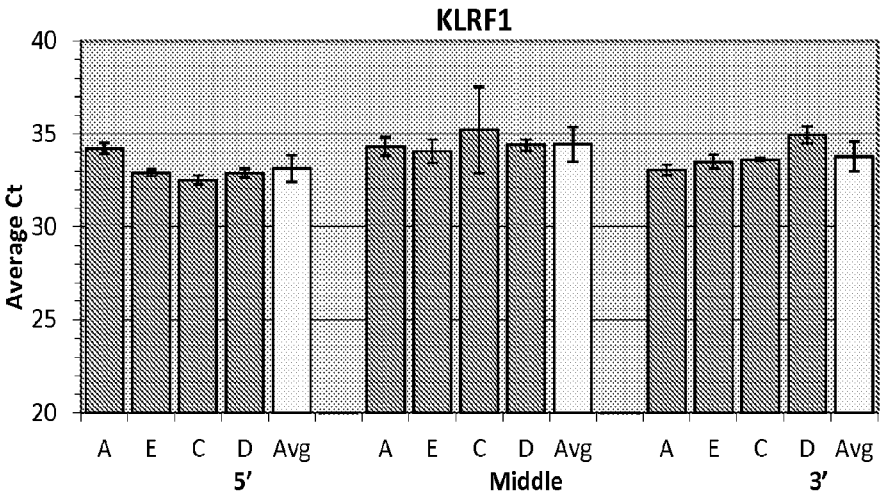
KLRF1
Average Ct
40
35
30
25
20
A E C D Avg A E C D Avg A E C D Avg
5′
Middle
3′

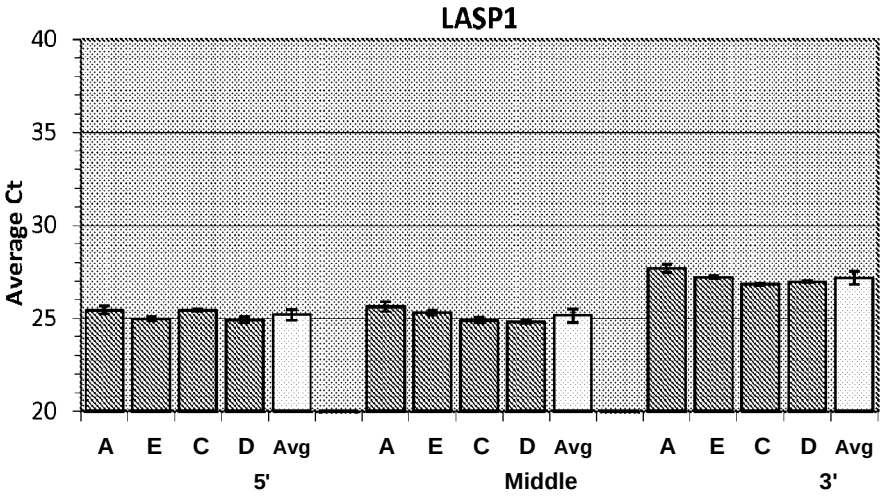
LASP1
Average Ct
40
35
30
25
20
A E C D Avg A E C D Avg A E C D Avg
5'
Middle
3'

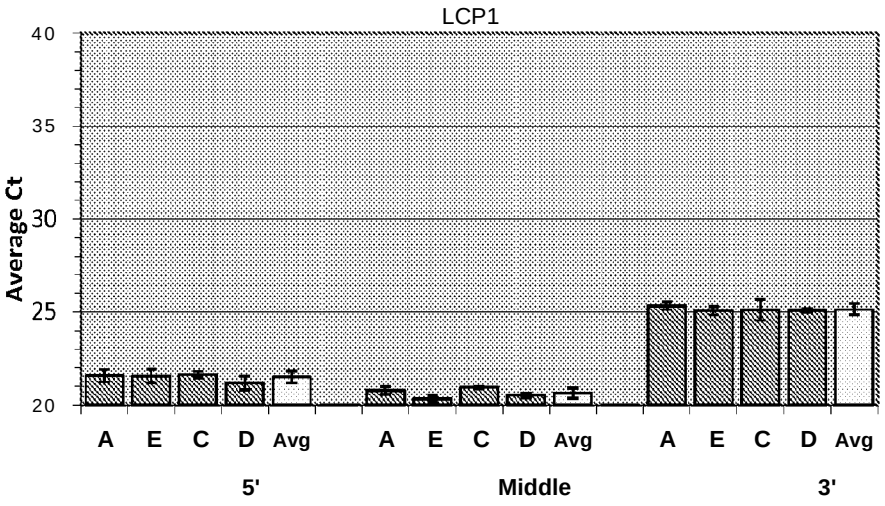
LCP1
Average Ct
40
35
30
25
20
A E C D Avg A E C D Avg A E C D Avg
5'
Middle
3'

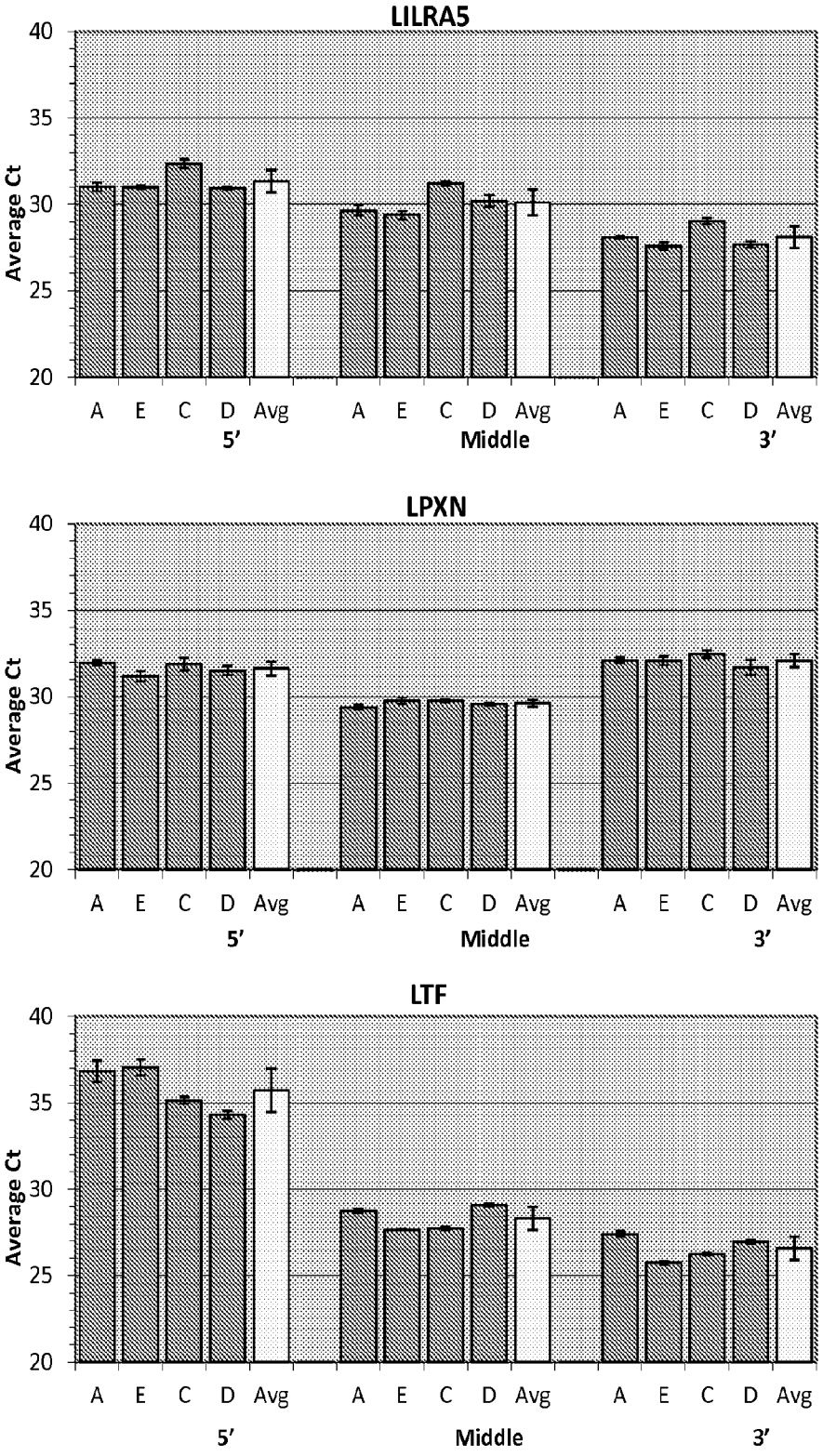
LILRA5
Average Ct
40
35
30
25
20
A E C D Avg A E C D Avg A E C D Avg
5′
Middle
3′
LPXN
Average Ct
40
35
30
25
20
A E C D Avg A E C D Avg A E C D Avg
5′
Middle
3′
LTF
Average Ct
40
35
30
25
20
A E C D Avg A E C D Avg A E C D Avg
5′
Middle
3′

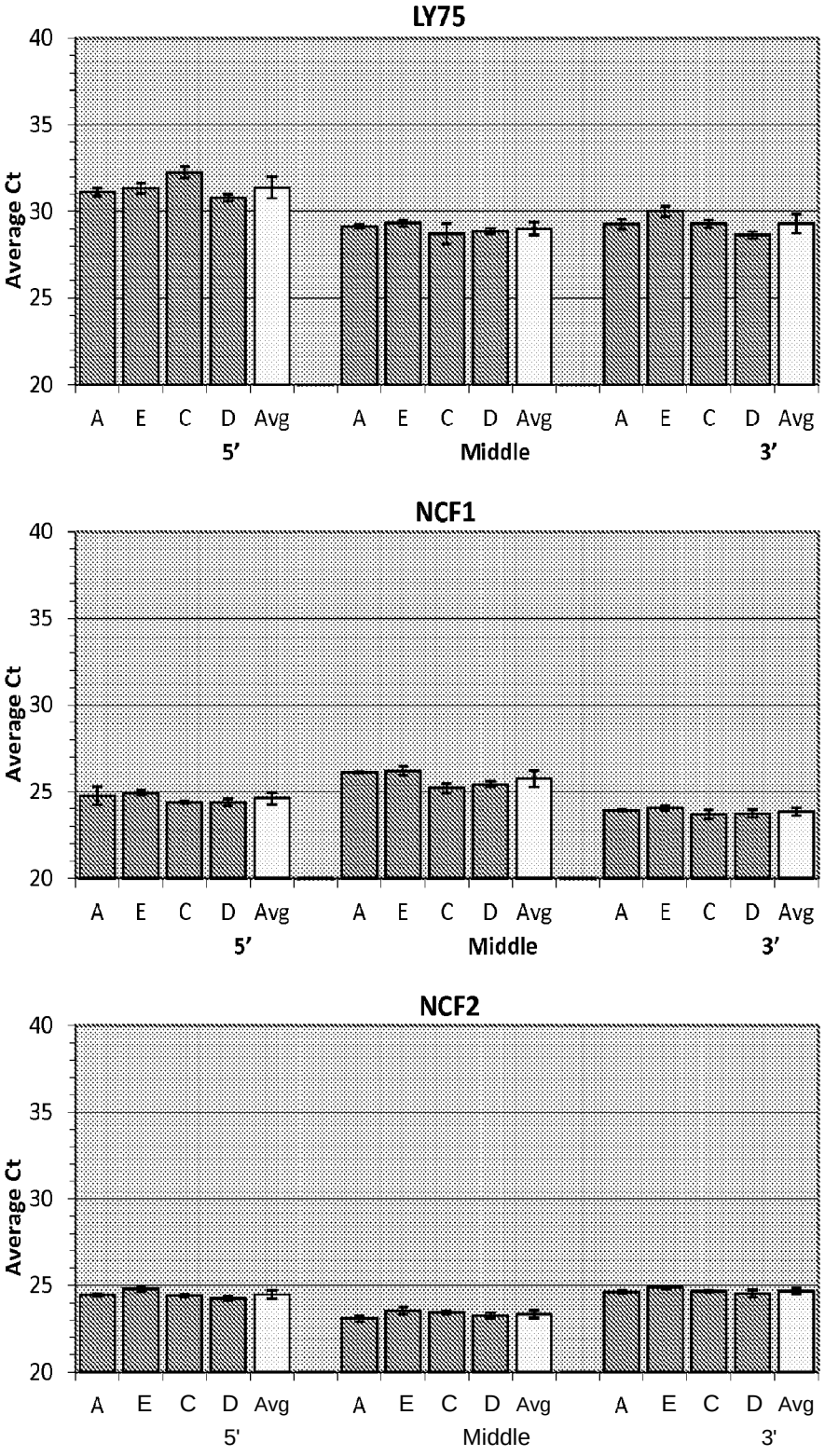
LY75
Average Ct
40
35
30
25
20
A E C D Avg A E C D Avg A E C D Avg
5'
Middle
3'
NCF1
Average Ct
40
35
30
25
20
A E C D Avg A E C D Avg A E C D Avg
5'
Middle
3'
NCF2
Average Ct
40
35
30
25
20
A E C D Avg A E C D Avg A E C D Avg
5'
Middle
3'

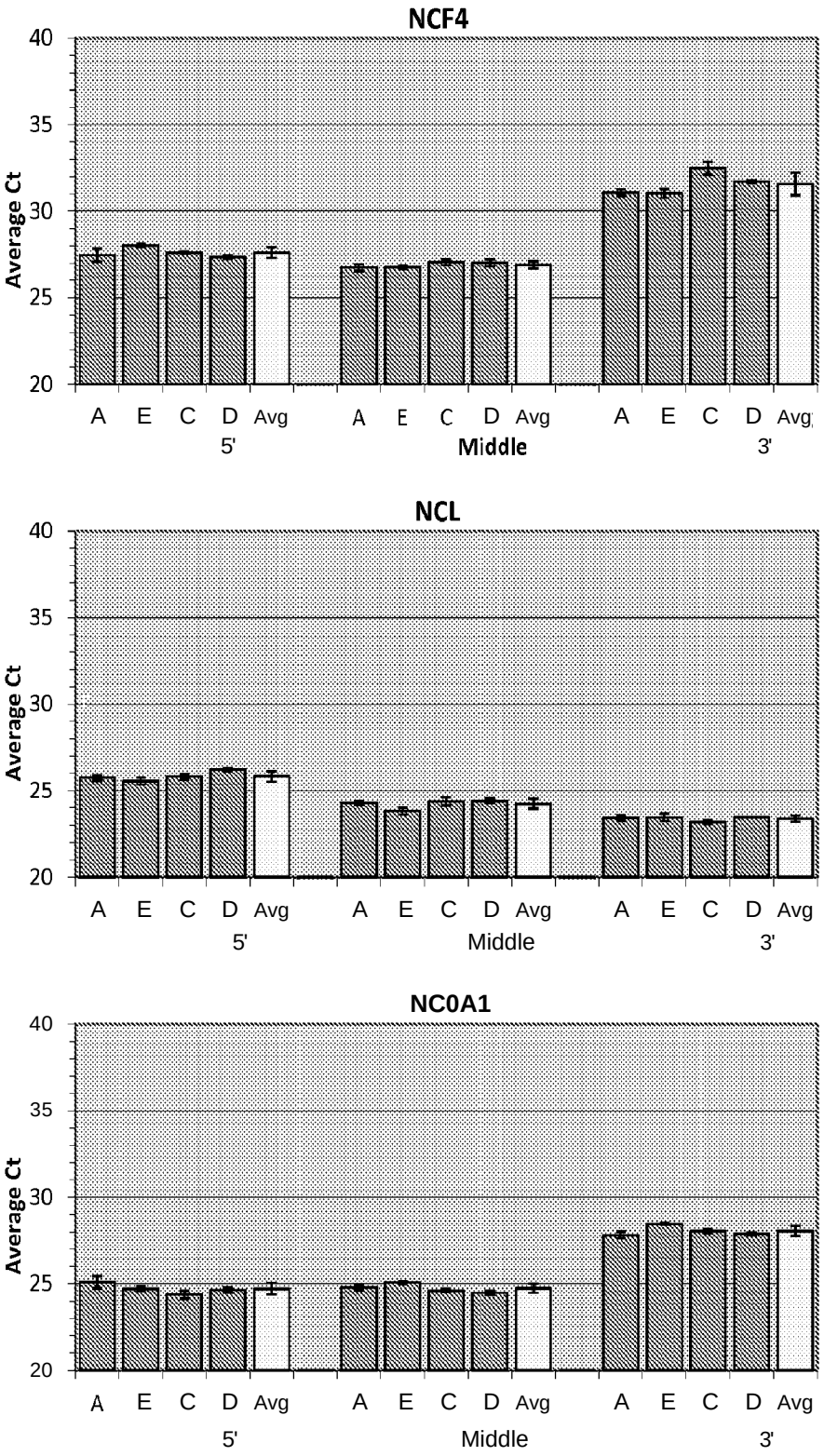
NCF4
Average Ct
40
35
30
25
20
A E C D Avg A E C D Avg A E C D Avg
5' Middle 3'
NCL
Average Ct
40
35
30
25
20
A E C D Avg A E C D Avg A E C D Avg
5' Middle 3'
NC0A1
Average Ct
40
35
30
25
20
A E C D Avg A E C D Avg A E C D Avg
5' Middle 3'

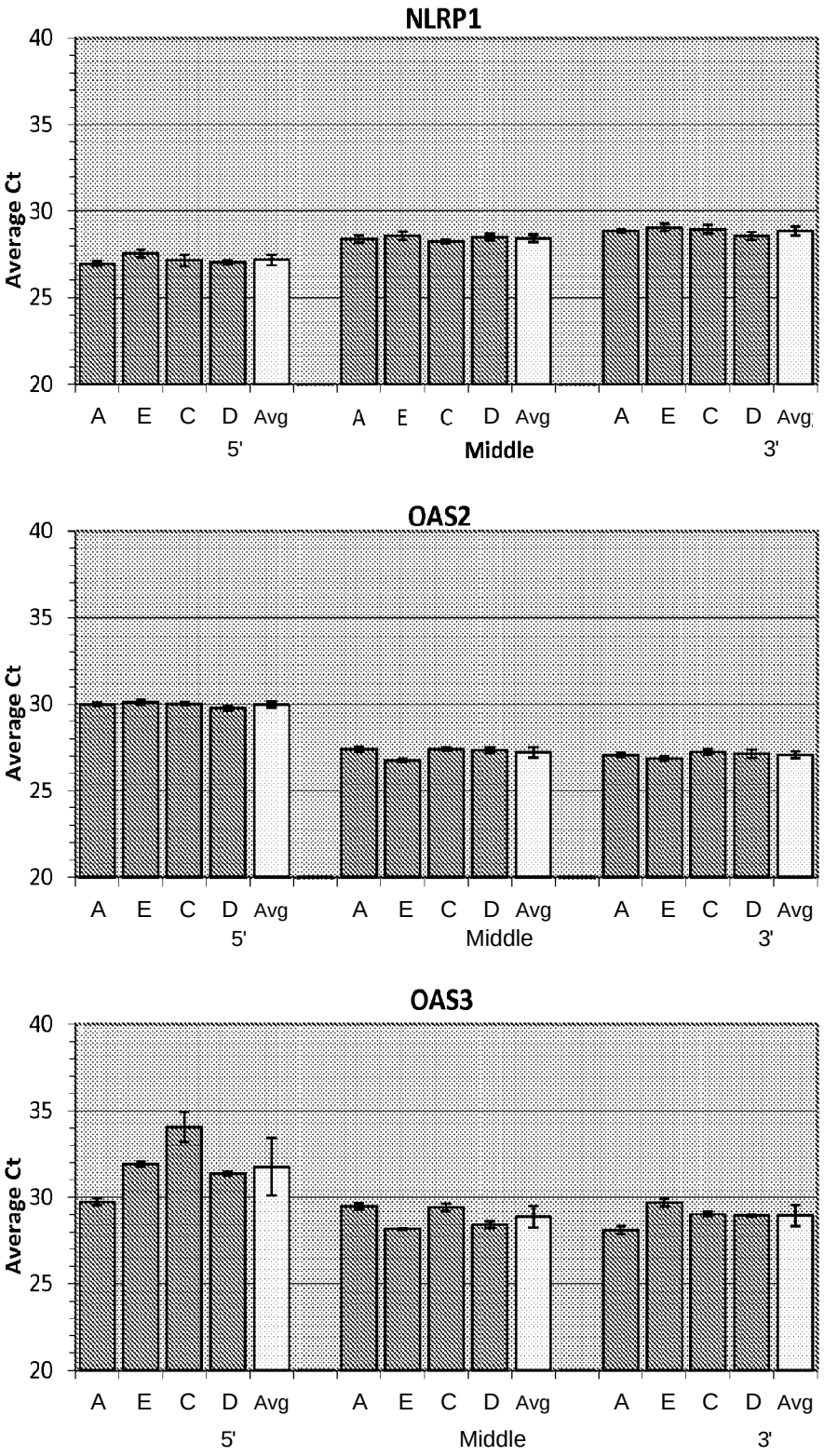
NLRP1
Average Ct
40
35
30
25
20
A E C D Avg A E C D Avg A E C D Avg
5' Middle 3'
OAS2
Average Ct
40
35
30
25
20
A E C D Avg A E C D Avg A E C D Avg
5' Middle 3'
OAS3
Average Ct
40
35
30
25
20
A E C D Avg A E C D Avg A E C D Avg
5' Middle 3'

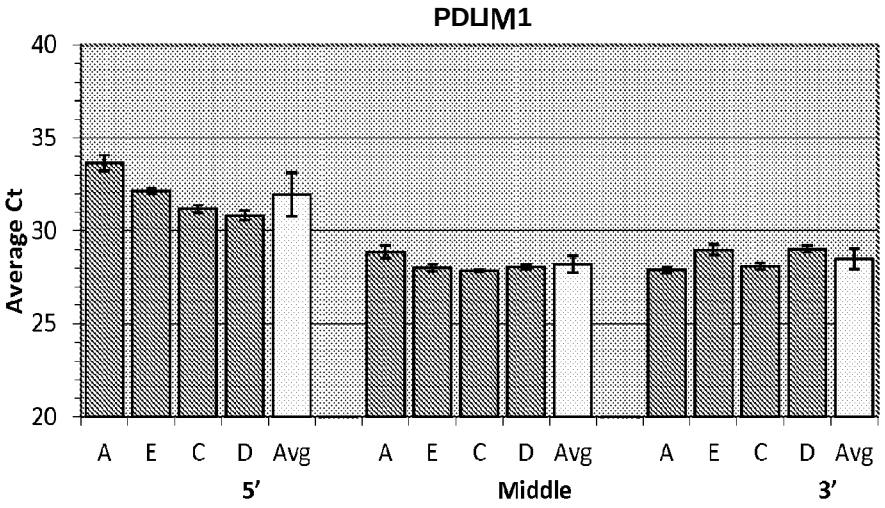
PDLIM1
Average Ct
40
35
30
25
20
A E C D Avg A E C D Avg A E C D Avg
5'
Middle
3'

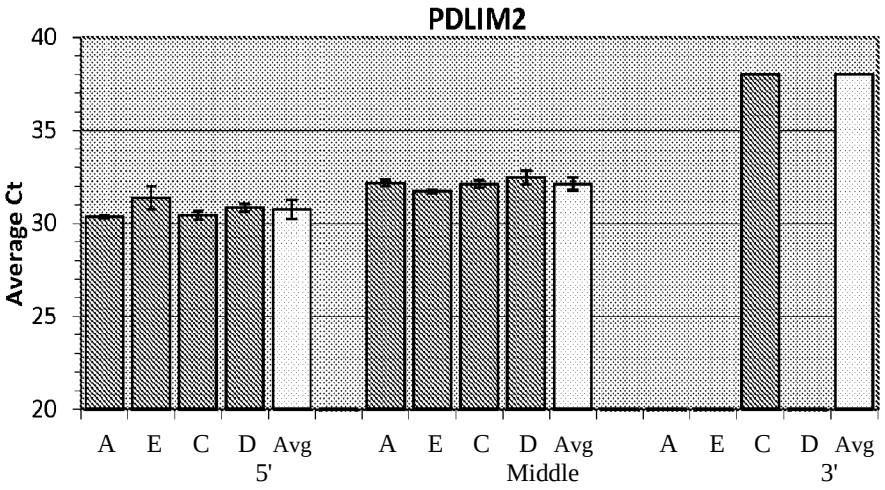
PDLIM2
Average Ct
40
35
30
25
20
A E C D Avg A E C D Avg A E C D Avg
5'
Middle
3'

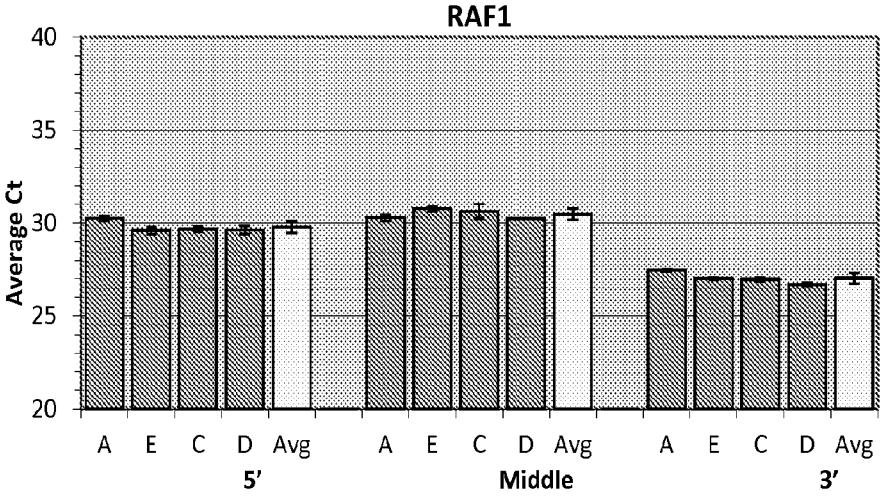
RAF1
Average Ct
40
35
30
25
20
A E C D Avg A E C D Avg A E C D Avg
5'
Middle
3'

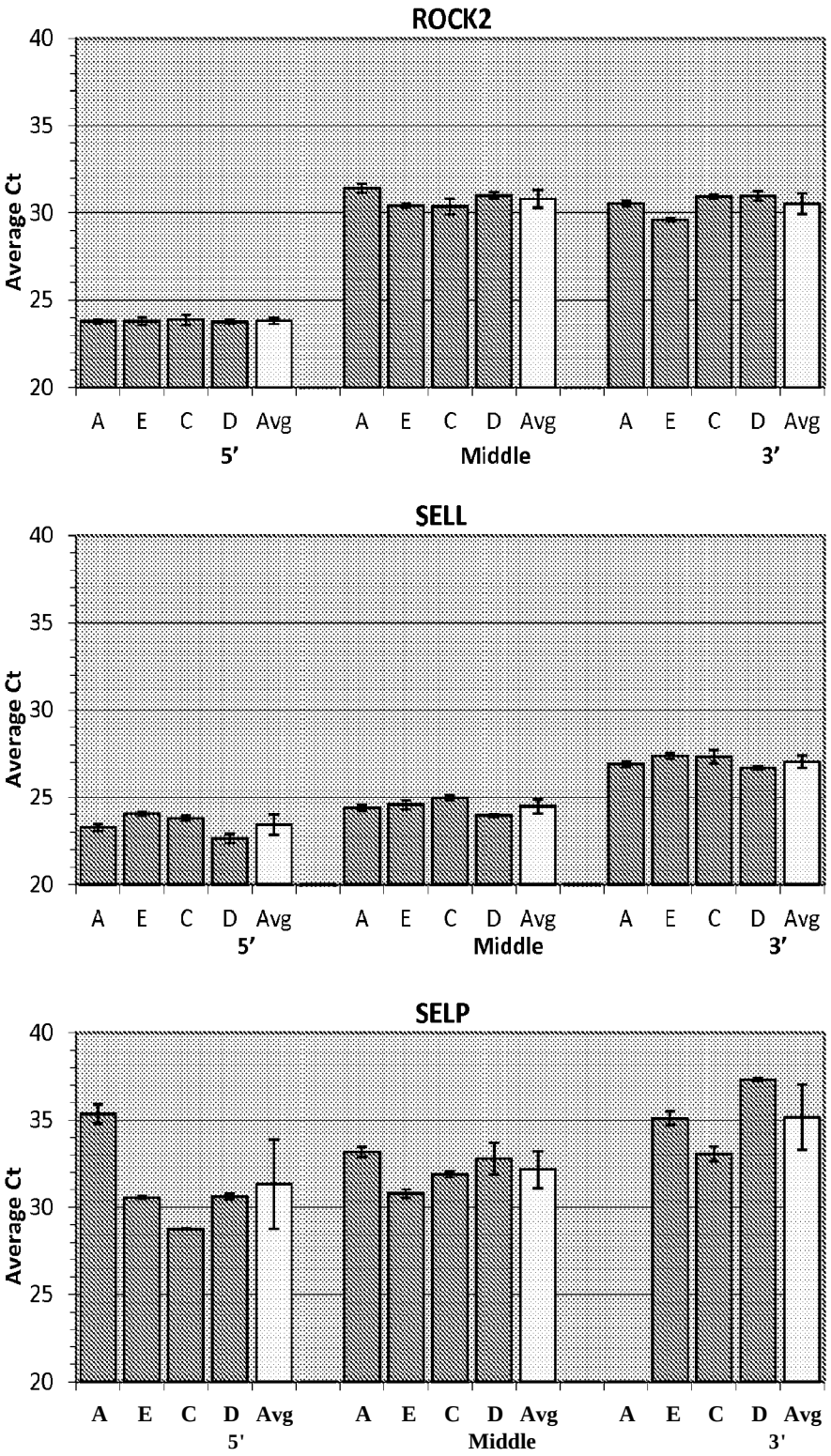
ROCK2
Average Ct
40
35
30
25
20
A E C D Avg A E C D Avg A E C D Avg
5'
Middle
3'
SELL
Average Ct
40
35
30
25
20
A E C D Avg A E C D Avg A E C D Avg
5'
Middle
3'
SELP
Average Ct
40
35
30
25
20
A E C D Avg A E C D Avg A E C D Avg
5'
Middle
3'

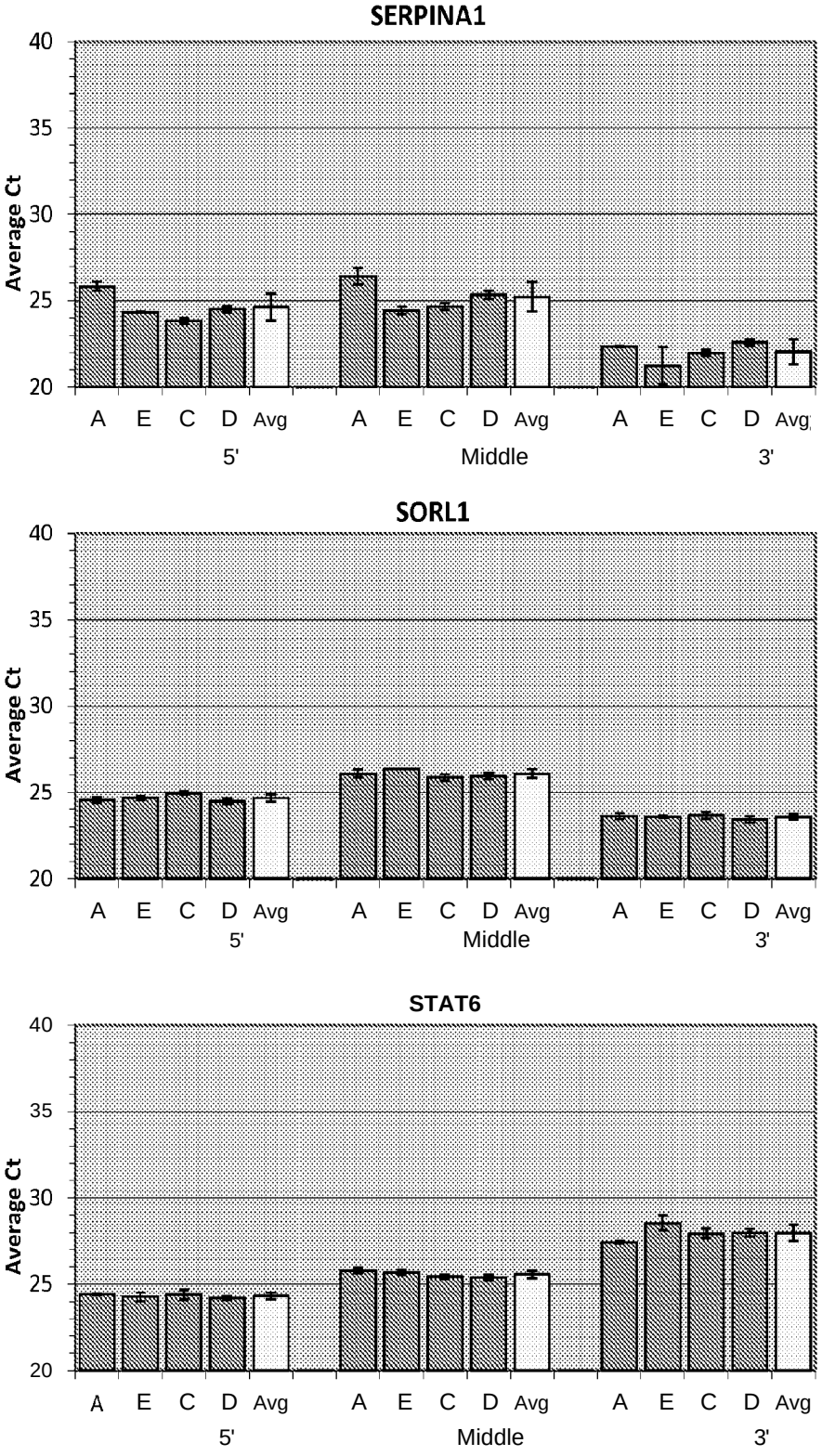
SERPINA1
Average Ct
40
35
30
25
20
A E C D Avg A E C D Avg A E C D Avg
5' Middle 3'
SORL1
Average Ct
40
35
30
25
20
A E C D Avg A E C D Avg A E C D Avg
5' Middle 3'
STAT6
Average Ct
40
35
30
25
20
A E C D Avg A E C D Avg A E C D Avg
5' Middle 3'

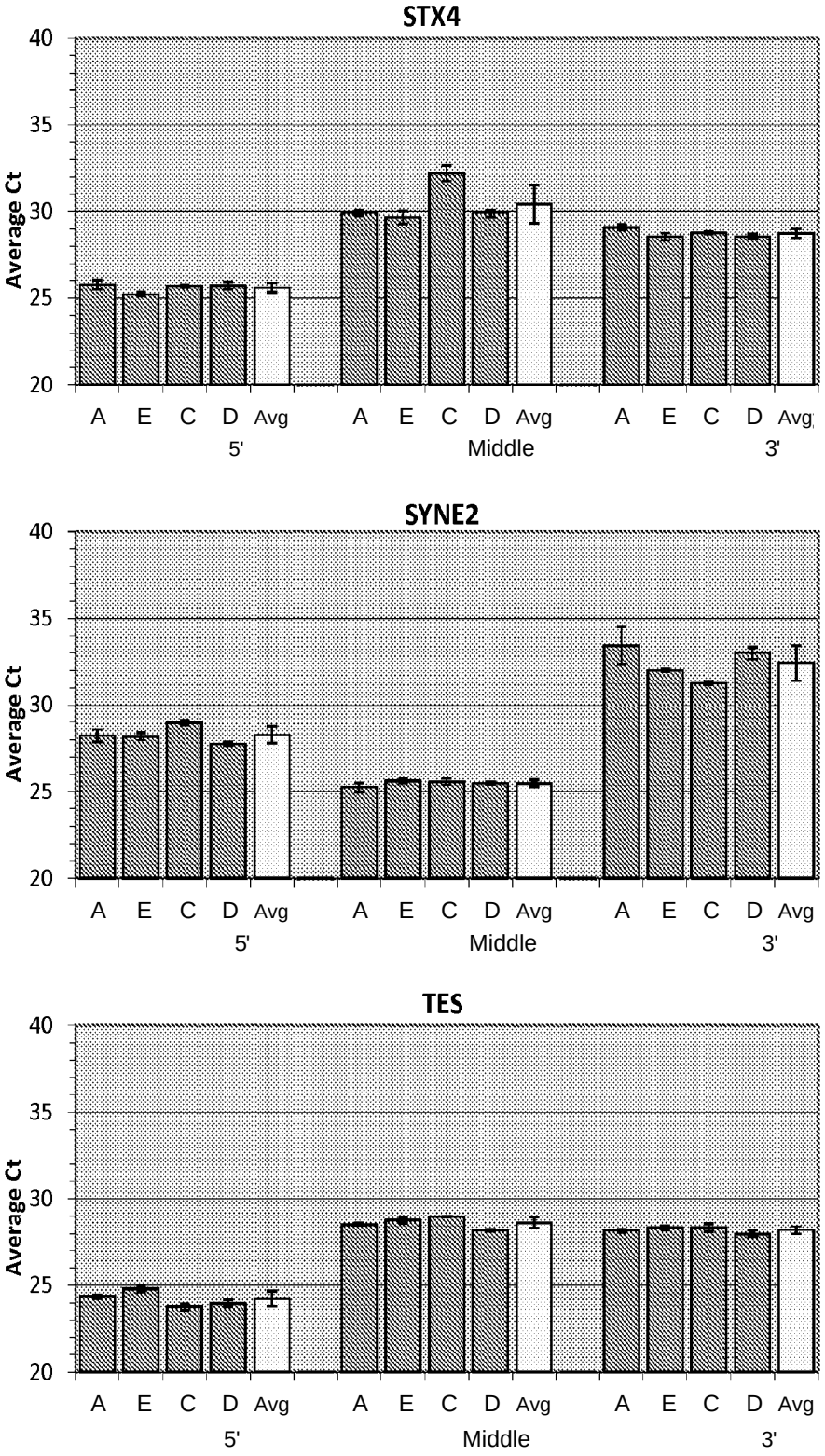
STX4
Average Ct
40
35
30
25
20
A E C D Avg A E C D Avg A E C D Avg
5' Middle 3'
SYNE2
Average Ct
40
35
30
25
20
A E C D Avg A E C D Avg A E C D Avg
5' Middle 3'
TES
Average Ct
40
35
30
25
20
A E C D Avg A E C D Avg A E C D Avg
5' Middle 3'

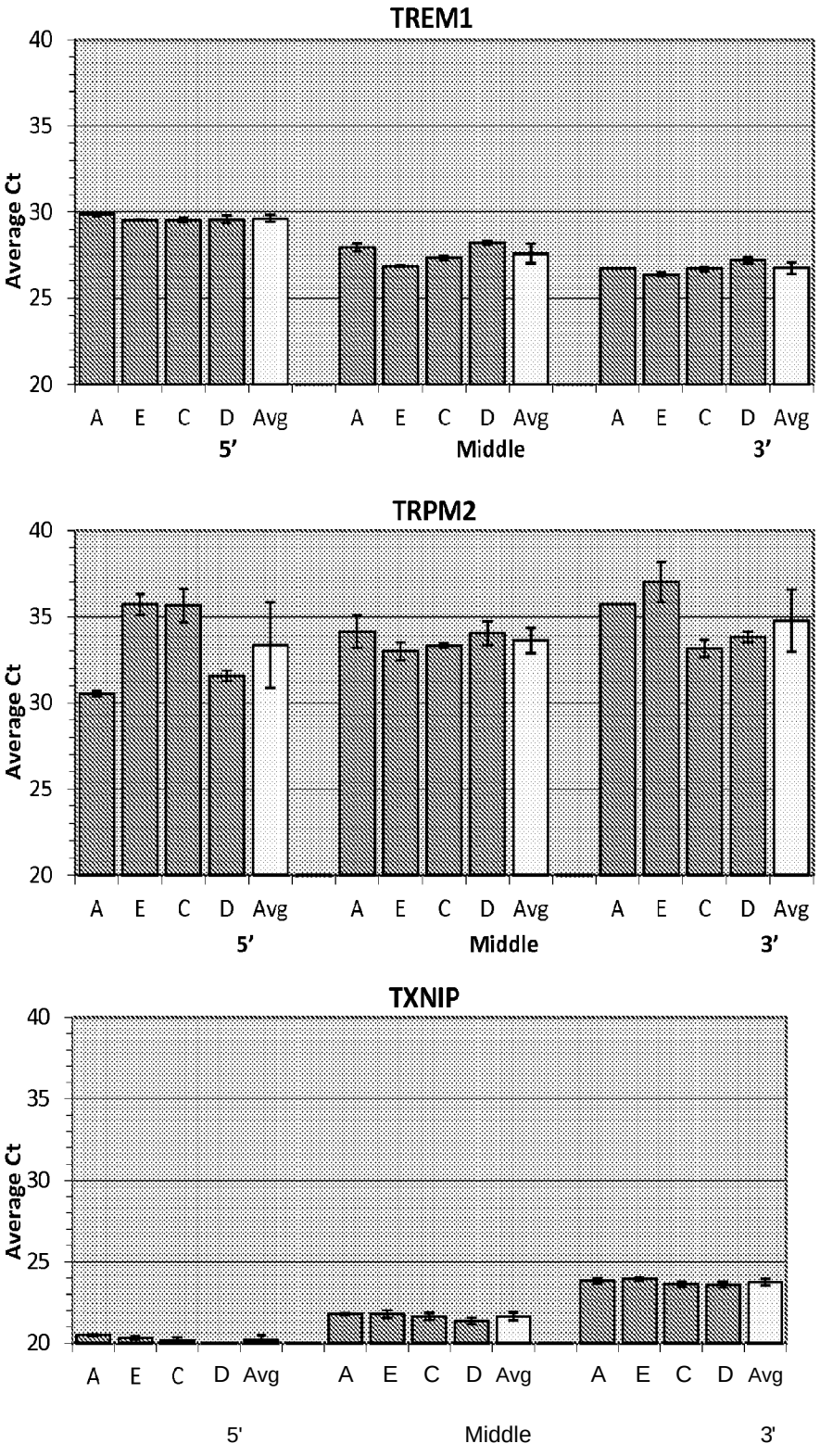
TREM1
Average Ct
40
35
30
25
20
A E C D Avg A E C D Avg A E C D Avg
5'
Middle
3'
TRPM2
Average Ct
40
35
30
25
20
A E C D Avg A E C D Avg A E C D Avg
5'
Middle
3'
TXNIP
Average Ct
40
35
30
25
20
A E C D Avg A E C D Avg A E C D Avg
5'
Middle
3'

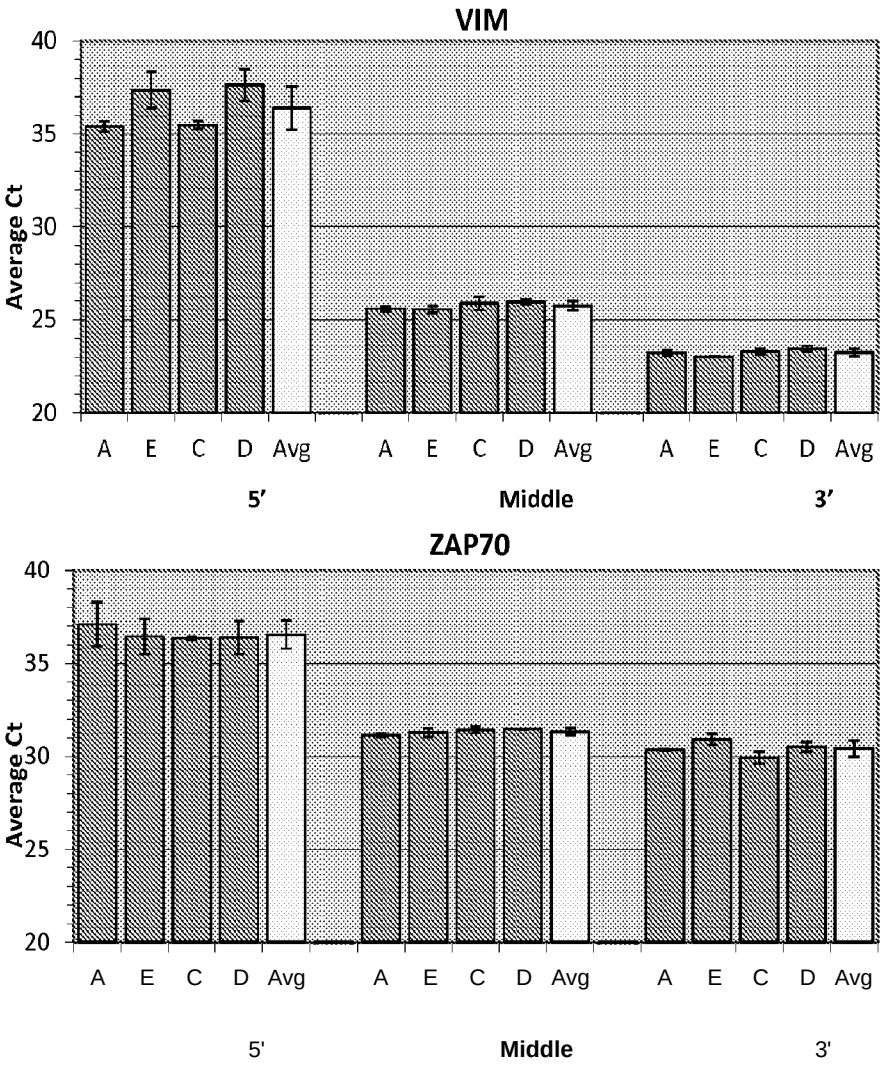

APPENDIX VIII

Assay Performance, Regional Consistency weighted most heavily:

- In 'Assay' column: L = 5' design, M = Middle design, R = 3' design

Performance Order	Assay	Regional Consistency	Amp. Plot Consistency	Matches Expression Expectation	Assay Avg. C_T	Expected Expression Score
1	**ADAR_M**	3	Y	Y	24.41	4500
2	**ARPC5_L**	3	Y	Y	21.99	5500
3	**ARPC5_M**	3	Y	Y	20.95	5500

4	**ARPC5_R**	3	Y	Y	21.96	5500
5	**F13A1_L**	3	Y	Y	27.12	2300
6	**F13A1_M**	3	Y	Y	26.28	2300
7	**F13A1_R**	3	Y	Y	27.07	2300
8	**FCN1_R**	3	Y	Y	24.81	9000
9	**IL10RBJ.**	3	Y	Y	30.27	850
10	**IL10RB_M**	3	Y	Y	31.06	850
11	**NCF1_L**	3	Y	Y	24.62	5500
12	**NCF1_R**	3	Y	Y	23.85	5500
13	**NCF2_L**	3	Y	Y	24.47	8500
14	**NCF2_M**	3	Y	Y	23.34	8500
15	**NCF2_R**	3	Y	Y	24.67	8500
16	**ADAR_R**	3	Y	Borderline	26.06	4500
17	**FCN1_L**	3	Y	Borderline	25.12	9000
18	**IL10RB_R**	3	Y	Borderline	29.29	850
19	**ITGB2_L**	3	Y	Borderline	25.38	10000
20	**ITGB2_M**	3	Y	Borderline	26.05	10000
21	**NCF1_M**	3	Y	Borderline	25.75	5500
22	**DDX58_L**	3	Y	N	27.76	350
23	**DDX58_M**	3	Y	N	26.23	350
24	**ITGB2_R**	3	Y	N	26.94	10000
25	**IVNS1ABP_L**	3	Y	N	27.32	750
26	**IVNS1ABP_M**	3	Y	N	27.75	750
27	**IVNS1ABP_R**	3	Y	N	27.04	750
28	**NLRP1_L**	3	Y	N	27.19	600
29	**NLRP1_M**	3	Y	N	28.43	600
30	**NLRP1_R**	3	Y	N	28.86	600
31	**KLRF1_L**	3	N	Y	33.13	650

32	KLRF1_M	3	N	Y	34.44	650
33	KLRF1_R	3	N	Y	33.78	650
34	TRPM2_L	3	N	Y	33.37	400
35	TRPM2_M	3	N	Y	33.62	400
36	TRPM2_R	3	N	Y	34.77	400
37	ADAR_L	3	N	Borderline	25.6	4500
38	FCN1_M	3	N	Borderline	25.54	9000
39	DDX58_R	3	N	N	27.8	350
40	ACTR2_M	2	Y	Y	25.6	2000
41	ADD3_L	2	Y	Y	28.52	1500
42	ADD3_M	2	Y	Y	27.52	1500
43	AIM1_R	2	Y	Y	25.87	1000
44	Clorf38_M	2	Y	Y	28.36	3000
45	CD53_M	2	Y	Y	24.8	8000
46	CDC42SE1_M	2	Y	Y	24.71	5000
47	CDC42SE1_R	2	Y	Y	23.98	5000
48	EEF2_M	2	Y	Y	24.21	7000
49	IL7R_M	2	Y	Y	28.7	3500
50	IL7R_R	2	Y	Y	25.75	3500
51	LCP1_L	2	Y	Y	21.5	6500
52	LCP1_M	2	Y	Y	20.64	6500
53	LPXN_M	2	Y	Y	29.63	1100
54	NCL_L	2	Y	Y	25.84	2000
55	PDLIM2_M	2	Y	Y	32.12	950
56	RAF1_L	2	Y	Y	29.79	3000
57	RAF1_R	2	Y	Y	27.03	3000
58	ROCK2_R	2	Y	Y	30.52	200
59	SERPINA1_R	2	Y	Y	22.03	7500

60	**ZAP70_M**	2	Y	Y	31.33	650
61	**ZAP70_R**	2	Y	Y	30.42	650
62	**ADD1_L**	2	Y	Borderline	29.43	750
63	**AIM1_M**	2	Y	Borderline	30.45	1000
64	**CD53_R**	2	Y	Borderline	25.9	8000
65	**EEF2_R**	2	Y	Borderline	25.62	7000
66	**LASP1_L**	2	Y	Borderline	25.2	4500
67	**LASP1_M**	2	Y	Borderline	25.16	4500
68	**LASP1_R**	2	Y	Borderline	27.18	4500
69	**LCP1_R**	2	Y	Borderline	25.14	6500
70	**LPXN_L**	2	Y	Borderline	31.64	1100
71	**LPXN_R**	2	Y	Borderline	32.09	1100
72	**LY75_M**	2	Y	Borderline	29.01	800
73	**LY75_R**	2	Y	Borderline	29.3	800
74	**NCF4_L**	2	Y	Borderline	27.61	4500
75	**NCF4_M**	2	Y	Borderline	26.89	4500
76	**OAS2_L**	2	Y	Borderline	29.97	500
77	**PDLIM1_R**	2	Y	Borderline	28.5	900
78	**RAF1_M**	2	Y	Borderline	30.47	3000
79	**TREM1_L**	2	Y	Borderline	29.63	4500
80	**TREM1_M**	2	Y	Borderline	27.6	4500
81	**TREM1_R**	2	Y	Borderline	26.76	4500
82	**ACTR2_L**	2	Y	N	22.72	2000
83	**ACTR2_R**	2	Y	N	23.17	2000
84	**ADD1_M**	2	Y	N	26.79	750
85	**ADD1_R**	2	Y	N	25.43	750
86	**ADD3_R**	2	Y	N	24.17	1500
87	**CAPN2_L**	2	Y	N	28.04	750

88	**CAPN2_M**	2	Y	N	23.88	750
89	**CAPN2_R**	2	Y	N	25.15	750
90	**CD163_R**	2	Y	N	27.83	200
91	**CD68_L**	2	Y	N	21.75	250
92	**CD68_R**	2	Y	N	26.03	250
93	**LTF_R**	2	Y	N	26.59	200
94	**NCF4_R**	2	Y	N	31.58	4500
95	**NCL_M**	2	Y	N	24.24	2000
96	**NCL_R**	2	Y	N	23.39	2000
97	**NCOA1J.**	2	Y	N	24.7	850
98	**NC0A1_M**	2	Y	N	24.74	850
99	**NC0A1_R**	2	Y	N	28.05	850
100	**OAS2_M**	2	Y	N	27.23	500
101	**OAS2_R**	2	Y	N	27.08	500
102	**OAS3_M**	2	Y	N	28.86	650
103	**OAS3_R**	2	Y	N	28.94	650
104	**PDLIM1_M**	2	Y	N	28.2	900
105	**ROCK2_L**	2	Y	N	23.81	200
106	**TES_L**	2	Y	N	24.23	750
107	**TES_M**	2	Y	N	28.61	750
108	**TES_R**	2	Y	N	28.19	750
109	**Clorf38_L**	2	N	Y	27.49	3000
110	**CD163_L**	2	N	Y	30.16	200
111	**CD27_M**	2	N	Y	32.29	650
112	**CD27_R**	2	N	Y	30.38	650
113	**CD300C_L**	2	N	Y	32.63	500
114	**CD300C_M**	2	N	Y	30.4	500
115	**CD300C_R**	2	N	Y	30.23	500

116	**CD53_L**	2	N	Y	23.36	8000
117	**CD83_L**	2	N	Y	36.63	150
118	**CD83_M**	2	N	Y	34.82	150
119	**CD83_R**	2	N	Y	30.62	150
120	**IL15RAJ.**	2	N	Y	35.19	300
121	**IL15RA_R**	2	N	Y	35.75	300
122	**IL7R_L**	2	N	Y	27.07	3500
123	**LTF_L**	2	N	Y	35.73	200
124	**LY75_L**	2	N	Y	31.38	800
125	**OAS3_L**	2	N	Y	31.77	650
126	**PDLIMIJ.**	2	N	Y	31.95	900
127	**PDLIM2_L**	2	N	Y	30.75	950
128	**PDLIM2_R**	2	N	Y	38.02	950
129	**ROCK2_M**	2	N	Y	30.81	200
130	**SERPINA1J.**	2	N	Y	24.63	7500
131	**ZAP70_L**	2	N	Y	36.56	650
132	**AIM1_L**	2	N	Borderline	30.33	1000
133	**Clorf38_R**	2	N	Borderline	32.82	3000
134	**SERPINA1_M**	2	N	Borderline	25.22	7500
135	**CD163_M**	2	N	N	28.45	200
136	**CD27_L**	2	N	N	29.18	650
137	**CD68_M**	2	N	N	27.65	250
138	**CDC42SE1_L**	2	N	N	30.86	5000
139	**EEF2_L**	2	N	N	28.43	7000
140	**IL15RA_M**	2	N	N	29.39	300
141	**LTF_M**	2	N	N	28.3	200
142	**ACTB_L**	0	Y	Y	23.94	10,000
143	**ACTB_R**	0	Y	Y	21.05	10,000

144	**CSF3R_R**	0	Y	Y	24.48	6500
145	**GAPDH_L**	0	Y	Y	24.86	10,000
146	**GZMB_R**	0	Y	Y	26.09	1500
147	**IL6R_L**	0	Y	Y	33.75	500
148	**LILRA5_L**	0	Y	Y	31.33	900
149	**SELL_L**	0	Y	Y	23.45	8500
150	**SELL_M**	0	Y	Y	24.48	8500
151	**S0RL1_L**	0	Y	Y	24.67	7500
152	**S0RL1_R**	0	Y	Y	23.58	7500
153	**STAT6_M**	0	Y	Y	25.57	1000
154	**STAT6_R**	0	Y	Y	27.98	1000
155	**TXNIP_L**	0	Y	Y	20.2	8000
156	**TXNIP_M**	0	Y	Y	21.64	8000
157	**TXNIP_R**	0	Y	Y	23.75	8000
158	**VIM_R**	0	Y	Y	23.24	9500
159	**LILRA5_R**	0	Y	Borderline	28.1	900
160	**SORLI_M**	0	Y	Borderline	26.09	7500
161	**VIM_M**	0	Y	Borderline	25.75	9500
162	**CSF3R_M**	0	Y	N	28.15	6500
163	**GAPDH_R**	0	Y	N	26.97	10,000
164	**IL6R_M**	0	Y	N	28.1	500
165	**IL6R_R**	0	Y	N	25.48	500
166	**SELL_R**	0	Y	N	27.05	8500
167	**STAT6_L**	0	Y	N	24.32	1000
168	**STX4_L**	0	Y	N	25.6	600
169	**STX4_R**	0	Y	N	28.74	600
170	**SYNE2_L**	0	Y	N	28.29	400
171	**SYNE2_M**	0	Y	N	25.49	400

172	**BACH2_L**	0	N	Y	34.45	150
173	**BACH2_R**	0	N	Y	30.93	150
174	**GZMB_L**	0	N	Y	29.68	1500
175	**GZMB_M**	0	N	Y	28.02	1500
176	**LILRA5_M**	0	N	Y	30.11	900
177	**SELPJ.**	0	N	Y	31.32	700
178	**SELP_M**	0	N	Y	32.15	700
179	**SELP_R**	0	N	Y	35.16	700
180	**STX4_M**	0	N	Y	30.42	600
181	**SYNE2_R**	0	N	Y	32.43	400
182	**CSF3R_L**	0	N	Borderline	26.1	6500
183	**BACH2_M**	0	N	N	27.36	150
184	**VIM_L**	0	N	N	36.39	9500

APPENDIX VIII (continued)

Assay Performance, Amplification Plot Consistency weighted most heavily:

- In 'Assay' column: L = 5' design, M = Middle design, R = 3' design

Performance Order	Assay	Amp. Plot Consistency	Regional Consistency	Matches Expression Expectation	Assay Avg C_T	Expected Expression Score
1	**ADAR_M**	Y	3	Y	24.41	4500
2	**ARPC5_L**	Y	3	Y	21.99	5500
3	**ARPC5_M**	Y	3	Y	20.95	5500
4	**ARPC5_R**	Y	3	Y	21.96	5500
5	**F13A1_L**	Y	3	Y	27.12	2300
6	**F13A1_M**	Y	3	Y	26.28	2300
7	**F13A1_R**	Y	3	Y	27.07	2300
8	**FCN1_R**	Y	3	Y	24.81	9000
9	**IL10RB_L**	Y	3	Y	30.27	850
10	**IL10RB_M**	Y	3	Y	31.06	850
11	**NCF1_L**	Y	3	Y	24.62	5500
12	**NCF1_R**	Y	3	Y	23.85	5500
13	**NCF2_L**	Y	3	Y	24.47	8500
14	**NCF2_M**	Y	3	Y	23.34	8500
15	**NCF2_R**	Y	3	Y	24.67	8500
16	**ADAR_R**	Y	3	Borderline	26.06	4500
17	**FCN1_L**	Y	3	Borderline	25.12	9000
18	**IL10RB_R**	Y	3	Borderline	29.29	850
19	**ITGB2_L**	Y	3	Borderline	25.38	10000
20	**ITGB2_M**	Y	3	Borderline	26.05	10000
21	**NCF1_M**	Y	3	Borderline	25.75	5500

22	DDX58_L	Y	3	N	27.76	350
23	DDX58_M	Y	3	N	26.23	350
24	ITGB2_R	Y	3	N	26.94	10000
25	IVNS1ABP_L	Y	3	N	27.32	750
26	IVNS1ABP_M	Y	3	N	27.75	750
27	IVNS1ABP_R	Y	3	N	27.04	750
28	NLRP1_L	Y	3	N	27.19	600
29	NLRP1_M	Y	3	N	28.43	600
30	NLRP1_R	Y	3	N	28.86	600
31	ACTR2_M	Y	2	Y	25.6	2000
32	ADD3_L	Y	2	Y	28.52	1500
33	ADD3_M	Y	2	Y	27.52	1500
34	AIM1_R	Y	2	Y	25.87	1000
35	Clorf38_M	Y	2	Y	28.36	3000
36	CD163_L	Y	2	Y	30.16	200
37	CD27_R	Y	2	Y	30.38	650
38	CD300C_R	Y	2	Y	30.23	500
39	CD53_M	Y	2	Y	24.8	8000
40	CD83_R	Y	2	Y	30.62	150
41	CDC42SE1_M	Y	2	Y	24.71	5000
42	CDC42SE1_R	Y	2	Y	23.98	5000
43	EEF2_M	Y	2	Y	24.21	7000
44	IL7R_M	Y	2	Y	28.7	3500
45	IL7R_R	Y	2	Y	25.75	3500
46	LCP1_L	Y	2	Y	21.5	6500
47	LCP1_M	Y	2	Y	20.64	6500
48	LPXN_M	Y	2	Y	29.63	1100
49	NCL_L	Y	2	Y	25.84	2000

50	**PDLIM2_M**	Y	2	Y	32.12	950
51	**RAF1_L**	Y	2	Y	29.79	3000
52	**RAF1_R**	Y	2	Y	27.03	3000
53	**ROCK2_R**	Y	2	Y	30.52	200
54	**SERPINA1_R**	Y	2	Y	22.03	7500
55	**ZAP70_M**	Y	2	Y	31.33	650
56	**ZAP70_R**	Y	2	Y	30.42	650
57	**ADD1_L**	Y	2	Borderline	29.43	750
58	**AIM1_M**	Y	2	Borderline	30.45	1000
59	**CD53_R**	Y	2	Borderline	25.9	8000
60	**EEF2_R**	Y	2	Borderline	25.62	7000
61	**LASP1_L**	Y	2	Borderline	25.2	4500
62	**LASP1_M**	Y	2	Borderline	25.16	4500
63	**LASP1_R**	Y	2	Borderline	27.18	4500
64	**LCP1_R**	Y	2	Borderline	25.14	6500
65	**LPXN_L**	Y	2	Borderline	31.64	1100
66	**LPXN_R**	Y	2	Borderline	32.09	1100
67	**LY75_M**	Y	2	Borderline	29.01	800
68	**LY75_R**	Y	2	Borderline	29.3	800
69	**NCF4_L**	Y	2	Borderline	27.61	4500
70	**NCF4_M**	Y	2	Borderline	26.89	4500
71	**OAS2_L**	Y	2	Borderline	29.97	500
72	**PDLIM1_R**	Y	2	Borderline	28.5	900
73	**RAF1_M**	Y	2	Borderline	30.47	3000
74	**TREM1_L**	Y	2	Borderline	29.63	4500
75	**TREM1_M**	Y	2	Borderline	27.6	4500
76	**TREM1_R**	Y	2	Borderline	26.76	4500
77	**ACTR2_L**	Y	2	N	22.72	2000

78	**ACTR2_R**	Y	2	N	23.17	2000
79	**ADD1JVI**	Y	2	N	26.79	750
80	**ADD1_R**	Y	2	N	25.43	750
81	**ADD3_R**	Y	2	N	24.17	1500
82	**CAPN2_L**	Y	2	N	28.04	750
83	**CAPN2_M**	Y	2	N	23.88	750
84	**CAPN2_R**	Y	2	N	25.15	750
85	**CD163_R**	Y	2	N	27.83	200
86	**CD68_L**	Y	2	N	21.75	250
87	**CD68_R**	Y	2	N	26.03	250
88	**LTF_R**	Y	2	N	26.59	200
89	**NCF4_R**	Y	2	N	31.58	4500
90	**NCL_M**	Y	2	N	24.24	2000
91	**NCL_R**	Y	2	N	23.39	2000
92	**NCOA1J.**	Y	2	N	24.7	850
93	**NC0A1_M**	Y	2	N	24.74	850
94	**NCOAl_R**	Y	2	N	28.05	850
95	**OAS2_M**	Y	2	N	27.23	500
96	**OAS2_R**	Y	2	N	27.08	500
97	**OAS3_M**	Y	2	N	28.86	650
98	**OAS3_R**	Y	2	N	28.94	650
99	**PDLIM1_M**	Y	2	N	28.2	900
100	**ROCK2_L**	Y	2	N	23.81	200
101	**TES_L**	Y	2	N	24.23	750
102	**TES_M**	Y	2	N	28.61	750
103	**TES_R**	Y	2	N	28.19	750
104	**ACTB_L**	Y	0	Y	23.94	10,000
105	**ACTB_R**	Y	0	Y	21.05	10,000

106	**CSF3R_R**	Y	0	Y	24.48	6500
107	**GAPDH_L**	Y	0	Y	24.86	10,000
108	**GZMB_R**	Y	0	Y	26.09	1500
109	**IL6R_L**	Y	0	Y	33.75	500
110	**LILRA5J.**	Y	0	Y	31.33	900
111	**SELLJ.**	Y	0	Y	23.45	8500
112	**SELL_M**	Y	0	Y	24.48	8500
113	**S0RL1_L**	Y	0	Y	24.67	7500
114	**S0RL1_R**	Y	0	Y	23.58	7500
115	**STAT6_M**	Y	0	Y	25.57	1000
116	**STAT6_R**	Y	0	Y	27.98	1000
117	**TXNIP_L**	Y	0	Y	20.2	8000
118	**TXNIP_M**	Y	0	Y	21.64	8000
119	**TXNIP_R**	Y	0	Y	23.75	8000
120	**VIM_R**	Y	0	Y	23.24	9500
121	**LILRA5_R**	Y	0	Borderline	28.1	900
122	**S0RL1_M**	Y	0	Borderline	26.09	7500
123	**VIM_M**	Y	0	Borderline	25.75	9500
124	**CSF3R_M**	Y	0	N	28.15	6500
125	**GAPDH_R**	Y	0	N	26.97	10,000
126	**IL6R_M**	Y	0	N	28.1	500
127	**IL6R_R**	Y	0	N	25.48	500
128	**SELL_R**	Y	0	N	27.05	8500
129	**STAT6_L**	Y	0	N	24.32	1000
130	**STX4_L**	Y	0	N	25.6	600
131	**STX4_R**	Y	0	N	28.74	600
132	**SYNE2_L**	Y	0	N	28.29	400
133	**SYNE2_M**	Y	0	N	25.49	400

134	**KLRF1_L**	N	3	Y	33.13	650
135	**KLRF1_M**	N	3	Y	34.44	650
136	**KLRF1_R**	N	3	Y	33.78	650
137	**TRPM2J.**	N	3	Y	33.37	400
138	**TRPM2_M**	N	3	Y	33.62	400
139	**TRPM2_R**	N	3	Y	34.77	400
140	**ADAR_L**	N	3	Borderline	25.6	4500
141	**FCN1_M**	N	3	Borderline	25.54	9000
142	**DDX58_R**	N	3	N	27.8	350
143	**Clorf38_L**	N	2	Y	27.49	3000
144	**CD27_M**	N	2	Y	32.29	650
145	**CD300C_L**	N	2	Y	32.63	500
146	**CD300C_M**	N	2	Y	30.4	500
147	**CD53_L**	N	2	Y	23.36	8000
148	**CD83_L**	N	2	Y	36.63	150
149	**CD83_M**	N	2	Y	34.82	150
150	**IL15RA_L**	N	2	Y	35.19	300
151	**IL15RA_R**	N	2	Y	35.75	300
152	**IL7R_L**	N	2	Y	27.07	3500
153	**LTF_L**	N	2	Y	35.73	200
154	**LY75_L**	N	2	Y	31.38	800
155	**OAS3_L**	N	2	Y	31.77	650
156	**PDLIM1_L**	N	2	Y	31.95	900
157	**PDLIM2_L**	N	2	Y	30.75	950
158	**PDLIM2_R**	N	2	Y	38.02	950
159	**ROCK2_M**	N	2	Y	30.81	200
160	**SERPINA1_L**	N	2	Y	24.63	7500
161	**ZAP70_L**	N	2	Y	36.56	650

162	**AIM1_L**	N	2	Borderline	30.33	1000
163	**Clorf38_R**	N	2	Borderline	32.82	3000
164	**SERPINA1_M**	N	2	Borderline	25.22	7500
165	**CD163_M**	N	2	N	28.45	200
166	**CD27_L**	N	2	N	29.18	650
167	**CD68_M**	N	2	N	27.65	250
168	**CDC42SE1_L**	N	2	N	30.86	5000
169	**EEF2_L**	N	2	N	28.43	7000
170	**IL15RA_M**	N	2	N	29.39	300
171	**LTF_M**	N	2	N	28.3	200
172	**BACH2_L**	N	0	Y	34.45	150
173	**BACH2_R**	N	0	Y	30.93	150
174	**GZMB_L**	N	0	Y	29.68	1500
175	**GZMB_M**	N	0	Y	28.02	1500
176	**LILRA5_M**	N	0	Y	30.11	900
177	**SELP_L**	N	0	Y	31.32	700
178	**SELP_M**	N	0	Y	32.15	700
179	**SELP_R**	N	0	Y	35.16	700
180	**STX4_M**	N	0	Y	30.42	600
181	**SYNE2_R**	N	0	Y	32.43	400
182	**CSF3R_L**	N	0	Borderline	26.1	6500
183	**BACH2_M**	N	0	N	27.36	150
184	**VIM_L**	N	0	N	36.39	9500

APPENDIX IX

RNA quality data for freeze/thaw cycle treatment (lanes 1-5) and heat treatment (lanes 6-10):

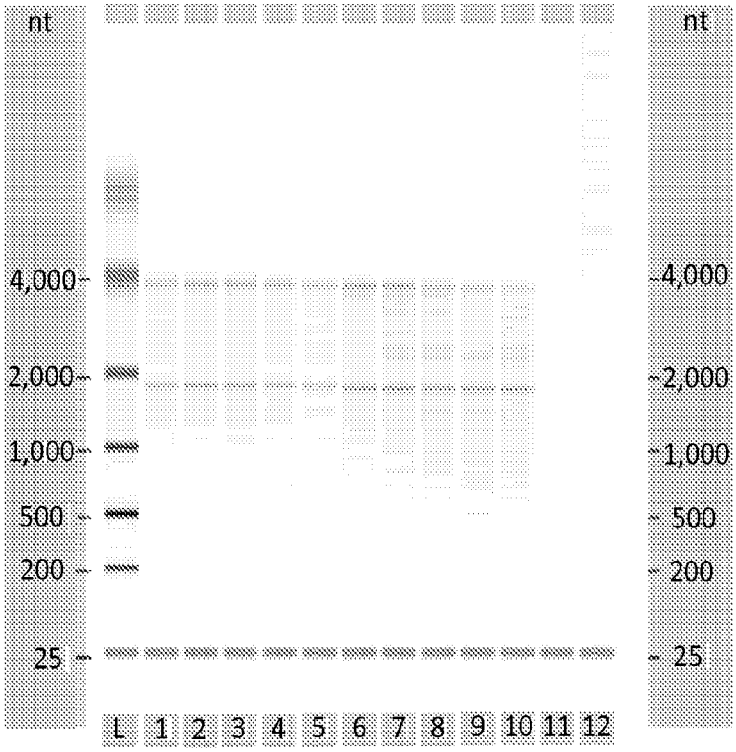

Lane Key:

Lane 1: F/T 0 cycles

Lane 2: F/T 3 cycles

Lane 3: F/T 6 cycles

Lane 4: F/T 9 cycles

Lane 5: F/T 12 cycles

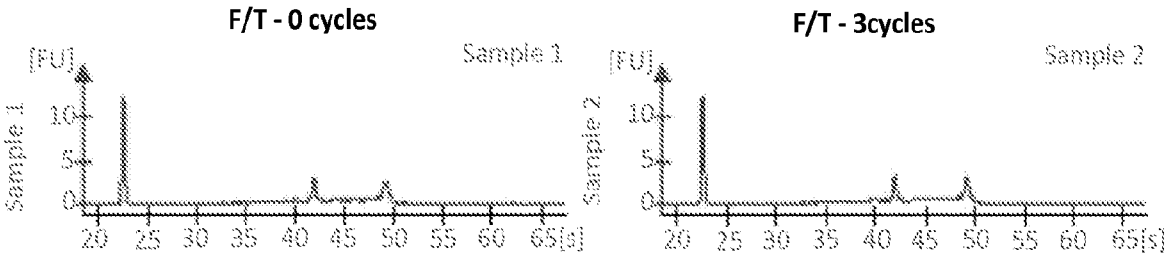

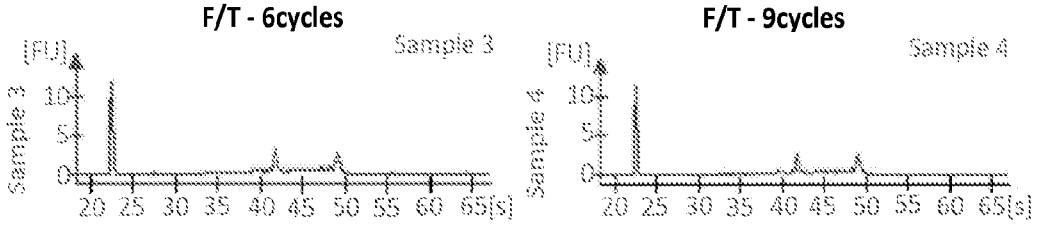
F/T - 6cycles
Sample 3
[FU]
Sample 3
10
5
0
20 25 30 35 40 45 50 55 60 65[s]
F/T - 9cycles
Sample 4
[FU]
Sample 4
10
5
0
20 25 30 35 40 45 50 55 60 65[s]

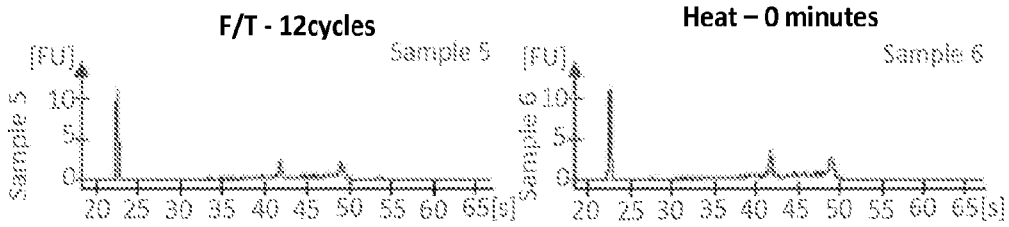
F/T - 12cycles
Sample 5
[FU]
Sample 5
10
5
0
20 25 30 35 40 45 50 55 60 65[s]
Heat – 0 minutes
Sample 6
[FU]
Sample 6
10
5
0
20 25 30 35 40 45 50 55 60 65[s]

5

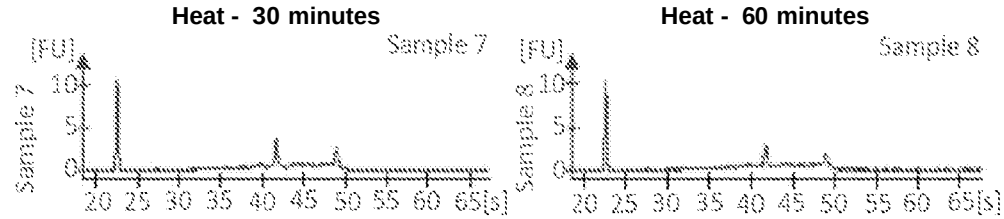
Heat - 30 minutes
Sample 7
[FU]
Sample 7
10
5
0
20 25 30 35 40 45 50 55 60 65[s]
Heat - 60 minutes
Sample 8
[FU]
Sample 8
10
5
0
20 25 30 35 40 45 50 55 60 65[s]

10

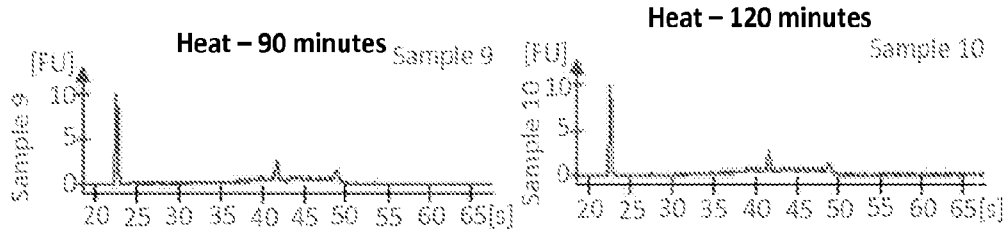
Heat – 90 minutes
Sample 9
[FU]
Sample 9
10
5
0
20 25 30 35 40 45 50 55 60 65[s]
Heat – 120 minutes
Sample 10
[FU]
Sample 10
10
5
0
20 25 30 35 40 45 50 55 60 65[s]

RNA quality data for RNase A degradation treatment (lanes 1-7):

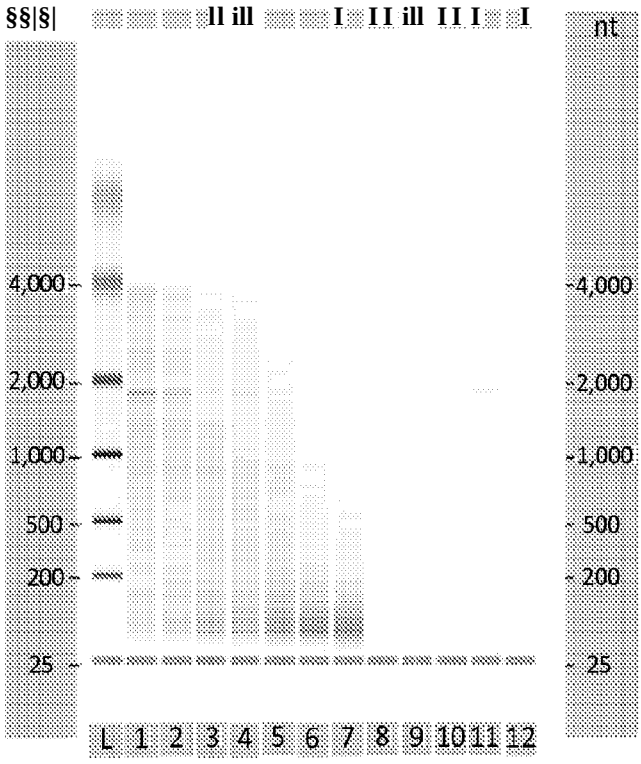

Lane Key:

Lane 1: F/T 0 cycles

Lane 2: F/T 3 cycles

Lane 3: F/T 6 cycles

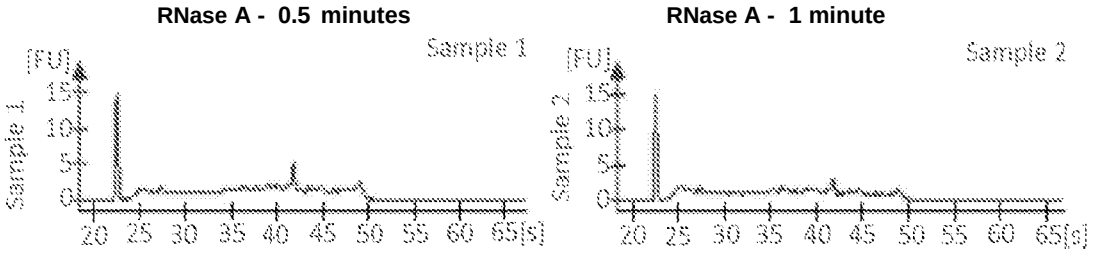

5

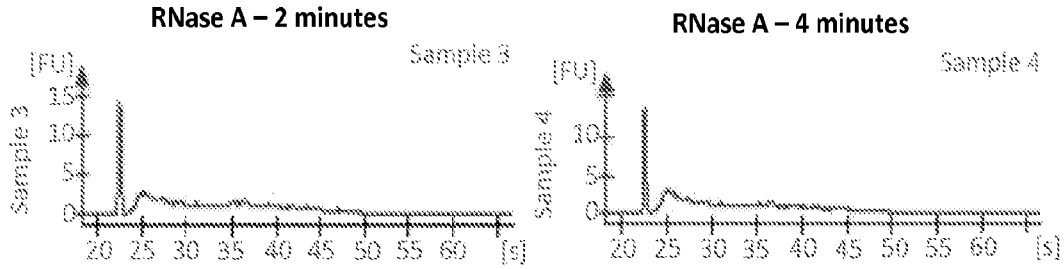

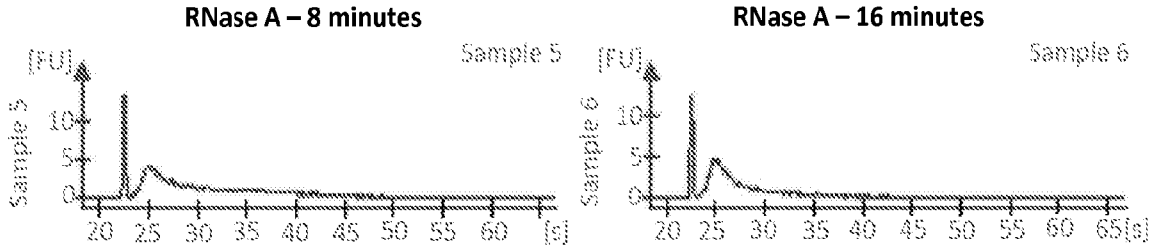
RNase A – 8 minutes
Sample 5
[FU]
Sample 5
10
5
0
20 25 30 35 40 45 50 55 60 [s]
RNase A – 16 minutes
Sample 6
[FU]
Sample 6
10
5
0
20 25 30 35 40 45 50 55 60 65[s]

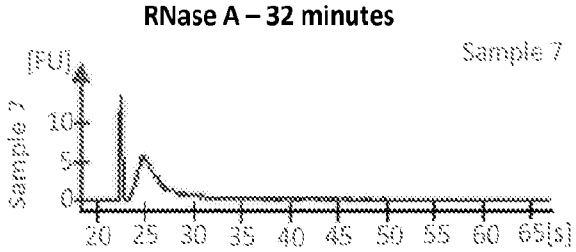
RNase A – 32 minutes
Sample 7
[FU]
Sample 7
10
5
0
20 25 30 35 40 45 50 55 60 65[s]

APPENDIX X

Nanodrop ND-8000 Native RNA Yield Data:

Sample ID	ng/µl	A260	A280	260/280	260/230	Constant	Yield (µg)
Pre-Cleanup	47.86	1.196	0.529	2.26	0.37	40.00	3.35
Post-Cleanup	48.38	1.209	0.591	2.04	1.77	40.00	3.38

Pre-Cleanup Bioanalyzer 2100 Data:

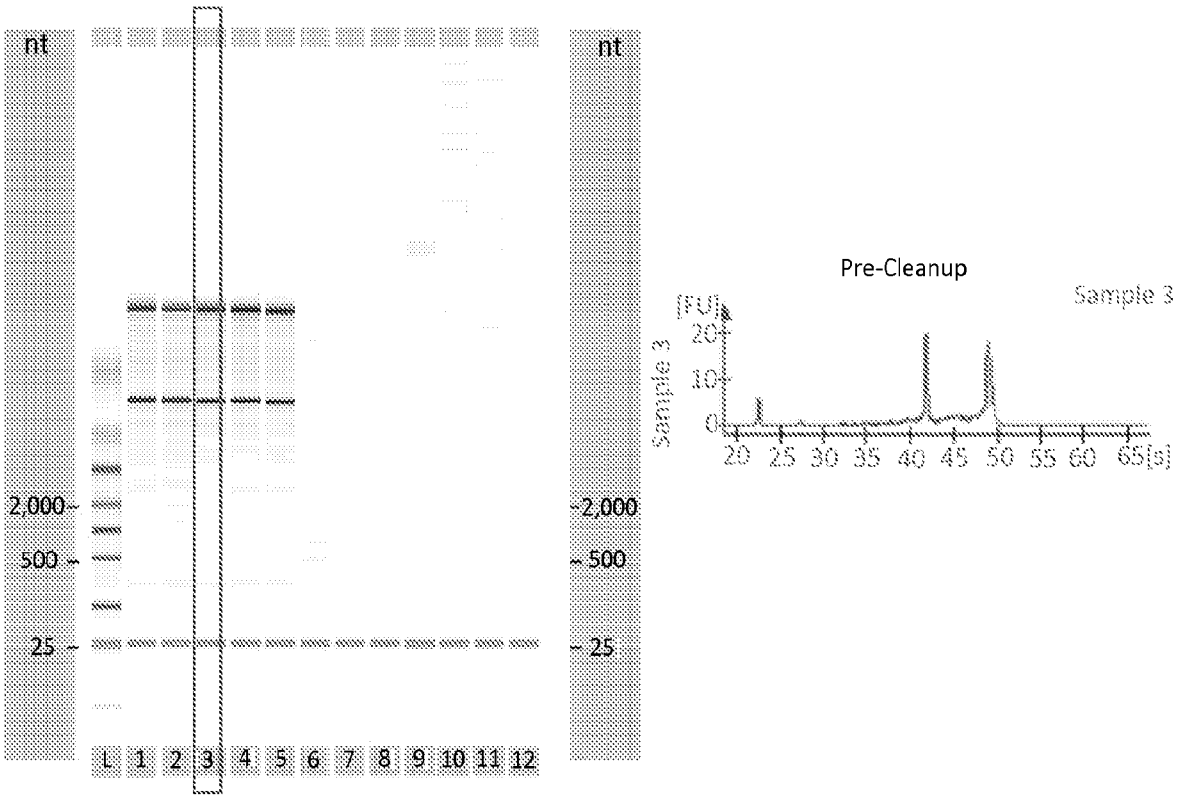

Post-Cleanup Bioanalyzer 2100 Data:

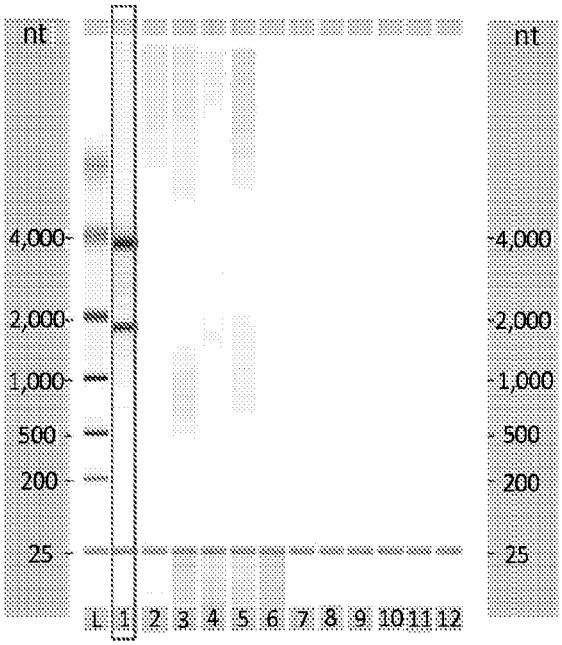

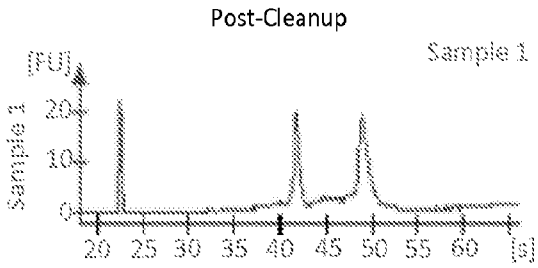

APPENDIX XI

Nanodrop ND-8000 Manually Extracted RNA Yield Data:

Sample ID	ng/µl	A260	A280	260/280	260/230	Constant	Yield (µg)
A	51.01	1.275	0.539	2.37	0.37	40	4.08
B	54.81	1.37	0.582	2.35	0.43	40	4.38
C	47.86	1.196	0.529	2.26	0.37	40	3.83
D	50.08	1.252	0.535	2.34	0.39	40	4.01
E	82.94	2.074	0.952	2.18	0.58	40	6.64

Manually Extracted RNA Bioanalyzer 2100 Data :

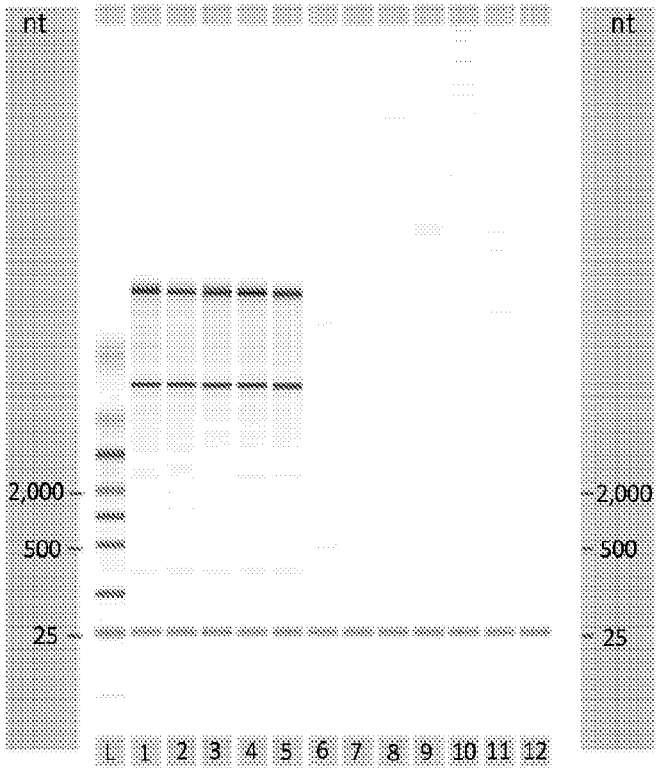

Lane Key:

Lane 1: Sample A

Lane 2: Sample B

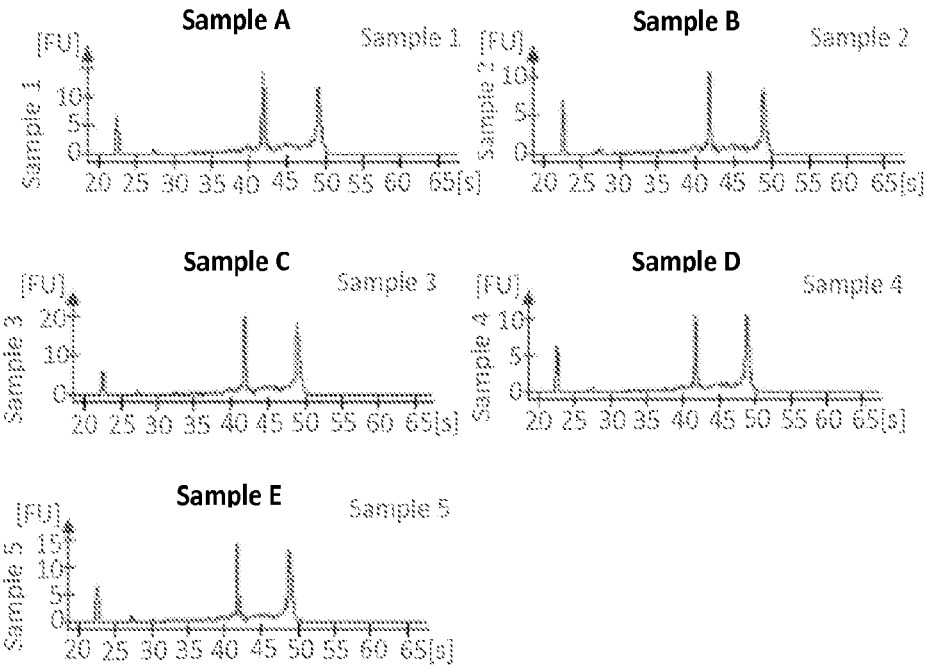

5

APPENDIX XII

Nanodrop ND-8000 RNase A Degradation and Column-Purified RNA Yield Data:

Sample ID	ng/µl	A260	A280	260/280	260/230	Constant
RNase A - 0.5 minute	21.55	0.539	0.298	1.81	0.39	40.00
RNase A - 1 minute	21.95	0.549	0.321	1.71	0.63	40.00
RNase A - 2 minutes	19.18	0.480	0.272	1.76	0.62	40.00
RNase A - 4 minutes	23.66	0.591	0.364	1.63	0.24	40.00
RNase A - 8 minutes	19.43	0.486	0.289	1.68	0.25	40.00
RNase A - 16 minutes	11.43	0.286	0.186	1.53	0.74	40.00

RNase A Degradation and Column-Purified RNA Bioanalyzer 2100 Data:

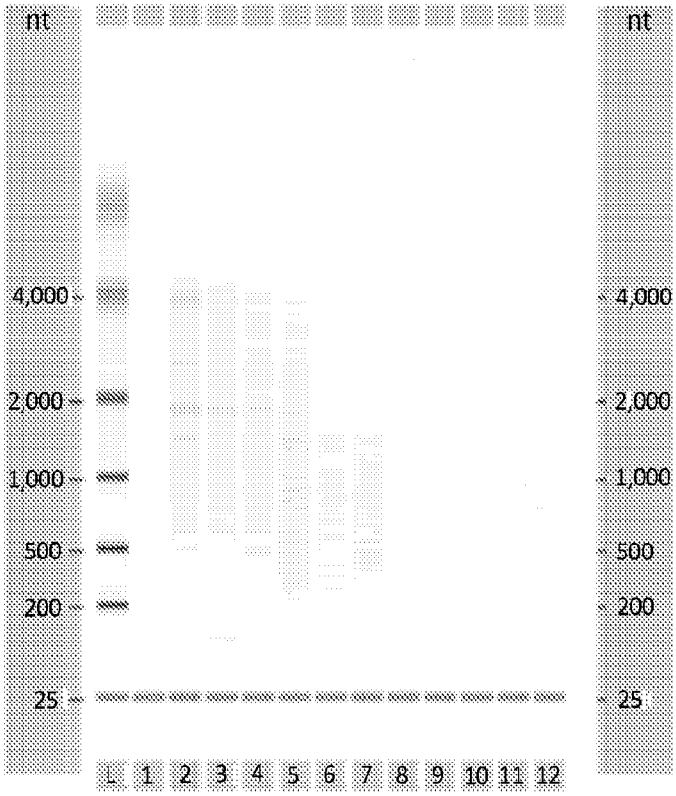

Lane Key:

Lane 2: RNase A – 0.5 minute

Lane 3: RNase A – 1 minute

Lane 4: RNase A – 2 minutes

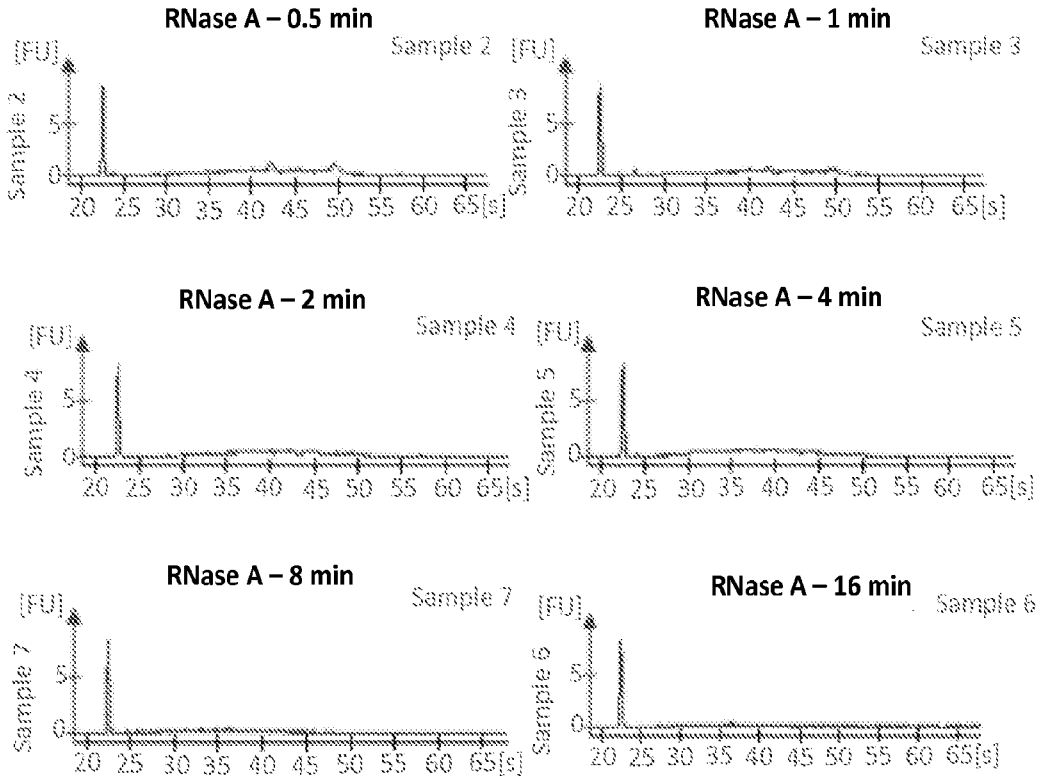
RNase A – 0.5 min
Sample 2
[FU]
Sample 2
5
0
20 25 30 35 40 45 50 55 60 65[s]
RNase A – 1 min
Sample 3
[FU]
Sample 3
5
0
20 25 30 35 40 45 50 55 60 65[s]
RNase A – 2 min
Sample 4
[FU]
Sample 4
5
0
20 25 30 35 40 45 50 55 60 65[s]
RNase A – 4 min
Sample 5
[FU]
Sample 5
5
0
20 25 30 35 40 45 50 55 60 65[s]
RNase A – 8 min
Sample 7
[FU]
Sample 7
5
0
20 25 30 35 40 45 50 55 60 65[s]
RNase A – 16 min
Sample 6
[FU]
Sample 6
5
0
20 25 30 35 40 45 50 55 60 65[s]

5

APPENDIX XIII

RNA Degradation: cDNA Synthesis and Amplification Quality Control Data

Nanodrop ND-8000 cDNA Yield Data:

Sample ID	ng/µl	A260	A280	260/280	260/230	Constant	Yield (µg)
RNase A - 0 minute	302.51	9.167	4.673	1.96	2.19	33	9.08
RNase A - 0.5 minute	233.56	7.077	3.624	1.95	2.17	33	7.01
RNase A - 1 minute	214.29	6.494	3.321	1.96	2.19	33	6.43
RNase A - 2 minutes	205.72	6.234	3.162	1.97	2.2	33	6.17
RNase A - 4 minutes	200.53	6.077	3.119	1.95	2.17	33	6.02
RNase A - 8 minutes	178.55	5.411	2.781	1.95	2.14	33	5.36
RNase A - 16 minutes	160	4.848	2.486	1.95	2.15	33	4.80

LabChip 90 HT Microcapillary Electrophoresis cDNAQuality Data:

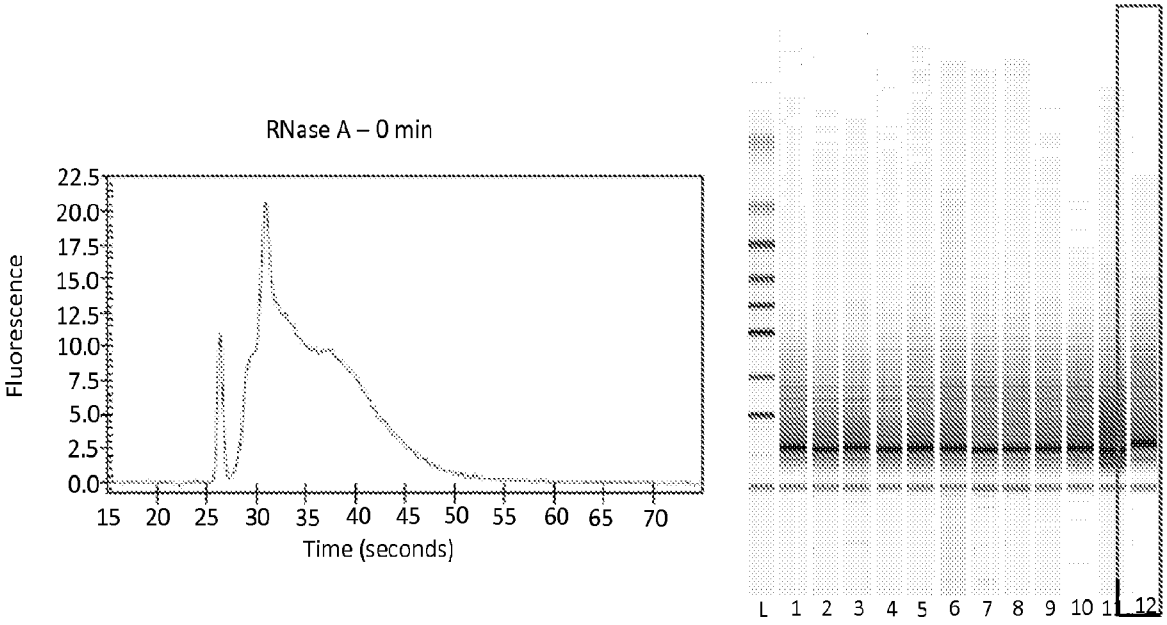

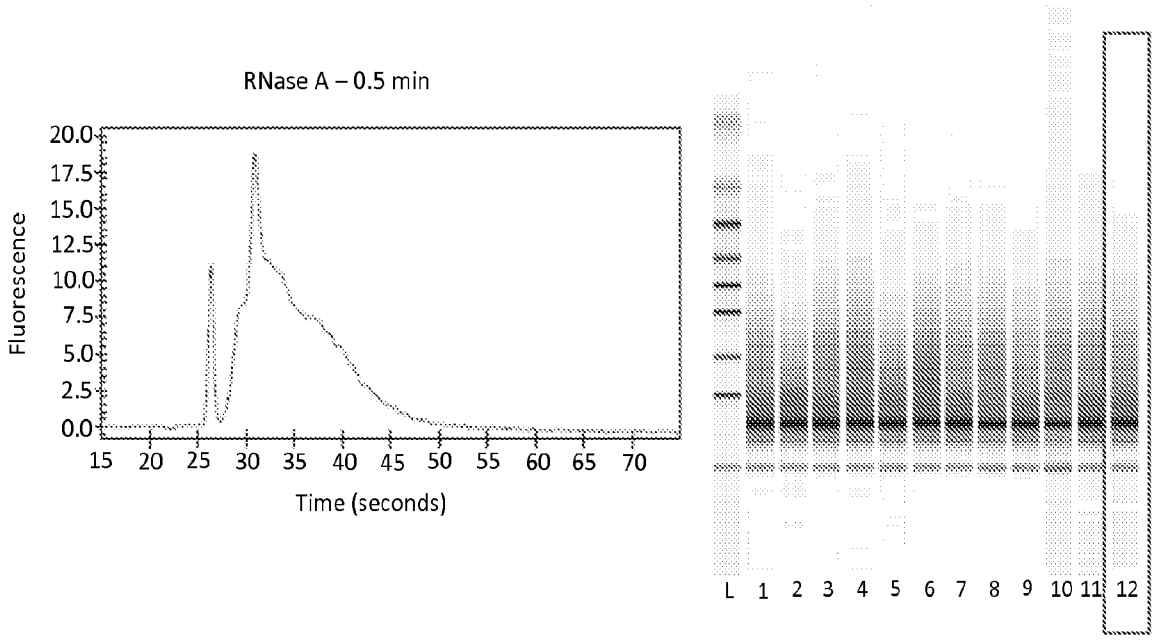

LabChip 90 HT Microcapillary Electrophoresis cDNAQuality Data (continued):

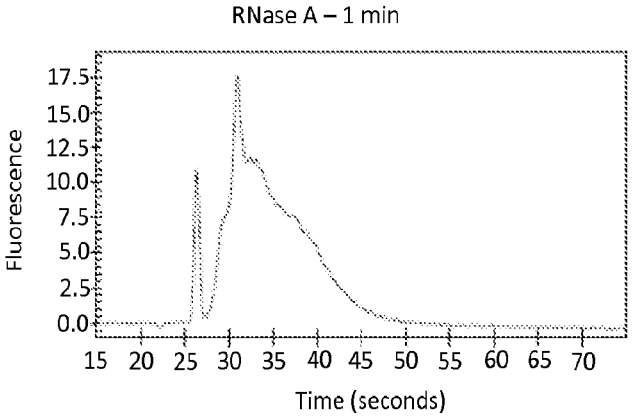

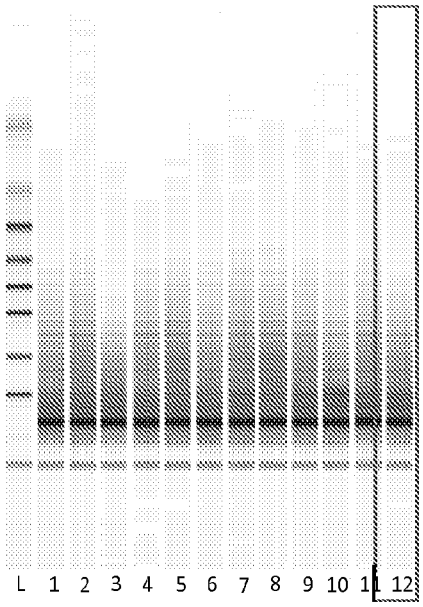

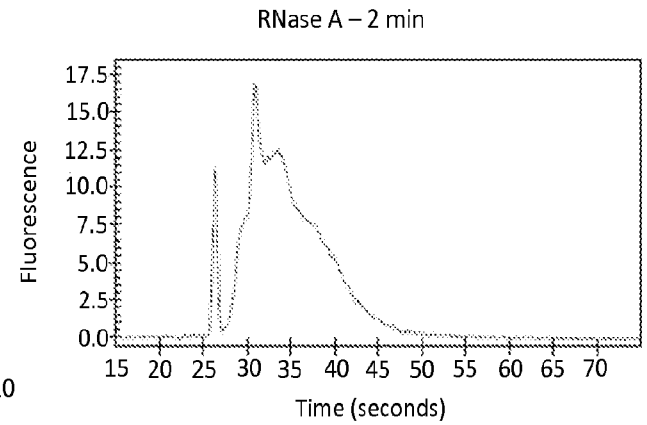

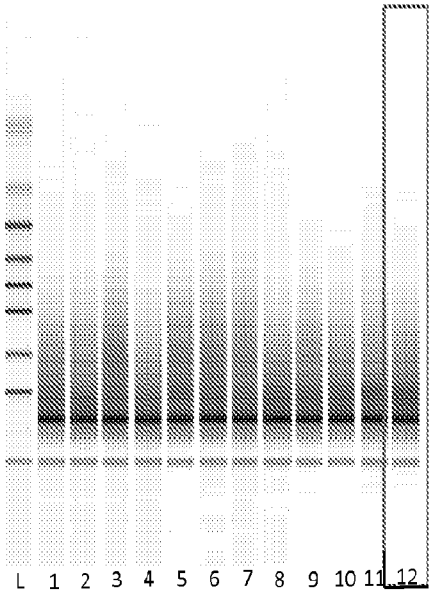

LabChip 90 HT Microcapillary Electrophoresis cDNAQuality Data (continued):

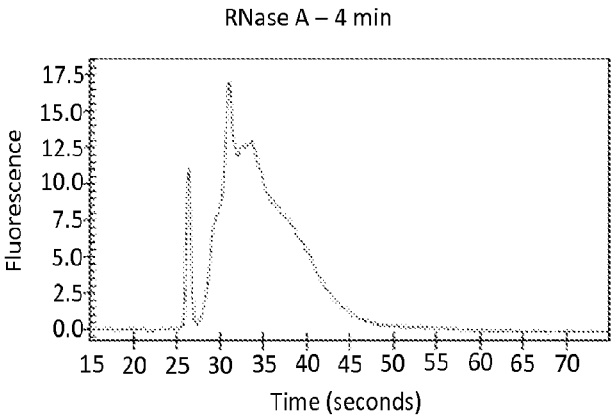

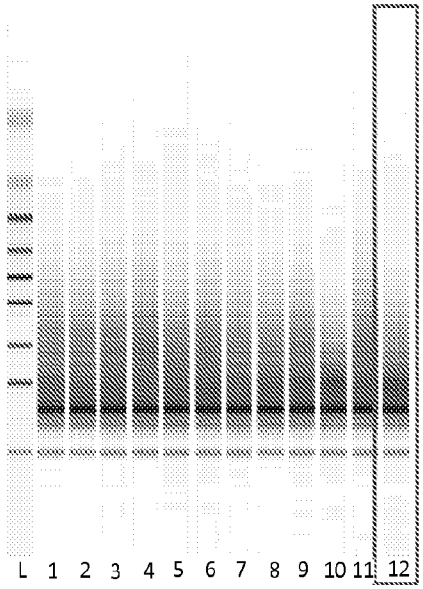

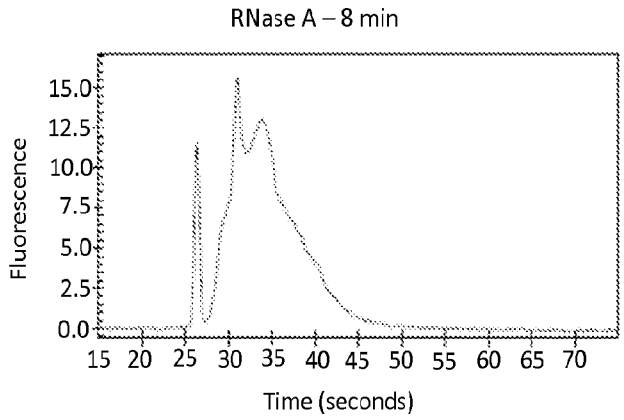

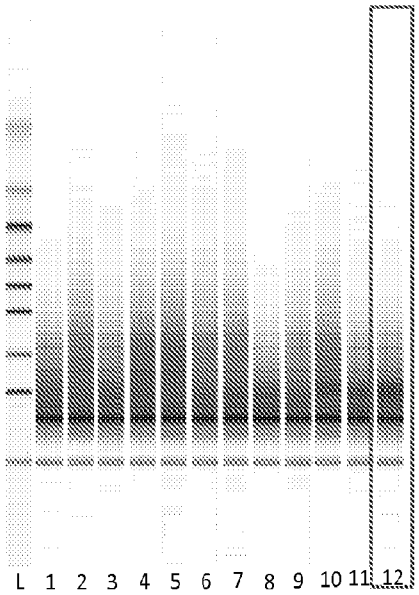

LabChip 90 HT Microcapillary Electrophoresis cDNAQuality Data (continued):

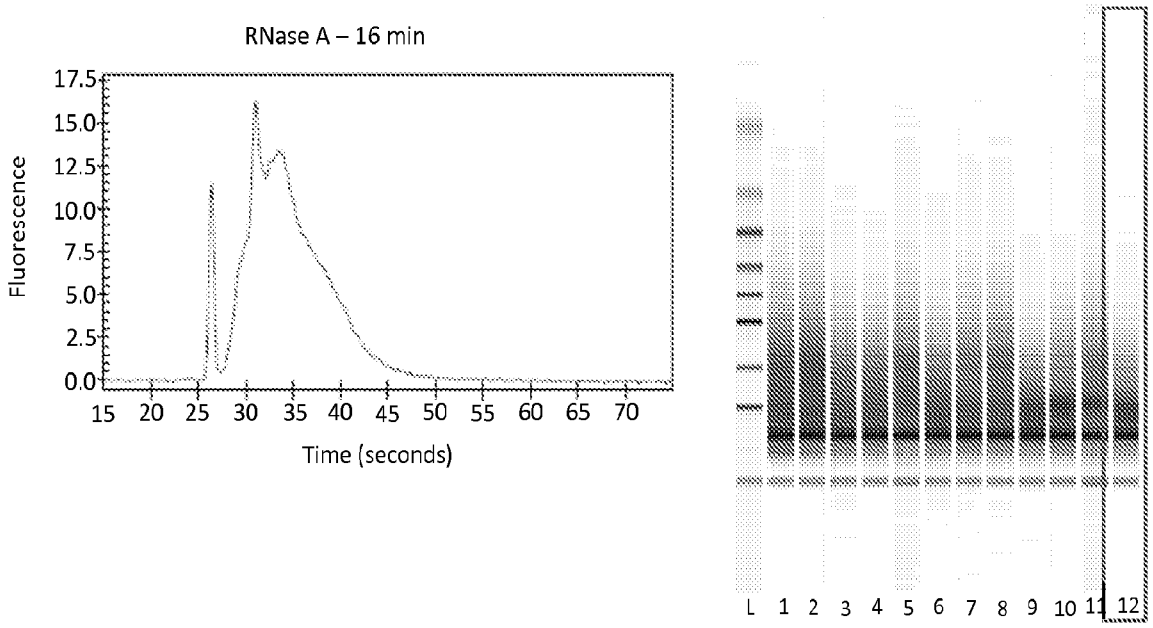

5

APPENDIX XIV

General Plate Map for Degraded RNA qPCR Reactions:

- Numbers refer to unique assays
- 'NTC' stands for No Template Control; these wells contain only assay master mix but no cDNA sample

		1	2	3	4	5	6	7	8	9	10	11	12	13	14	15	16	17	18	19	20	21	22	23	24
0	A	1	1	2	2	3	3	4	4	5	5	6	6	7	7	8	8	9	9	10	10	11	11	12	12
	B	1	NTC	2	NTC	3	NTC	4	NTC	5	NTC	6	NTC	7	NTC	8	NTC	9	NTC	10	NTC	11	NTC	12	NTC
0.5	C	1	1	2	2	3	3	4	4	5	5	6	6	7	7	8	8	9	9	10	10	11	11	12	12
	D	1	NTC	2	NTC	3	NTC	4	NTC	5	NTC	6	NTC	7	NTC	8	NTC	9	NTC	10	NTC	11	NTC	12	NTC
1	E	1	1	2	2	3	3	4	4	5	5	6	6	7	7	8	8	9	9	10	10	11	11	12	12
	F	1	NTC	2	NTC	3	NTC	4	NTC	5	NTC	6	NTC	7	NTC	8	NTC	9	NTC	10	NTC	11	NTC	12	NTC
2	G	1	1	2	2	3	3	4	4	5	5	6	6	7	7	8	8	9	9	10	10	11	11	12	12
	H	1	NTC	2	NTC	3	NTC	4	NTC	5	NTC	6	NTC	7	NTC	8	NTC	9	NTC	10	NTC	11	NTC	12	NTC
4	I	1	1	2	2	3	3	4	4	5	5	6	6	7	7	8	8	9	9	10	10	11	11	12	12
	J	1	NTC	2	NTC	3	NTC	4	NTC	5	NTC	6	NTC	7	NTC	8	NTC	9	NTC	10	NTC	11	NTC	12	NTC
8	K	1	1	2	2	3	3	4	4	5	5	6	6	7	7	8	8	9	9	10	10	11	11	12	12
	L	1	NTC	2	NTC	3	NTC	4	NTC	5	NTC	6	NTC	7	NTC	8	NTC	9	NTC	10	NTC	11	NTC	12	NTC
16	M	1	1	2	2	3	3	4	4	5	5	6	6	7	7	8	8	9	9	10	10	11	11	12	12
	N	1	NTC	2	NTC	3	NTC	4	NTC	5	NTC	6	NTC	7	NTC	8	NTC	9	NTC	10	NTC	11	NTC	12	NTC
	O	-	-	-	-	-	-	-	-	-	-	-	-	-	-	-	-	-	-	-	-	-	-	-	-
	P	-	-	-	-	-	-	-	-	-	-	-	-	-	-	-	-	-	-	-	-	-	-	-	-

APPENDIX XV

Degraded RNA: Expression Data and Descriptive Statistics

- Average C_T is the average of three technical replicates
- Overall Average C_T is the average of three technical replicates of all four samples
- 'Undet.' indicates that the C_T value was undetermined for that sample

Detector	Threshold	Avg C_T 0 min	Avg C_T 0.5 min	Avg C_T 1 min	Avg C_T 2 min	Avg C_T 4 min	Avg C_T 8 min	Avg C_T 16 min	Overall Avg C_T	Overall StDev
ACTB_L	0.051	24.98	25.5	25.82	25.95	25.74	25.98	26.31	25.75	0.5
ACTB_R	0.065	21.72	22.31	23.01	22.91	22.78	23.18	23.5	22.77	0.593
ARPC5_L	0.076	21.79	22.41	23.34	23.27	22.89	23.94	23.88	23.07	0.747
ARPC5_M	0.146	20.98	21.62	22.47	22.86	22.52	23.18	23.62	22.46	0.879
ARPC5_R	0.061	21.28	22.15	22.59	22.97	22.83	23.72	24.3	22.84	0.949
F13A1_L	0.116	28.51	29.18	29.73	28.06	30.26	30	29.32	29.27	0.788
F13A1_M	0.158	27.49	29.45	29.54	30.55	31.14	31.16	36.83	30.58	2.478
F13A1_R	0.161	28.14	29.52	29.23	31.04	29.7	31.42	31.35	30.06	1.19
IL10RB_L	0.086	29.73	31.22	30.53	33.3	32.47	36.23	35.79	32.75	2.416
IL10RB_M	0.104	30.64	31.59	31.79	32.53	31.48	33.71	33.83	32.22	1.174
IL10RB_R	0.096	29.92	30.49	31.91	32.15	30.13	33.59	34.03	31.75	1.599
ITGB2_L	0.125	27.48	27.81	28.64	28.77	28.7	29.82	32.1	29.04	1.469
ITGB2_M	0.078	27.59	28.43	28.56	27.71	28.26	29.09	28.03	28.22	0.563
ITGB2_R	0.035	28.92	29.34	30.7	30.23	30.15	29.84	31.24	30.06	0.999
IVNS1ABP_L	0.112	27.48	28.81	28.86	29.41	28.62	31.63	26.31	28.73	1.573
IVNS1ABP_M	0.035	27.82	28.31	29.57	28.87	29.95	30.35	31.73	29.51	1.309
IVNS1ABP_R	0.075	27.07	28.55	28.03	29.25	28.21	30.69	32.27	29.15	1.699
KLRF1_L	0.04	31.48	32.5	32.36	34.74	31.53	35.81	37.69	33.53	2.165
KLRF1_M	0.026	32.6	33.81	34.61	34.95	33.91	36.54	38.48	34.59	1.596
KLRF1_R	0.099	33.5	34.89	35.17	33.94	33.18	35.68	33.05	34.2	1.004
NCF1_L	0.119	25.11	25.59	25.67	26.11	26.21	27.22	26.84	26.11	0.709

NCF1_M	0.116	26.02	26.4	26.55	27.24	27.1	27.7	27.63	26.95	0.65
NCF1_R	0.115	24.8	24.64	25.17	24.32	24.3	23.99	24.67	24.56	0.385
NCF2_L	0.09	24.81	25.16	25.35	25.57	25.37	25.43	25.47	25.31	0.264
NCF2_M	0.193	23.97	24.4	24.82	25.17	24.72	24.9	26.01	24.85	0.623
NCF2_R	0.086	24.75	25.88	25.99	26.49	26.36	26.7	29.11	26.47	1.262
NLRP1_L	0.091	27.99	28.42	29.56	30.71	27.9	28.71	29.79	29.01	1.002
NLRP1_M	0.183	27.91	29.23	28.84	30.04	27.77	31.47	31.26	29.5	1.416
NLRP1_R	0.061	29.77	30.46	29.47	33.78	32.27	32.45	33.47	31.67	1.689
TRPM2_L	0.067	34.34	35.72	37.76	37.72	34.73	Undet.	37.07	35.96	1.528
TRPM2_M	0.102	34.86	34.59	37.49	Undet.	35.29	33.08	Undet.	34.58	1.292
TRPM2_R	0.071	36.99	35.44	Undet.	Undet.	Undet.	Undet.	Undet.	35.83	1.228
ZAP70_L	0.097	37.45	Undet.	32.5	38.27	Undet.	Undet.	Undet.	35.11	2.927
ZAP70_M	0.13	31.34	32.36	31.76	33.25	32.34	34.57	Undet.	32.6	1.102
ZAP70_R	0.143	31.37	30.6	34.49	33.31	34.54	32.02	33.74	32.87	1.493

APPENDIX XVI

RNA Degradation Assay Histograms: Sample Average and Overall Average C_T Values

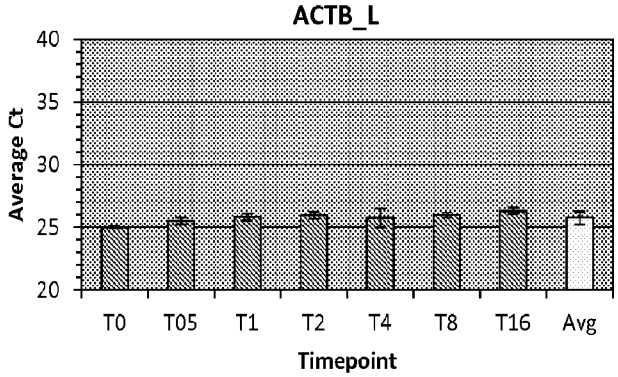

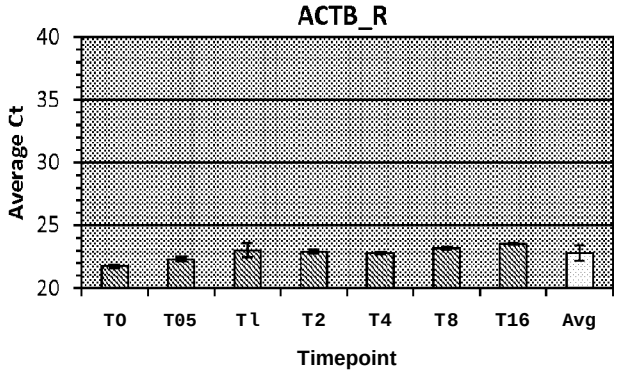

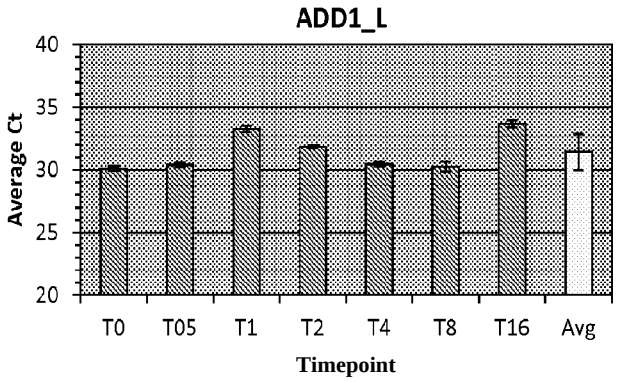
ADD1_L
Average Ct
40
35
30
25
20
T0
T05
T1
T2
T4
T8
T16
Avg
Timepoint

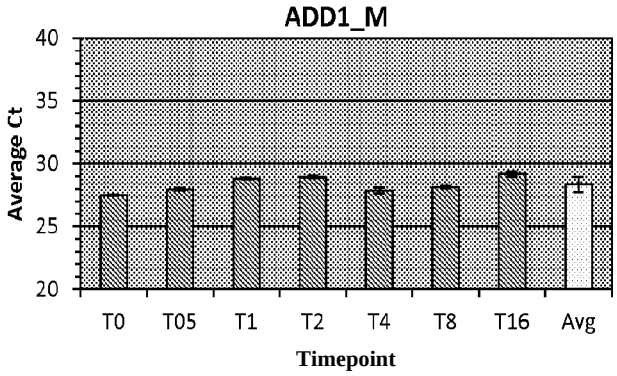
ADD1_M
Average Ct
40
35
30
25
20
T0
T05
T1
T2
T4
T8
T16
Avg
Timepoint

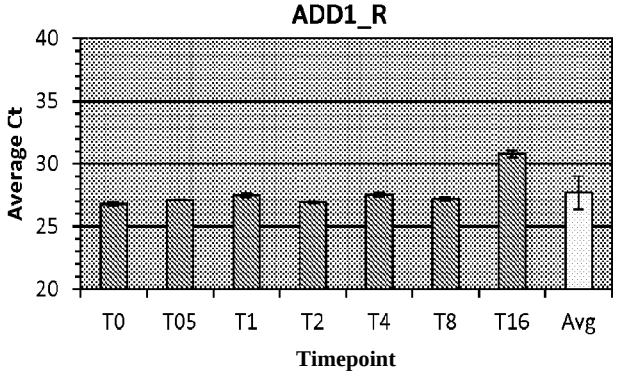
ADD1_R
Average Ct
40
35
30
25
20
T0
T05
T1
T2
T4
T8
T16
Avg
Timepoint

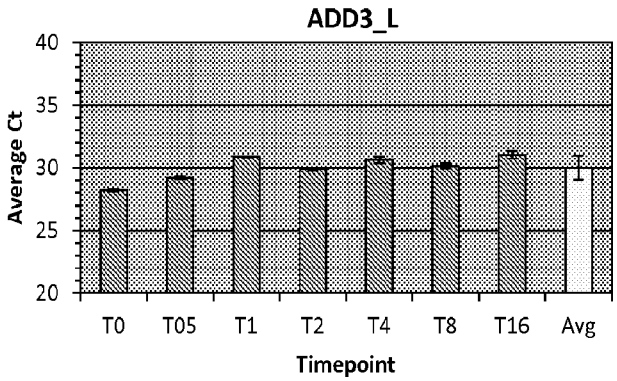
ADD3_L
Average Ct
40
35
30
25
20
T0
T05
T1
T2
T4
T8
T16
Avg
Timepoint

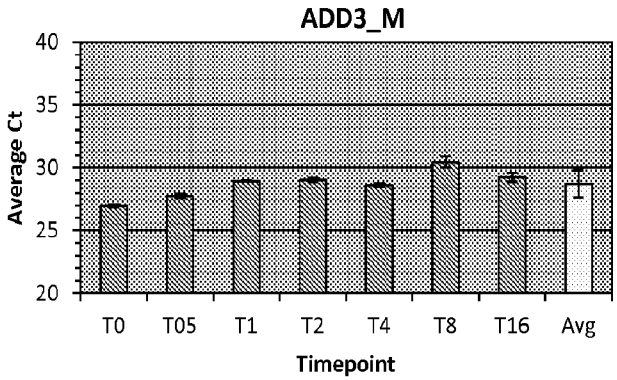
ADD3_M
Average Ct
40
35
30
25
20
T0
T05
T1
T2
T4
T8
T16
Avg
Timepoint

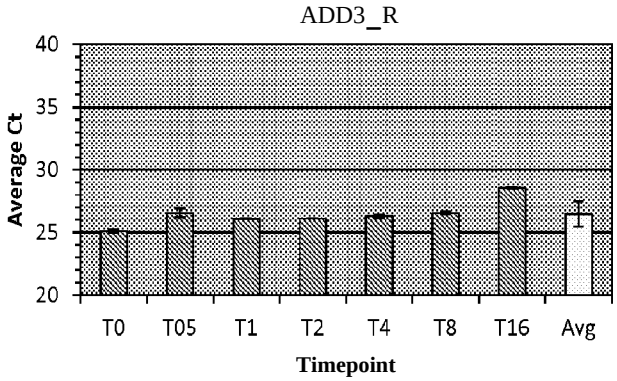
ADD3_R
Average Ct
40
35
30
25
20
T0
T05
T1
T2
T4
T8
T16
Avg
Timepoint

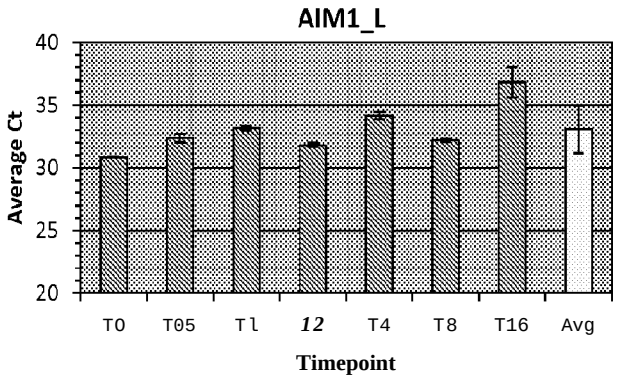
AIM1_L
Average Ct
40
35
30
25
20
T0
T05
Tl
12
T4
T8
T16
Avg
Timepoint

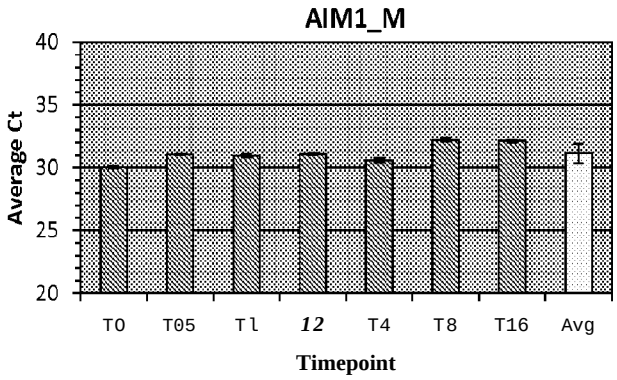
AIM1_M
Average Ct
40
35
30
25
20
T0
T05
Tl
12
T4
T8
T16
Avg
Timepoint

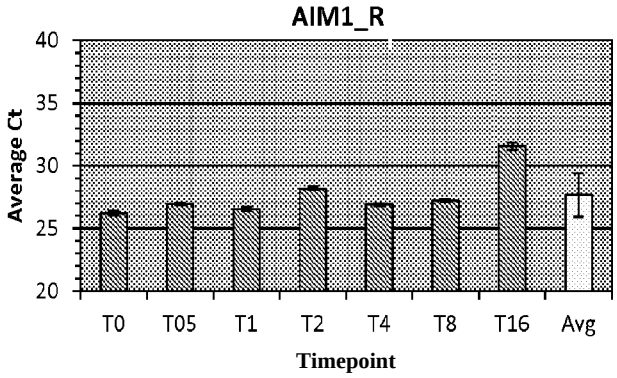
AIM1_R
Average Ct
40
35
30
25
20
T0
T05
T1
T2
T4
T8
T16
Avg
Timepoint

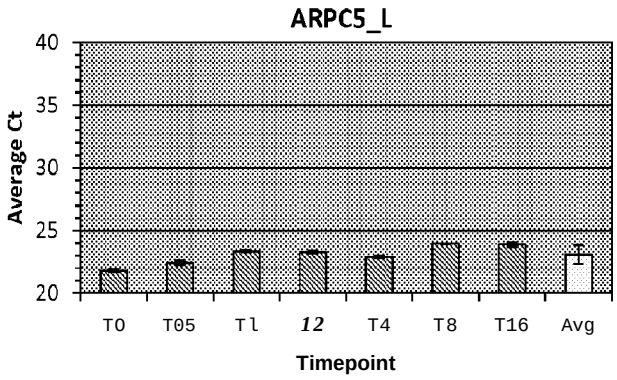
ARPC5_L
Average Ct
40
35
30
25
20
T0
T05
Tl
12
T4
T8
T16
Avg
Timepoint

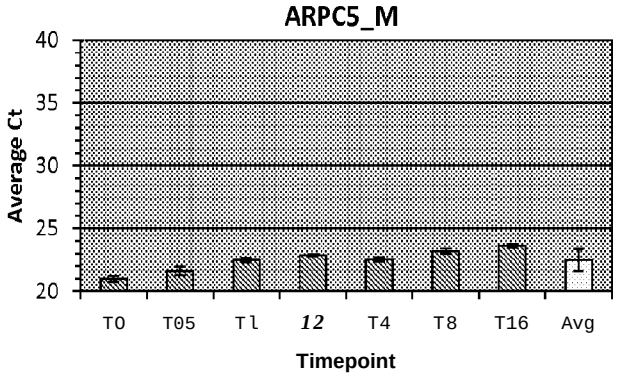
ARPC5_M
Average Ct
40
35
30
25
20
T0
T05
Tl
12
T4
T8
T16
Avg
Timepoint

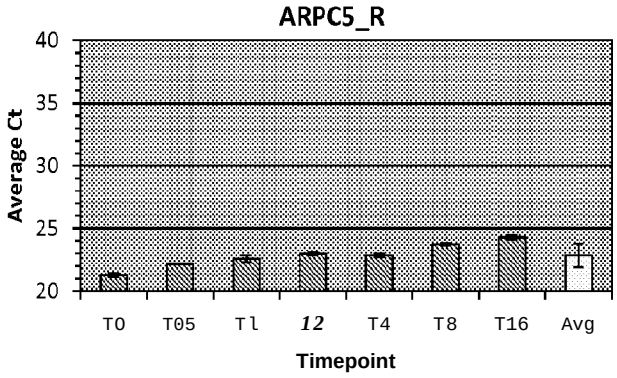
ARPC5_R
Average Ct
40
35
30
25
20
T0
T05
Tl
12
T4
T8
T16
Avg
Timepoint

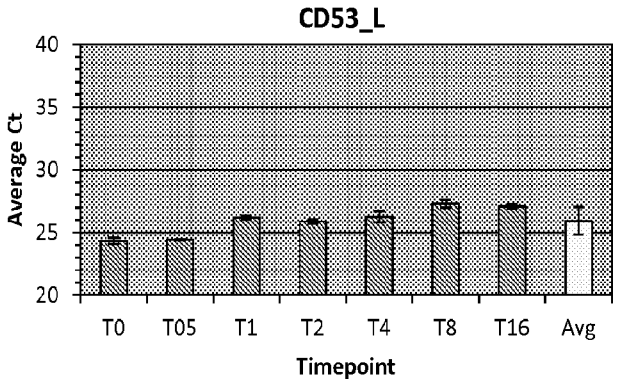
CD53_L
Average Ct
40
35
30
25
20
T0
T05
T1
T2
T4
T8
T16
Avg
Timepoint

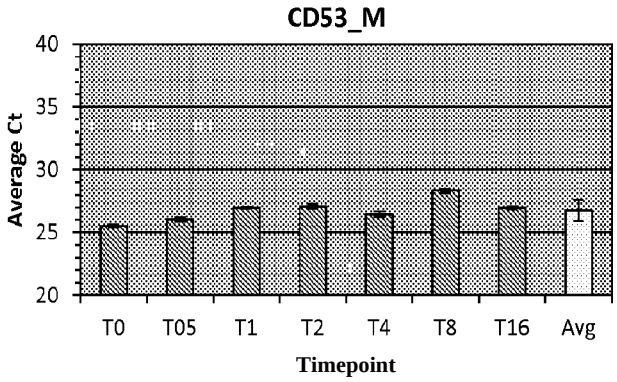
CD53_M
Average Ct
40
35
30
25
20
T0
T05
T1
T2
T4
T8
T16
Avg
Timepoint

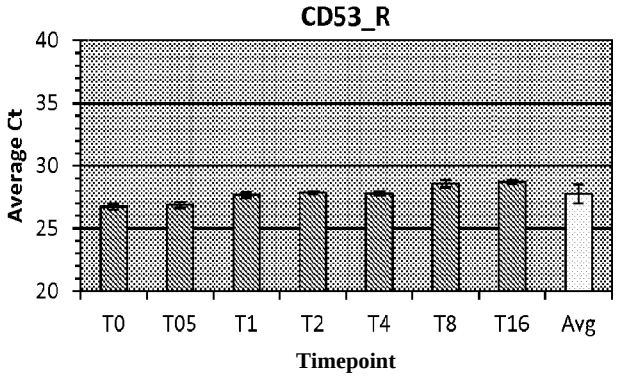
CD53_R
Average Ct
40
35
30
25
20
T0
T05
T1
T2
T4
T8
T16
Avg
Timepoint

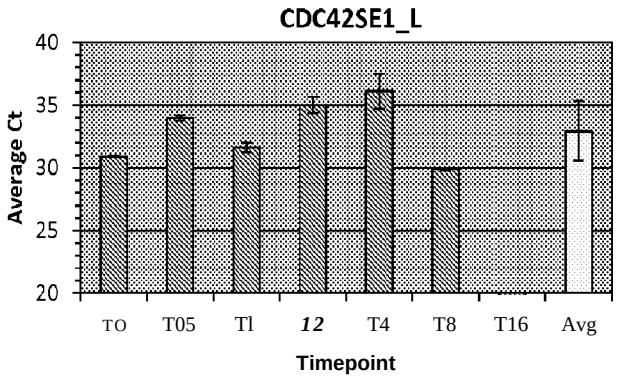
CDC42SE1_L
Average Ct
40
35
30
25
20
TO
T05
Tl
12
T4
T8
T16
Avg
Timepoint

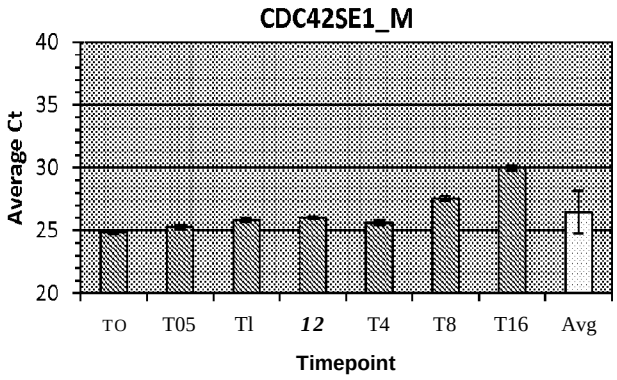
CDC42SE1_M
Average Ct
40
35
30
25
20
TO
T05
Tl
12
T4
T8
T16
Avg
Timepoint

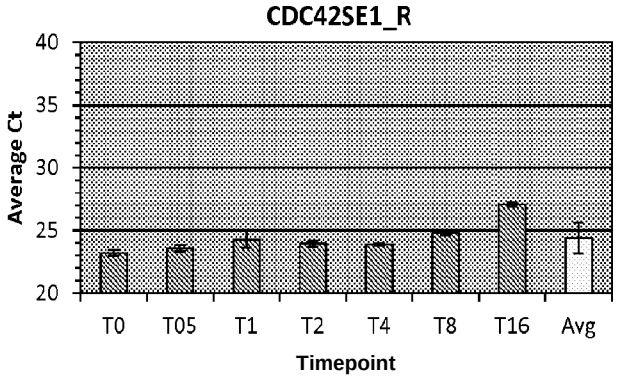
CDC42SE1_R
Average Ct
40
35
30
25
20
T0
T05
T1
T2
T4
T8
T16
Avg
Timepoint

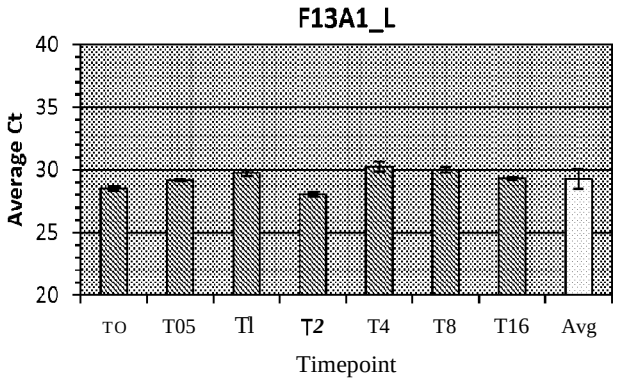
F13A1_L
Average Ct
40
35
30
25
20
TO
T05
Tl
T2
T4
T8
T16
Avg
Timepoint

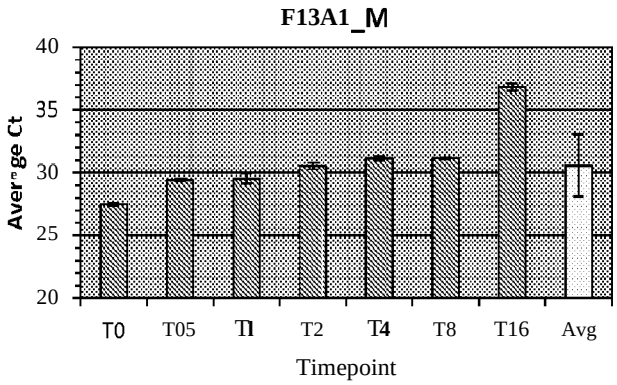
F13A1_M
Average Ct
40
35
30
25
20
T0
T05
Tl
T2
T4
T8
T16
Avg
Timepoint

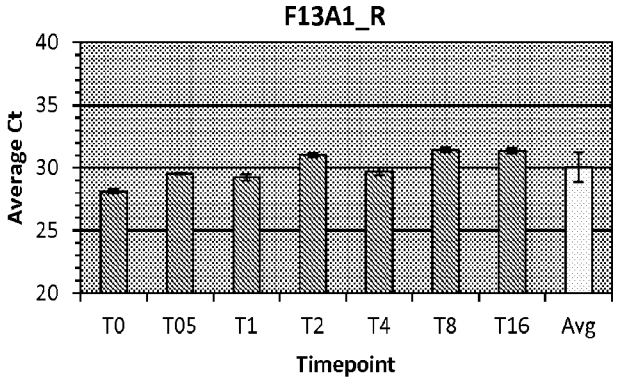
F13A1_R
Average Ct
40
35
30
25
20
T0
T05
T1
T2
T4
T8
T16
Avg
Timepoint

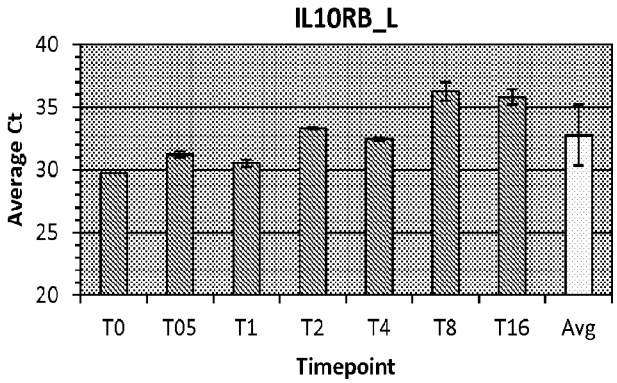
IL10RB_L
Average Ct
40
35
30
25
20
T0
T05
T1
T2
T4
T8
T16
Avg
Timepoint

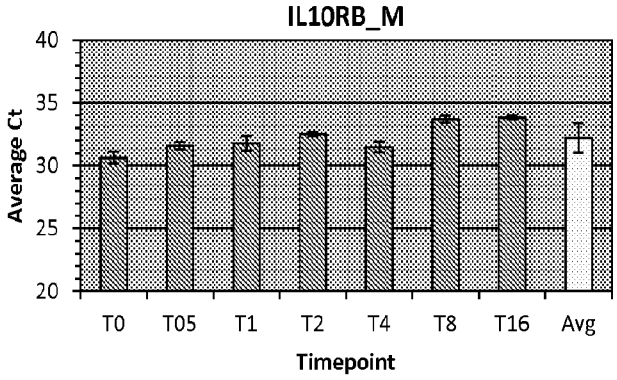
IL10RB_M
Average Ct
40
35
30
25
20
T0
T05
T1
T2
T4
T8
T16
Avg
Timepoint

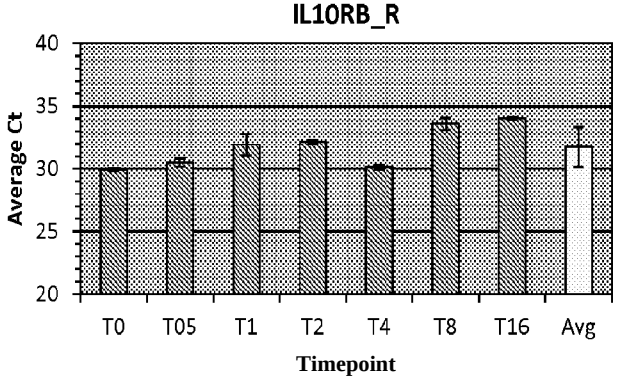
IL10RB_R
Average Ct
40
35
30
25
20
T0
T05
T1
T2
T4
T8
T16
Avg
Timepoint

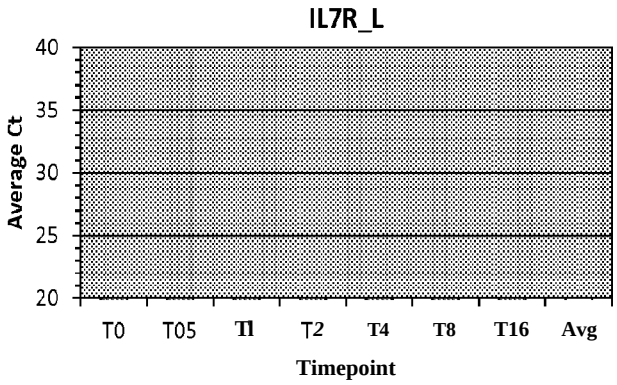
IL7R_L
Average Ct
40
35
30
25
20
T0
T05
T1
T2
T4
T8
T16
Avg
Timepoint

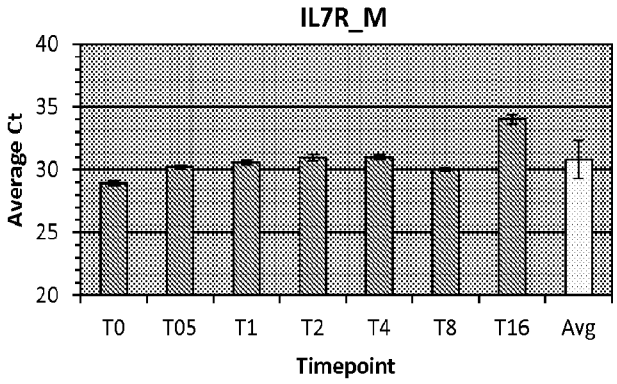
IL7R_M
Average Ct
40
35
30
25
20
T0
T05
T1
T2
T4
T8
T16
Avg
Timepoint

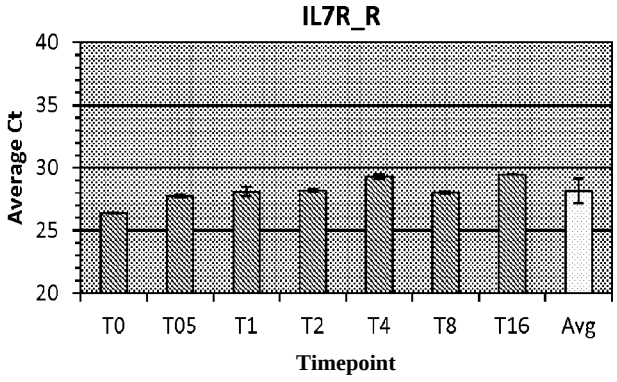
IL7R_R
Average Ct
40
35
30
25
20
T0
T05
T1
T2
T4
T8
T16
Avg
Timepoint

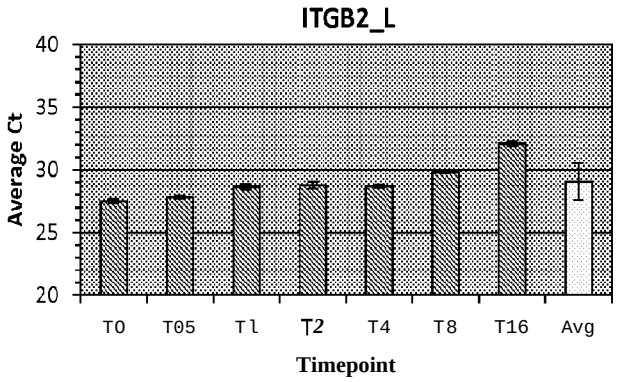
ITGB2_L
Average Ct
40
35
30
25
20
T0
T05
Tl
T2
T4
T8
T16
Avg
Timepoint

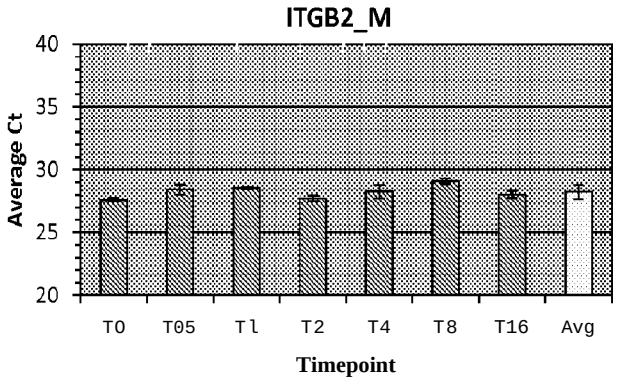
ITGB2_M
Average Ct
40
35
30
25
20
T0
T05
Tl
T2
T4
T8
T16
Avg
Timepoint

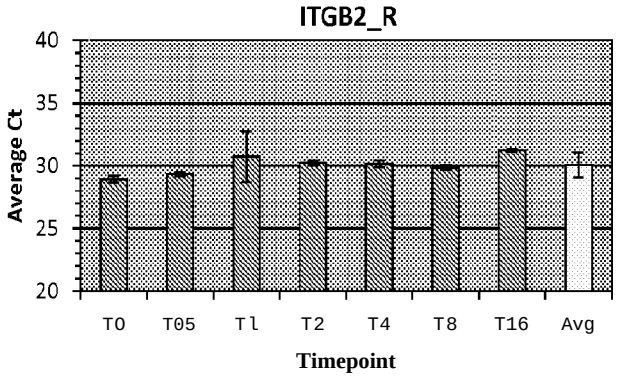
ITGB2_R
Average Ct
40
35
30
25
20
T0
T05
Tl
T2
T4
T8
T16
Avg
Timepoint

IVNS1ABPJ.

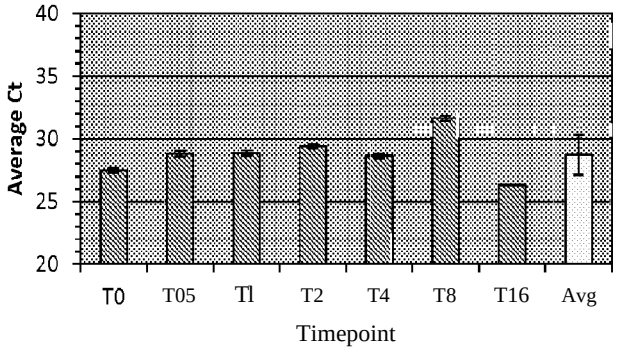
40
35
30
25
20
Average Ct
T0
T05
Tl
T2
T4
T8
T16
Avg
Timepoint

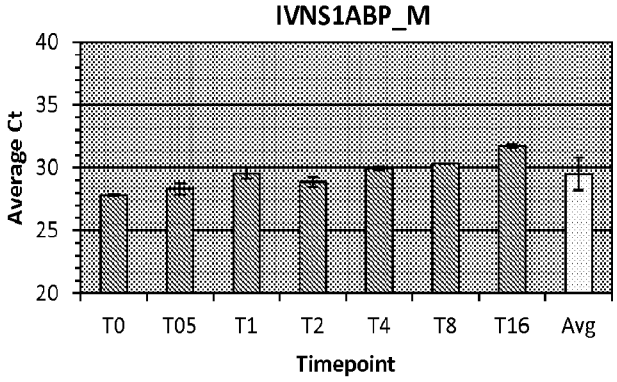
IVNS1ABP_M
40
35
30
25
20
Average Ct
T0
T05
T1
T2
T4
T8
T16
Avg
Timepoint

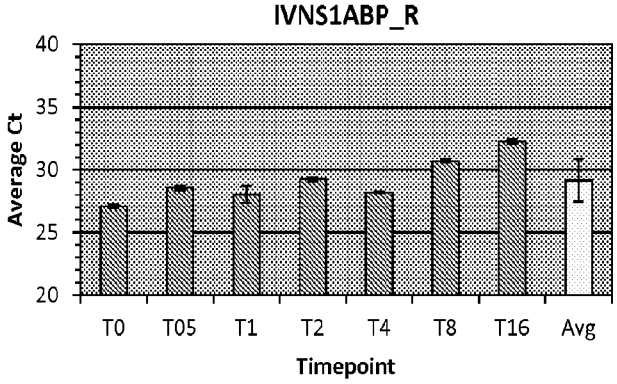
IVNS1ABP_R
40
35
30
25
20
Average Ct
T0
T05
T1
T2
T4
T8
T16
Avg
Timepoint

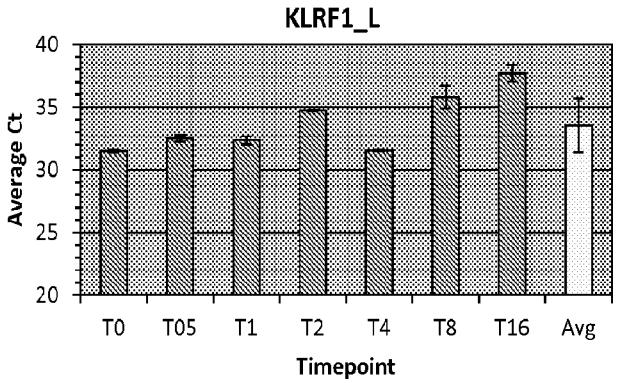
KLRF1_L
Average Ct
40
35
30
25
20
T0
T05
T1
T2
T4
T8
T16
Avg
Timepoint

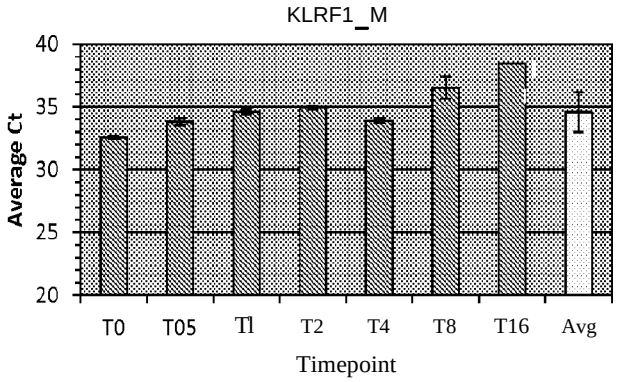
KLRF1_M
Average Ct
40
35
30
25
20
T0
T05
Tl
T2
T4
T8
T16
Avg
Timepoint

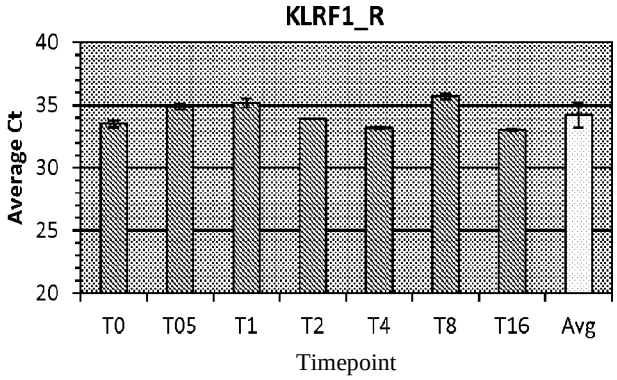
KLRF1_R
Average Ct
40
35
30
25
20
T0
T05
T1
T2
T4
T8
T16
Avg
Timepoint

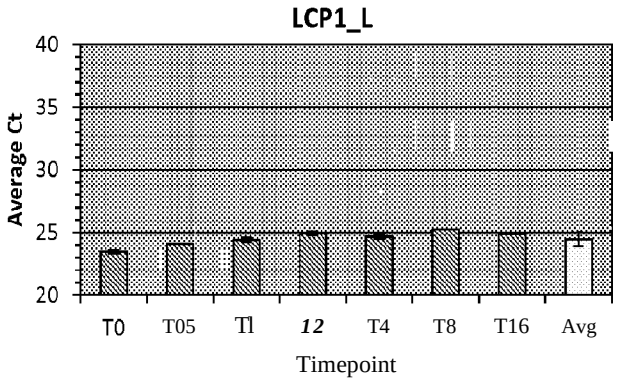
LCP1_L
Average Ct
40
35
30
25
20
T0
T05
Tl
12
T4
T8
T16
Avg
Timepoint

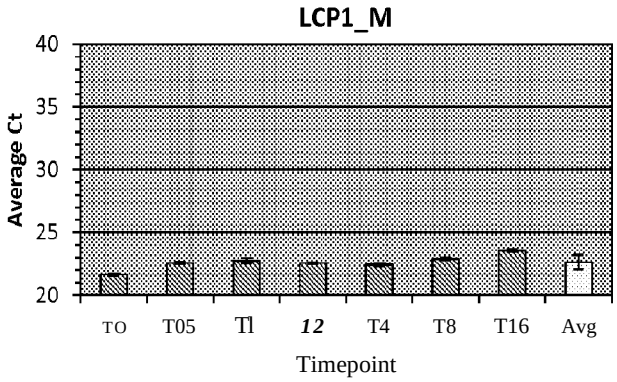
LCP1_M
Average Ct
40
35
30
25
20
TO
T05
Tl
12
T4
T8
T16
Avg
Timepoint

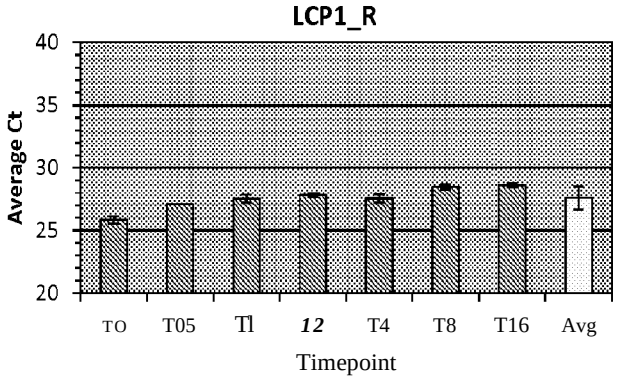
LCP1_R
Average Ct
40
35
30
25
20
TO
T05
Tl
12
T4
T8
T16
Avg
Timepoint

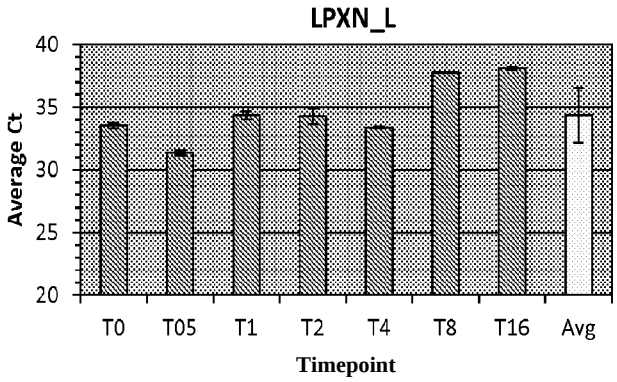
LPXN_L
Average Ct
40
35
30
25
20
T0
T05
T1
T2
T4
T8
T16
Avg
Timepoint

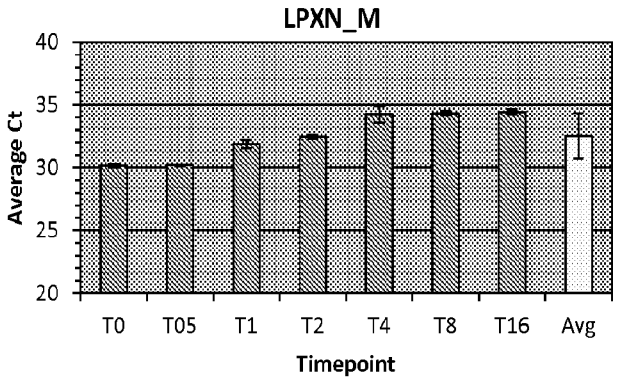
LPXN_M
Average Ct
40
35
30
25
20
T0
T05
T1
T2
T4
T8
T16
Avg
Timepoint

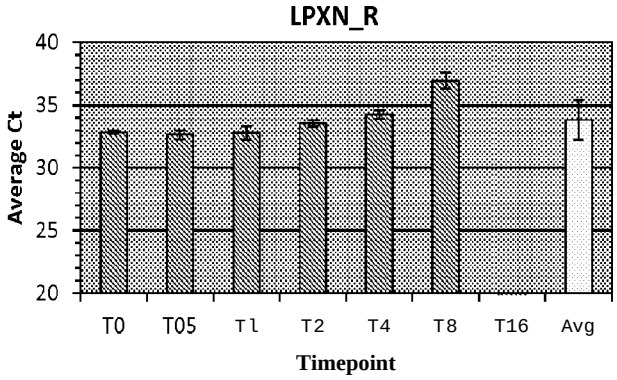
LPXN_R
Average Ct
40
35
30
25
20
T0
T05
Tl
T2
T4
T8
T16
Avg
Timepoint

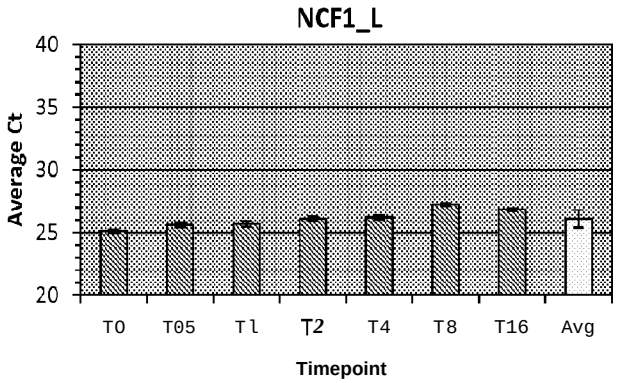
NCF1_L
Average Ct
40
35
30
25
20
T0
T05
T1
T2
T4
T8
T16
Avg
Timepoint

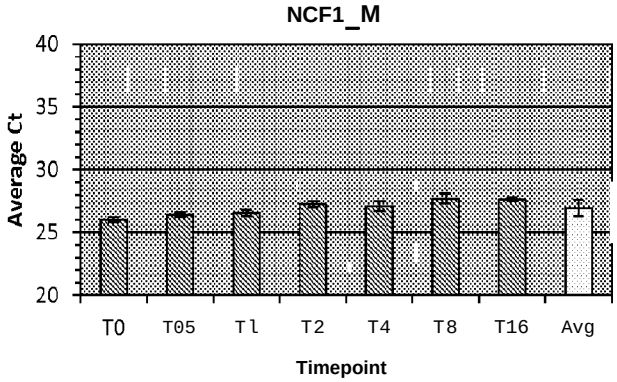
NCF1_M
Average Ct
40
35
30
25
20
T0
T05
T1
T2
T4
T8
T16
Avg
Timepoint

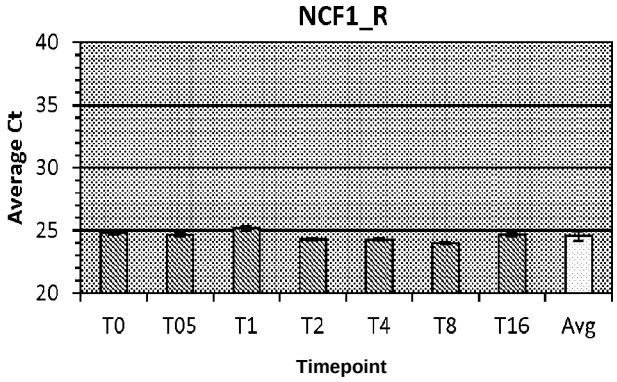
NCF1_R
Average Ct
40
35
30
25
20
T0
T05
T1
T2
T4
T8
T16
Avg
Timepoint

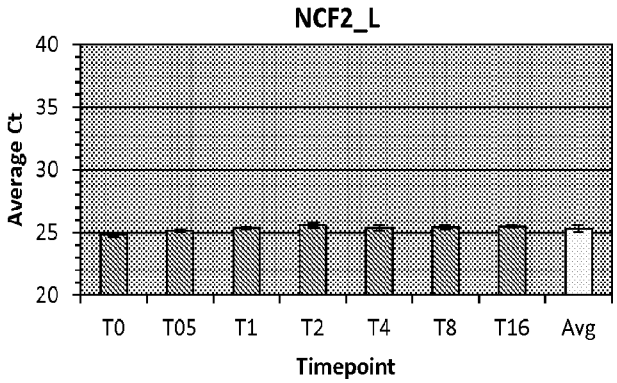
NCF2_L
Average Ct
40
35
30
25
20
T0
T05
T1
T2
T4
T8
T16
Avg
Timepoint

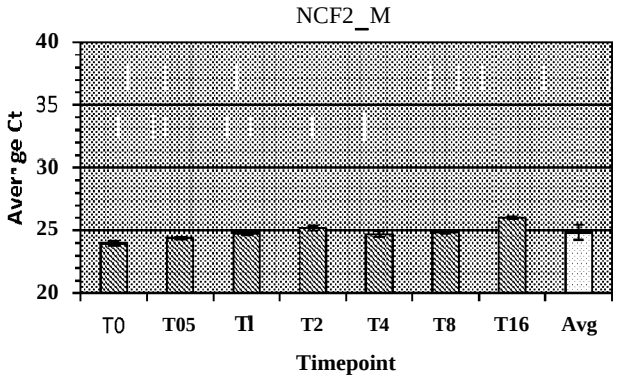
NCF2_M
Average Ct
40
35
30
25
20
T0
T05
T1
T2
T4
T8
T16
Avg
Timepoint

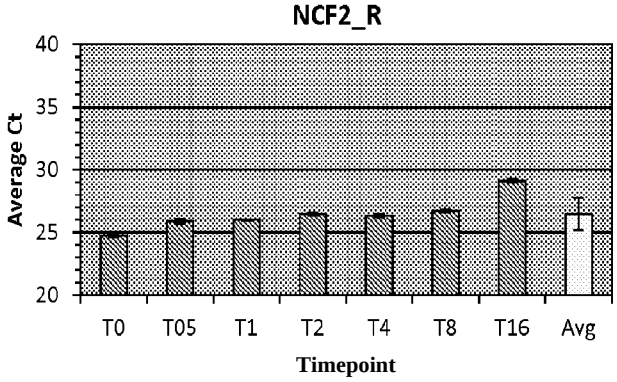
NCF2_R
Average Ct
40
35
30
25
20
T0
T05
T1
T2
T4
T8
T16
Avg
Timepoint

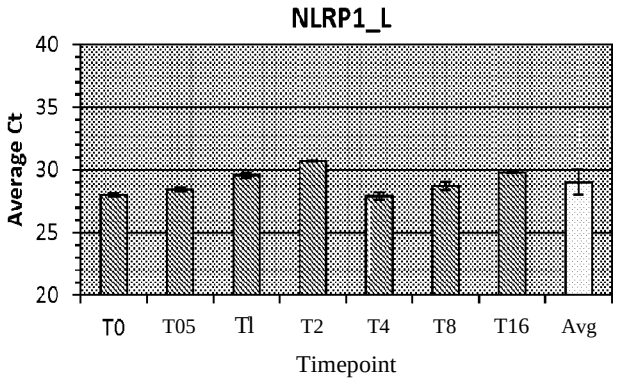
NLRP1_L
Average Ct
40
35
30
25
20
T0
T05
Tl
T2
T4
T8
T16
Avg
Timepoint

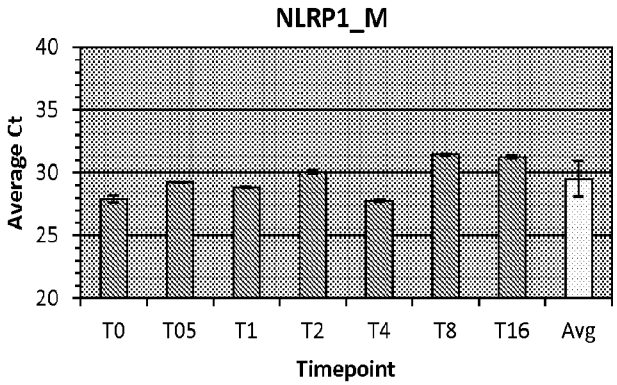
NLRP1_M
Average Ct
40
35
30
25
20
T0
T05
T1
T2
T4
T8
T16
Avg
Timepoint

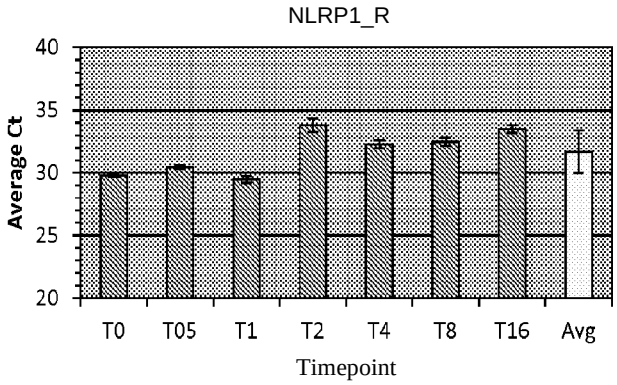
NLRP1_R
Average Ct
40
35
30
25
20
T0
T05
T1
T2
T4
T8
T16
Avg
Timepoint

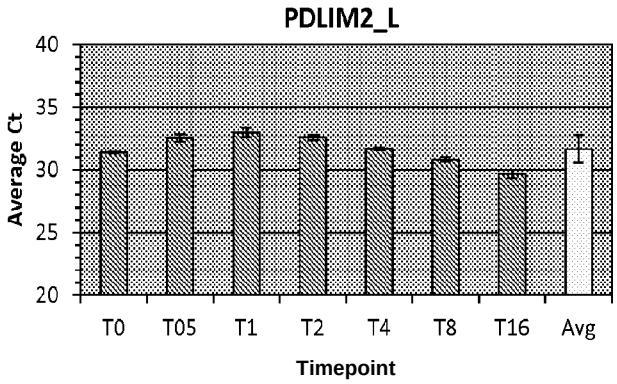
PDLIM2_L
Average Ct
40
35
30
25
20
T0
T05
T1
T2
T4
T8
T16
Avg
Timepoint

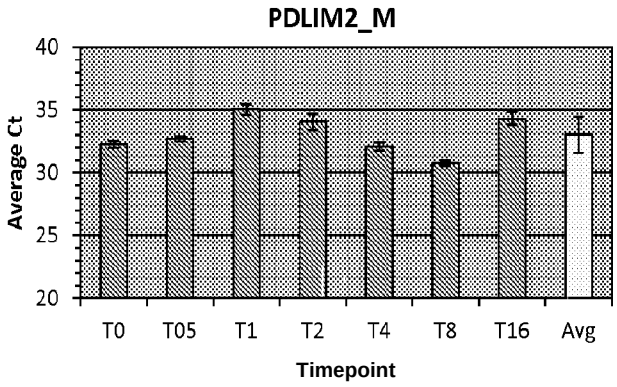
PDLIM2_M
Average Ct
40
35
30
25
20
T0
T05
T1
T2
T4
T8
T16
Avg
Timepoint

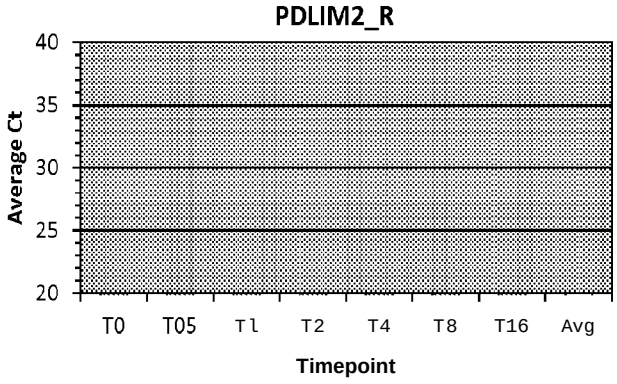
PDLIM2_R
Average Ct
40
35
30
25
20
T0
T05
Tl
T2
T4
T8
T16
Avg
Timepoint

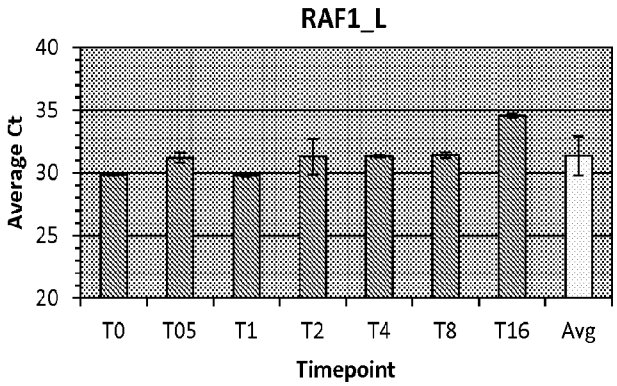
RAF1_L
Average Ct
40
35
30
25
20
T0
T05
T1
T2
T4
T8
T16
Avg
Timepoint

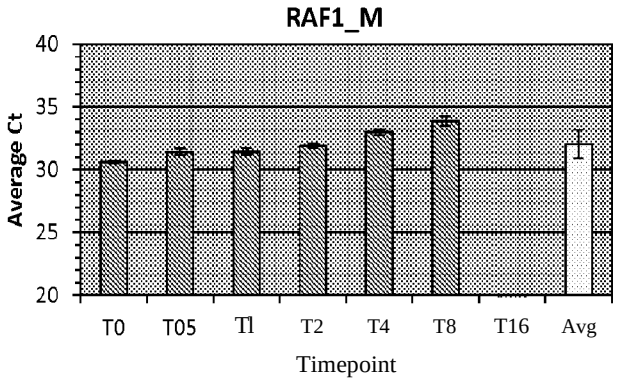
RAF1_M
Average Ct
40
35
30
25
20
T0
T05
Tl
T2
T4
T8
T16
Avg
Timepoint

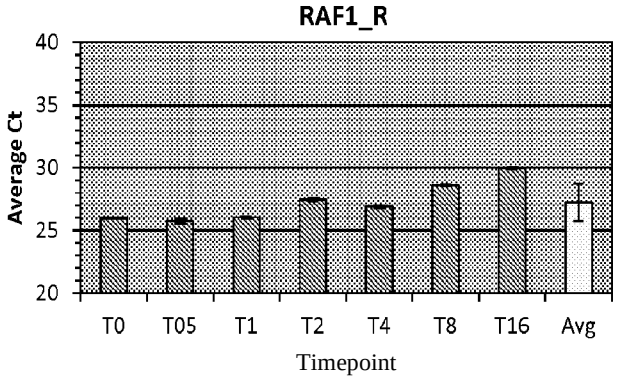
RAF1_R
Average Ct
40
35
30
25
20
T0
T05
T1
T2
T4
T8
T16
Avg
Timepoint

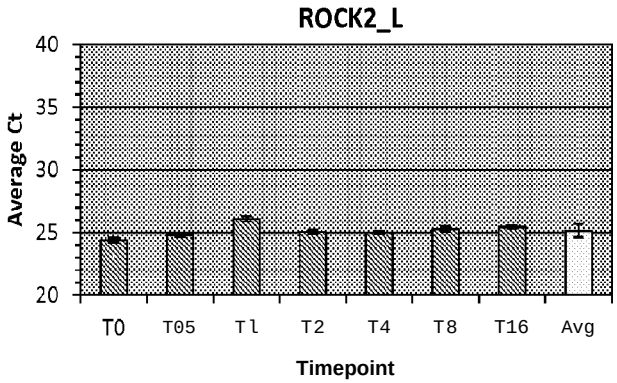
ROCK2_L
Average Ct
40
35
30
25
20
T0
T05
Tl
T2
T4
T8
T16
Avg
Timepoint

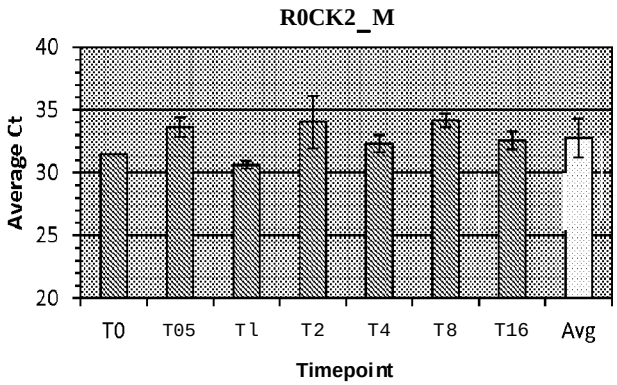
R0CK2_M
Average Ct
40
35
30
25
20
T0
T05
Tl
T2
T4
T8
T16
Avg
Timepoint

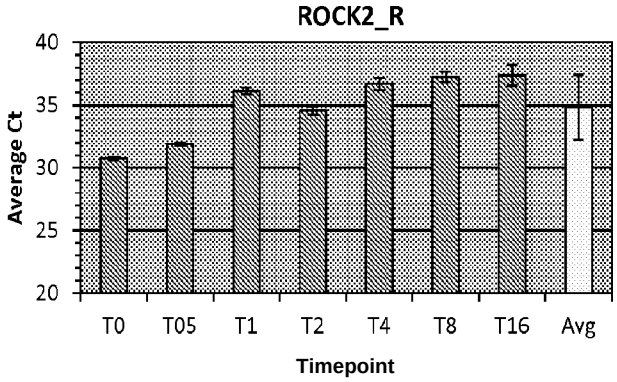
ROCK2_R
Average Ct
40
35
30
25
20
T0
T05
T1
T2
T4
T8
T16
Avg
Timepoint

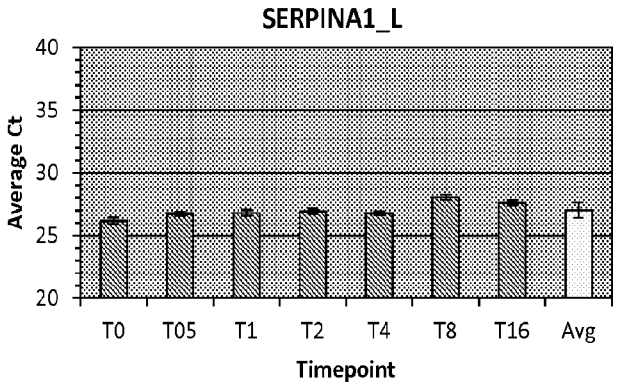
SERPINA1_L
Average Ct
40
35
30
25
20
T0
T05
T1
T2
T4
T8
T16
Avg
Timepoint

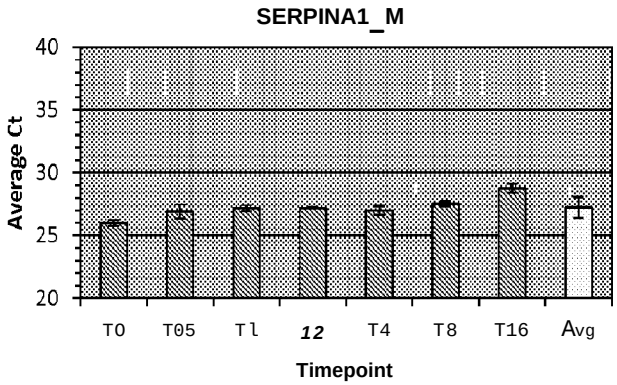
SERPINA1_M
Average Ct
40
35
30
25
20
T0
T05
Tl
12
T4
T8
T16
Avg
Timepoint

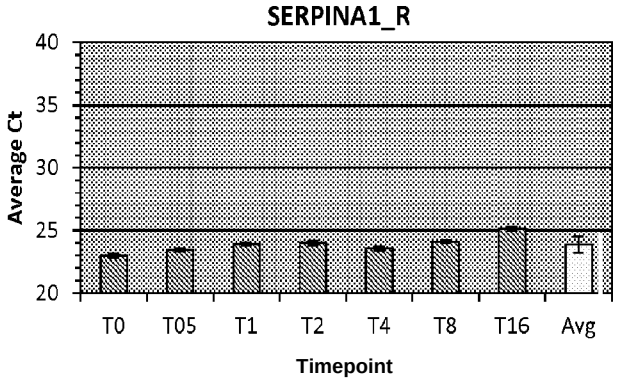
SERPINA1_R
Average Ct
40
35
30
25
20
T0
T05
T1
T2
T4
T8
T16
Avg
Timepoint

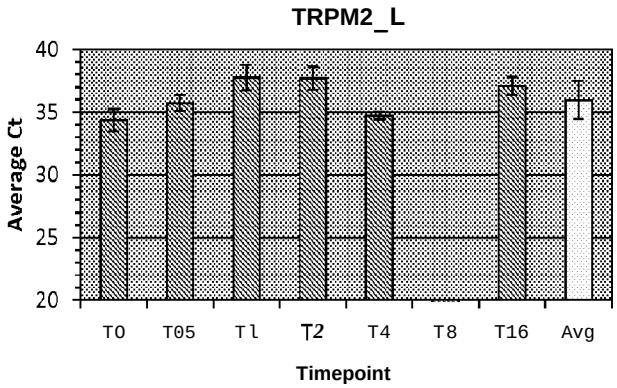
TRPM2_L
Average Ct
40
35
30
25
20
T0
T05
Tl
T2
T4
T8
T16
Avg
Timepoint

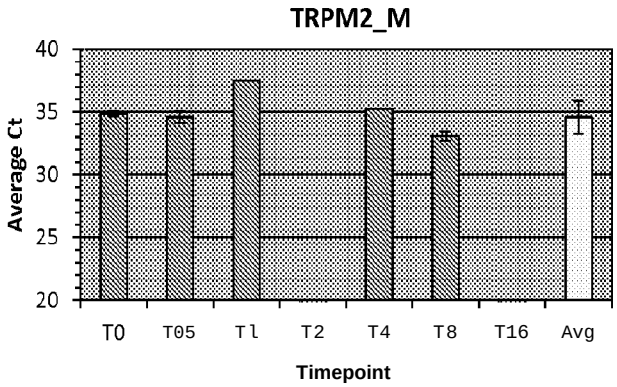
TRPM2_M
Average Ct
40
35
30
25
20
T0
T05
Tl
T2
T4
T8
T16
Avg
Timepoint

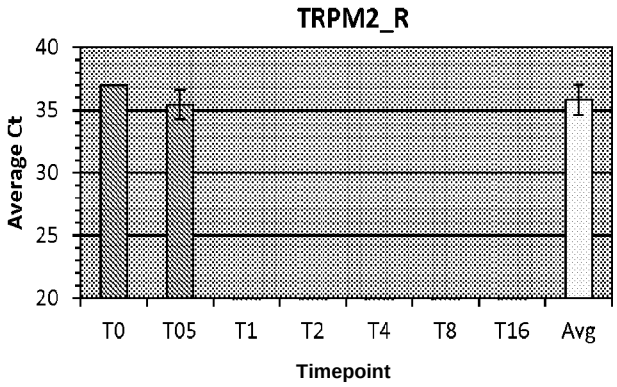
TRPM2_R
Average Ct
40
35
30
25
20
T0
T05
T1
T2
T4
T8
T16
Avg
Timepoint

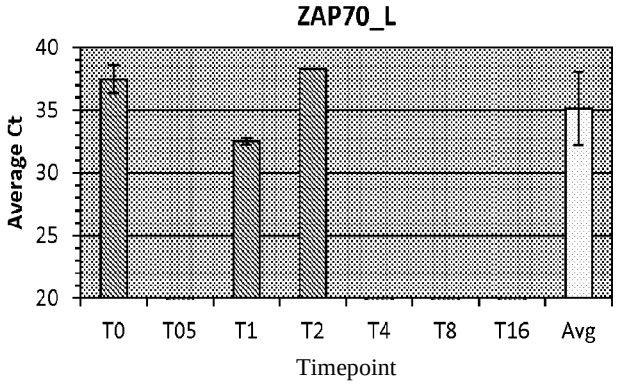
ZAP70_L
Average Ct
40
35
30
25
20
T0
T05
T1
T2
T4
T8
T16
Avg
Timepoint

0

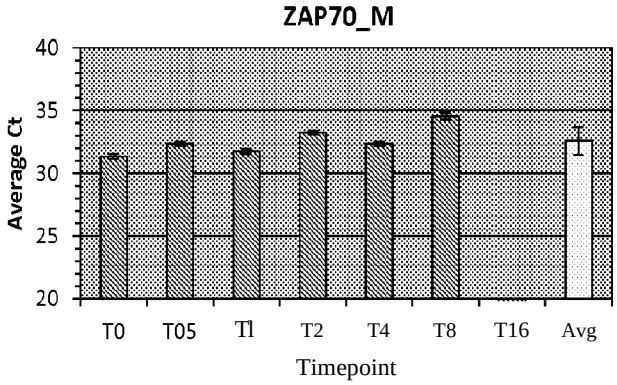
ZAP70_M
Average Ct
40
35
30
25
20
T0
T05
Tl
T2
T4
T8
T16
Avg
Timepoint

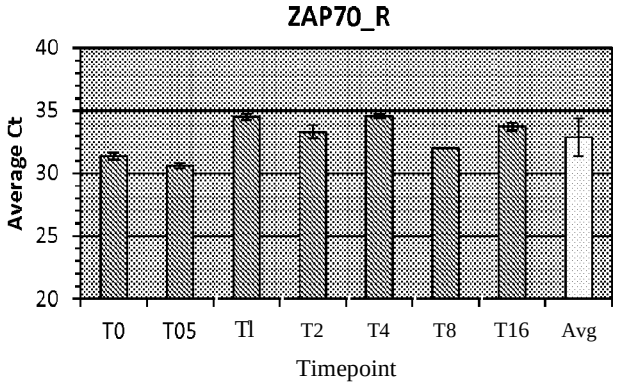
ZAP70_R
Average Ct
40
35
30
25
20
T0
T05
Tl
T2
T4
T8
T16
Avg
Timepoint

5

REFERENCES

1. Vermeulen, J., K. De Preter, S. Lefever, J. Nuytens, F. De Vloed, S. Derveaux, J. Hellemans, F. Speleman, and J. Vandesompele, *Measurable impact of RNA quality on gene expression results from quantitative PCR.* Nucleic Acids Res, 2011. **39**(9): p. e63.

2. Strand, C , J. Enell, I. Hedenfalk, and M. Ferno, *RNA quality in frozen breast cancer samples and the influence on gene expression analysis-a comparison of three evaluation methods using microcapillary electrophoresis traces.* BMC Mol Biol, 2007. **8**: p. 38.

3. Schroeder, A., O. Mueller, S. Stacker, R. Salowsky, M. Leiber, M. Gassmann, S. Lightfoot, W. Menzel, M. Granzow, and T. Ragg, *The RIN: an RNA integrity number for assigning integrity values to RNA measurements.* BMC Mol Biol, 2006. **7**: p. 3.

4. Houseley, J. and D. Tollervey, *The many pathways of RNA degradation.* Cell, 2009. **136**(**4**): p. 763-76.

5. Samuel, M.A., K. Whitby, B.C. Keller, A. Marri, W. Barchet, B.R. Williams, R.H. Silverman, M. Gale, Jr., and M.S. Diamond, *PKR and RNase L contribute to protection against lethal West Nile Virus infection by controlling early viral spread in the periphery and replication in neurons.* J Virol, 2006. **80**(14): p. 7009-19.

6. Li, X.L., J.A. Blackford, and B.A. Hassel, *RNase L mediates the antiviral effect of interferon through a selective reduction in viral RNA during encephalomyocarditis virus infection.* J Virol, 1998. **72**(4): p. 2752-9.

7. Beelman, C.A. and R. Parker, *Degradation of mRNA in eukaryotes.* Cell, 1995. **81**(2): p. 179-83.

8. Watson, J.D., *Molecular biology of the gene, 6th edition.* 2008, Cold Spring Harbor, N.Y.: Cold Spring Harbor Laboratory Press.

9. Newbury, S.F., O. Muhlemann, and G. Stoecklin, *Turnover in the Alps: an mRNA perspective. Workshops on mechanisms and regulation of mRNA turnover.* EMBO Rep, 2006. **7**(2): p. 143-8.

10. Takano, E.A., T. Mikeska, A. Dobrovic, **D.J.** Byrne, and S.B. Fox, *A multiplex endpoint RT-PCR assay for quality assessment of RNA extracted from formalin-fixed paraffin-embedded tissues.* BMC Biotechnol, 2010. **10:** p. 89.

11. Baechler, E.C., F.M. Batliwalla, G. Karypis, P.M. Gaffney, K. Moser, W.A. Ortmann, K.J. Espe, S. Balasubramanian, K.M. Hughes, J.P. Chan, A. Begovich, S.Y. Chang, P.K. Gregersen, and T.W. Behrens, *Expression levels for many genes in human*

peripheral blood cells are highly sensitive to ex vivo incubation. Genes Immun, 2004. **5**(5): p. 347-53.

12. Probst, J., S. Brechtel, B. Scheel, I. Hoerr, G. Jung, H.G. Rammensee, and S. Pascolo, *Characterization of the ribonuclease activity on the skin surface.* Genet Vaccines Ther, 2006. **4**: p. 4.

13. Thompson, K.L., P.S. Pine, B.A. Rosenzweig, Y. Turpaz, and J. Retief, *Characterization of the effect of sample quality on high density oligonucleotide microarray data using progressively degraded rat liver RNA.* BMC Biotechnol, 2007. **7**: p. 57.

14. Opitz, L., G. Salinas-Riester, M. Grade, K. Jung, P. Jo, G. Emons, B.M. Ghadimi, **T.** Beissbarth, and J. Gaedcke, *Impact of RNA degradation on gene expression profiling.* BMC Med Genomics, 2010. **3**: p. 36.

15. Gingrich, J., T. Rubio, and C. Karlak, *Effect of RNA Degradation on Data Quality in Quantitative PCR and Microarray Experiments.* Bio-Rad Bulletin #5452, 2006.

16. Quellhorst, G., Y. Han, and R. Blanchard, *Validating Microarray Data Using RT^2 Real-Time PCR.* SABiosciences, 2005.

17. Morey, J.S., J.C. Ryan, and F.M. Van Dolah, *Microarray validation: factors influencing correlation between oligonucleotide microarrays and real-time PCR.* Biol Proced Online, 2006. 8: p. 175-93.

18. Nolan, **T.,** R.E. Hands, and S.A. Bustin, *Quantification of mRNA using real-time RT-PCR.* Nat Protoc, 2006. **1**(3): p. 1559-82.

19. Biosystems, A., *Essentials of Real Time PCR.* 2006.

20. Bustin, S.A. and **T.** Nolan, *Pitfalls of quantitative real-time reverse-transcription polymerase chain reaction.* J Biomol Tech, 2004. **15**(3): p. 155-66.

21. Becker, C , A. Hammerle-Fickinger, I. Riedmaier, and M.W. Pfaffl, *mRNA and microRNA quality control for RT-qPCR analysis.* Methods, 2010. **50**(4): p. 237-43.

22. Fleige, S. and M.W. Pfaffl, *RNA integrity and the effect on the real-time qRT-PCR performance.* Mol Aspects Med, 2006. **27**(2-3): p. 126-39.

23. Schoor, O., **T.** Weinschenk, J. Hennenlotter, S. Corvin, A. Stenzl, H.G. Rammensee, and S. Stevanovic, *Moderate degradation does not preclude microarray analysis of small amounts of RNA.* Biotechniques, 2003. **35**(6): p. 1192-6, 1198-201.

24. Mueller, O., K. Hahnenberger, M. Dittmann, H. Yee, R. Dubrow, R. Nagle, and D. llsley, *A microfluidic system for high-speed reproducible DNA sizing and quantitation.* Electrophoresis, 2000. **21**(1): p. 128-34.

25. Kuschel, M. and W. Ausserer, *Characterization of RNA quality using the Agilent 2100 Bioanalyzer.* Agilent Application Note, 2000.

26. Palmer, M. and E. Prediger, *Assessing RNA Quality.* Ambion TechNotes, 2004. **11**(1).

27. Auer, H., S. Lyianarachchi, D. Newsom, M.I. Klisovic, G. Marcucci, and K. Kornacker, *Chipping away at the chip bias: RNA degradation in microarray analysis.* Nat Genet, 2003. **35**(4): p. 292-3.

28. Mueller, 0., S. Lightfoot, and A. Schroeder, *RNA Integrity Number (RIN) - Standardization of RNA Quality Control.* Agilent Technologies Application Note, 2004.

29. Pfaffl, M.W., S. Fleige, and I. Riedmaier, *Validation of lab-on-chip capillary electrophoresis systems for total RNA quality and quantity control.* Biotechnology & Biotechnological Equipment, 2008. **22**(3): p. 829-834.

30. Riedmaier, L, M. Bergmaier, and M.W. Pfaffl, *Comparison of two available platforms for determination of RNA quality.* Biotechnology & Biotechnological Equipment, 2010. **24**(4): p. 2154-2159.

31. Port, M., H.U. Schmelz, T. Stassen, K. Mueller, M. Stockinger, R. Obermair, and M. Abend, *Correcting false gene expression measurements from degraded RNA using RTQ-PCR.* DiagnMol Pathol, 2007. **16**(1): p. 38-49.

32. Copois, V., F. Bibeau, C. Bascoul-Mollevi, N. Salvetat, P. Chalbos, C. Bareil, L. Candeil, C. Fraslon, E. Conseiller, V. Granci, P. Maziere, A. Kramar, M. Ychou, B. Pau, P. Martineau, F. Molina, and M. Del Rio, *Impact of RNA degradation on gene expression profiles: assessment of different methods to reliably determine RNA quality.* J Biotechnol, 2007. **127**(**4**): p. 549-59.

33. Su, A.I., T. Wiltshire, S. Batalov, H. Lapp, K.A. Ching, D. Block, J. Zhang, R. Soden, M. Hayakawa, G. Kreiman, M.P. Cooke, J.R. Walker, and J.B. Hogenesch, *A gene atlas of the mouse and human protein-encoding transcriptomes.* Proc Natl Acad Sci U S A, 2004. **101**(16): p. 6062-7.

34. Pant, P.V., H. Tao, E.J. Beilharz, D.G. Ballinger, D.R. Cox, and K.A. Frazer, *Analysis of allelic differential expression in human white blood cells.* Genome Res, 2006. **16**(3): p. 33 1-9.

35. Safran, M., V. Chalifa-Caspi, O. Shmueli, T. Olender, M. Lapidot, N. Rosen, M. Shmoish, Y. Peter, G. Glusman, E. Feldmesser, A. Adato, I. Peter, M. Khen, T. Atarot, Y. Groner, and D. Lancet, *Human Gene-Centric Databases at the Weizmann Institute of Science: GeneCards, UDB, CroW 21 and HORDE.* Nucleic Acids Res, 2003. **31**(1): p. 142-6.

36. Min, J.L., A. Barrett, T. Watts, F.H. Pettersson, H.E. Lockstone, CM. Lindgren, J.M. Taylor, M. Allen, K.T. Zondervan, and M.I. McCarthy, *Variability of gene expression*

profiles in human blood and lymphoblastoid cell lines. BMC Genomics, 2010. **11:** p. 96.

37. Yanai, I., H. Benjamin, M. Shmoish, V. Chalifa-Caspi, M. Shklar, R. Ophir, A. Bar-Even, S. Horn-Saban, M. Safran, E. Domany, D. Lancet, and O. Shmueli, *Genome-wide midrange transcription profiles reveal expression level relationships in human tissue specification.* Bioinformatics, 2005. **21**(5): p. 650-9.

38. Shmueli, O., S. Horn-Saban, V. Chalifa-Caspi, M. Shmoish, R. Ophir, H. Benjamin-Rodrig, M. Safran, E. Domany, and D. Lancet, *GeneNote: whole genome expression profiles in normal human tissues.* C R Biol, 2003. **326**(10-11): p. 1067-72.

39. Wu, C., C. Orozco, J. Boyer, M. Leglise, J. Goodale, S. Batalov, C.L. Hodge, J. Haase, J. Janes, J.W. Huss, 3rd, and A.I. Su, *BioGPS: an extensible and customizable portal for querying and organizing gene annotation resources.* Genome Biol, 2009. **10**(11): p. R130.

40. Bijlani, R., Y. Cheng, D.A. Pearce, A.I. Brooks, and M. Ogihara, *Prediction of biologically significant components from microarray data: Independently Consistent Expression Discriminator (ICED).* Bioinformatics, 2003. **19**(1): p. 62-70.

41. Troyanskaya, O.G., M.E. Garber, P.O. Brown, D. Botstein, and R.B. Altman, *Nonparametric methods for identifying differentially expressed genes in microarray data.* Bioinformatics, 2002. **18**(11): p. 1454-61.

42. Roche, *RealTime Ready Universal ProbeLibrary: Redefining and revolutionizing real-time qPCR assays.* 2009.

43. Qiagen/PreAnalytiX, *PAXgene Blood RNA Kit Handbook.* 2009.

44. Wilkes, T.M., A.S. Devonshire, S.L. Ellison, and C.A. Foy, *Evaluation of a novel approach for the measurement of RNA quality.* BMC Res Notes, 2010. **3:** p. 89.

45. Ibberson, D., V. Benes, M.U. Muckenthaler, and M. Castoldi, *RNA degradation compromises the reliability of microRNA expression profiling.* BMC Biotechnol, 2009. **9:** p. 102.

46. Breaker, R.R., G.M. Emilsson, D. Lazarev, S. Nakamura, I.J. Puskarz, A. Roth, and N. Sudarsan, *A common speed limit for RNA-cleaving ribozymes and deoxyribozymes.* RNA, 2003. **9**(8): p. 949-57.

47. Emilsson, G.M., S. Nakamura, A. Roth, and R.R. Breaker, *Ribozyme speed limits.* RNA, 2003. **9**(8): p. 907-18.

48. Ambion, *TRIzol® Reagent Manual.* 2010.

49. Qiagen, *RNeasy Mini Kit Handbook.* 2010.

50. Raines, R.T., *Ribonuclease A.* Chem Rev, 1998. **98**(3): p. 1045-1066.

While certain of the preferred embodiments of the present invention have been described and specifically exemplified above, it is not intended that the invention be limited to such embodiments. Various modifications may be made thereto without departing from the scope and spirit of the present invention, as set forth in the following claims.

What is claimed is:

1. A method for quantitatively evaluating the extent of RNA degradation in a sample, comprising;

a) identifying a candidate gene set and determining an arbitrary expression score for each gene present in said set, said gene set being specifically expressed in said tissue or said blood specimen and sorting said genes into at least two tiers based on said expression score;

b) generating a plurality of amplification plots and CT profiles from a set of candidate genes encoding RNAs exposed to differential degradation conditions thereby providing a series of differentially weighted CT profiles correlating to the degradation state of said RNA, said scores corresponding to intact and incrementally degraded RNAs; and

c) subjecting RNA in said sample to quantitative amplification, thereby generating an amplification plot and a CT score; said Cx score being correlated with those determined in step b) said score providing the degree of degradation of said sample.

2. The method of claim 1, wherein said sample is an environmental sample.

3. The method of claim 1, wherein said sample is obtained from a human.

4. The method of claim 1, wherein said sample is a tissue sample.

5. The method of claim 1, wherein said sample is a fluid.

6. The method of claim 1, wherein said sample comprises whole blood.

7. The method of claim 6, further comprising the step of d) analyzing a gene expression profile employing said sample.

8. The method of claim 7, further comprising the step of e) assessing disease status or progression using said gene expression profile.

9. The method of claim 1, further comprising the step of d) discarding said sample without conducting a gene expression profile analysis if said degree of degradation is unsuitable.

10. The method of claim 1, wherein said RNA is converted to cDNA during or prior to quantitative amplification.

11. The method of claim 1, wherein said quantitative amplification comprises PCR.

12. A system configured to carry out the method of any of claims 1-11.

13. The system of claim 12, comprising a computer processor that generates said plurality of amplification plots and Cx profiles.

14. The system of claim 11, comprising a thermocycler.

15. The system of claim 11, comprising a sample processing component.

16. The system of claim 15, wherein said sample processing components purifies or isolates RNA from cells or tissue.

17. The system of claim 11, comprising a detection component.

18. The system of claim 17, wherein said detection component detects mass, optical signals, heat, pH changes, or radioactivity.

Figure 1

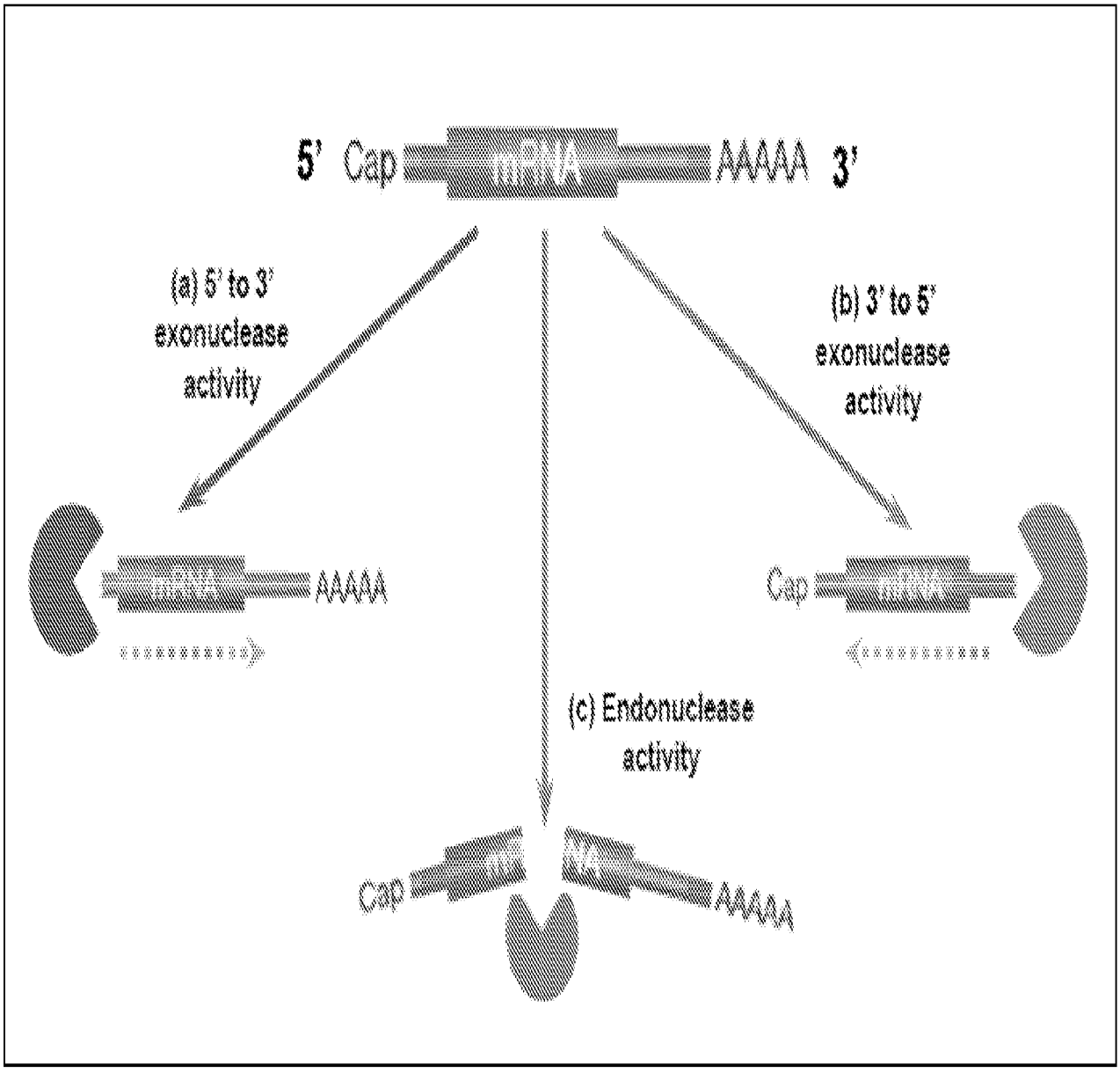
5' Cap mRNA AAAAA 3'
(a) 5' to 3' exonuclease activity
(b) 3' to 5' exonuclease activity
(c) Endonuclease activity
AAAAA
Cap
Cap
AAAAA

Figure 2

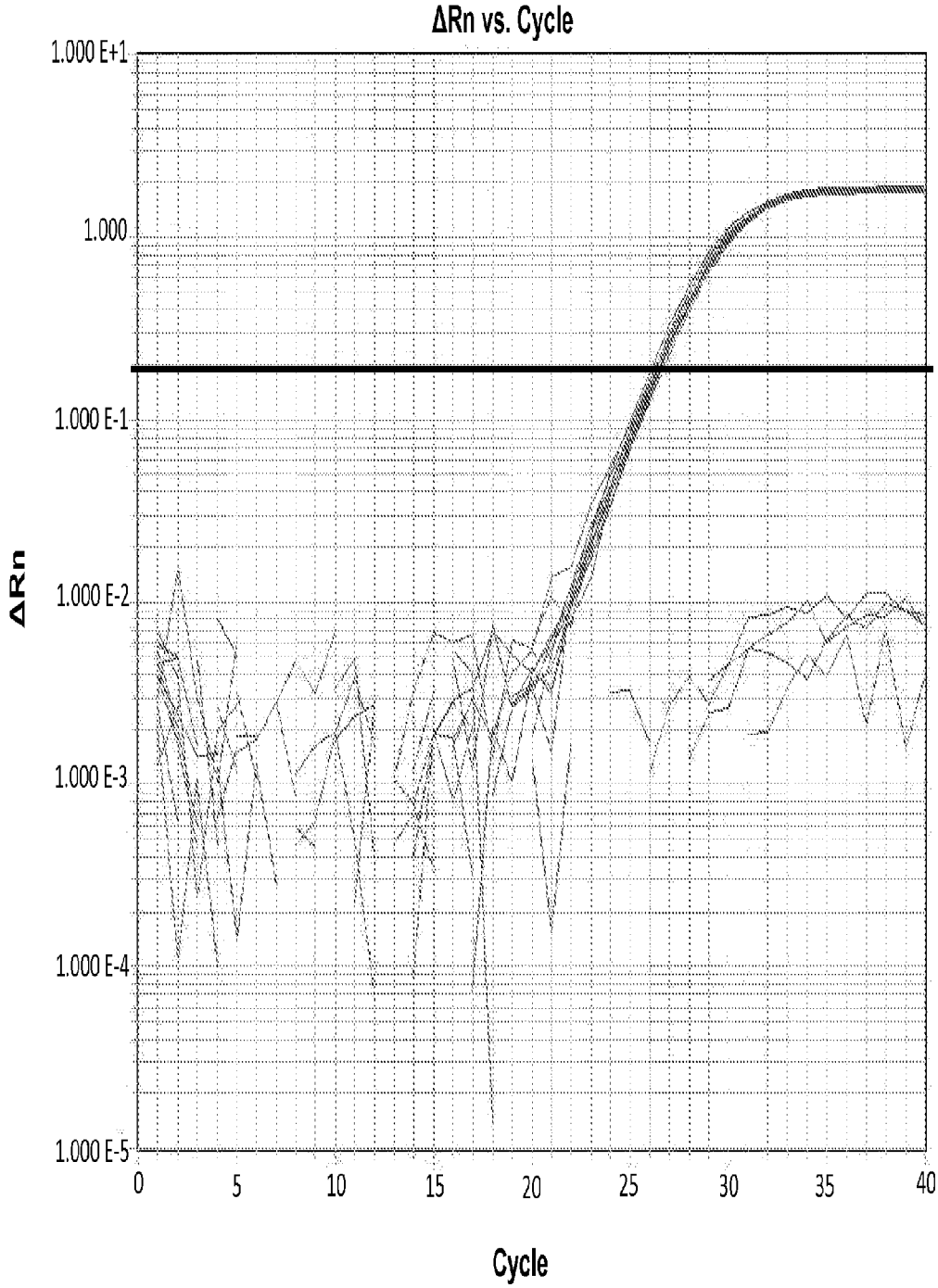
ΔRn vs. Cycle
1.000 E+1
1.000
1.000 E-1
1.000 E-2
1.000 E-3
1.000 E-4
1.000 E-5
ΔRn
0
5
10
15
20
25
30
35
40
Cycle

Figure 3

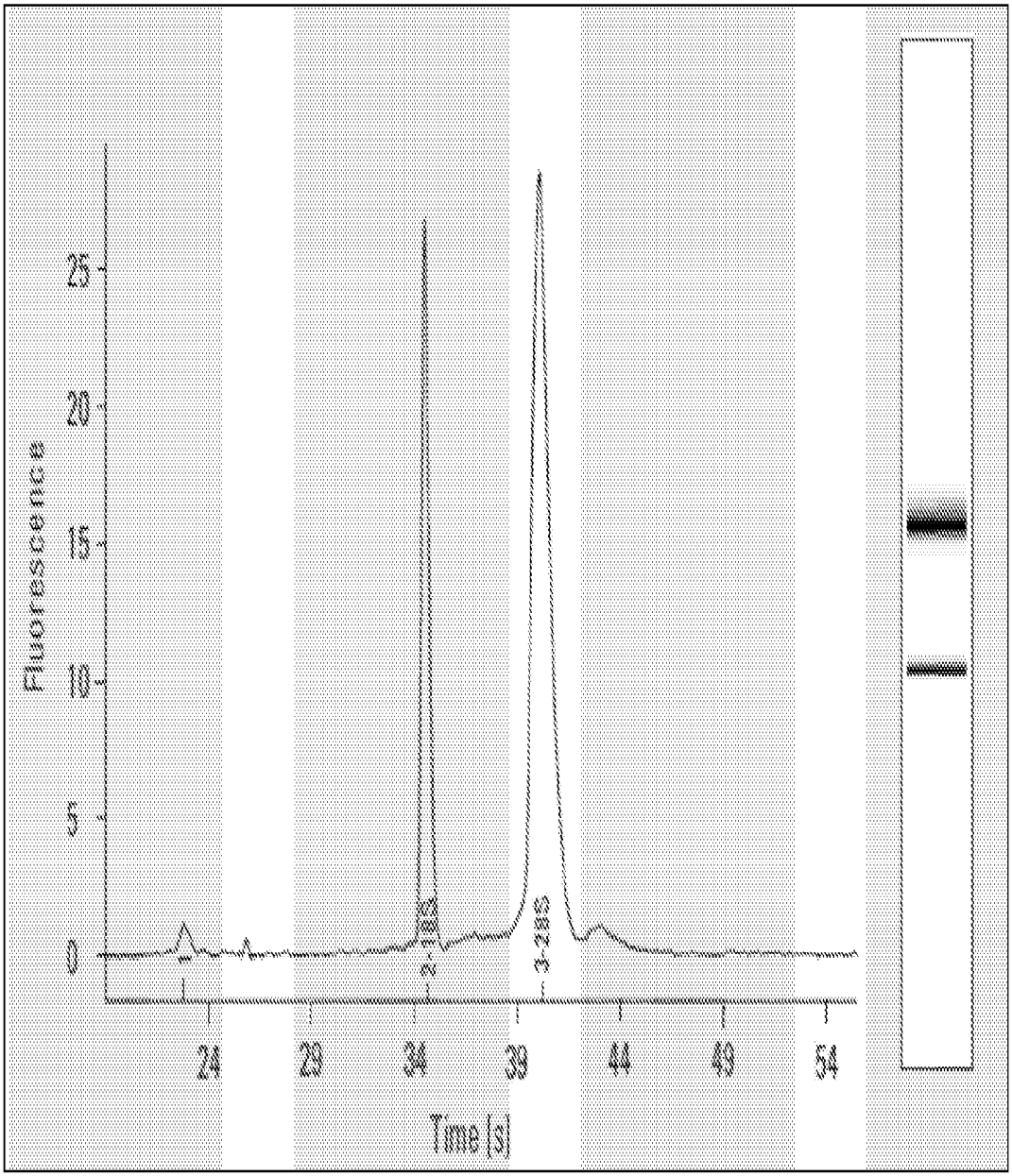

Figure 4

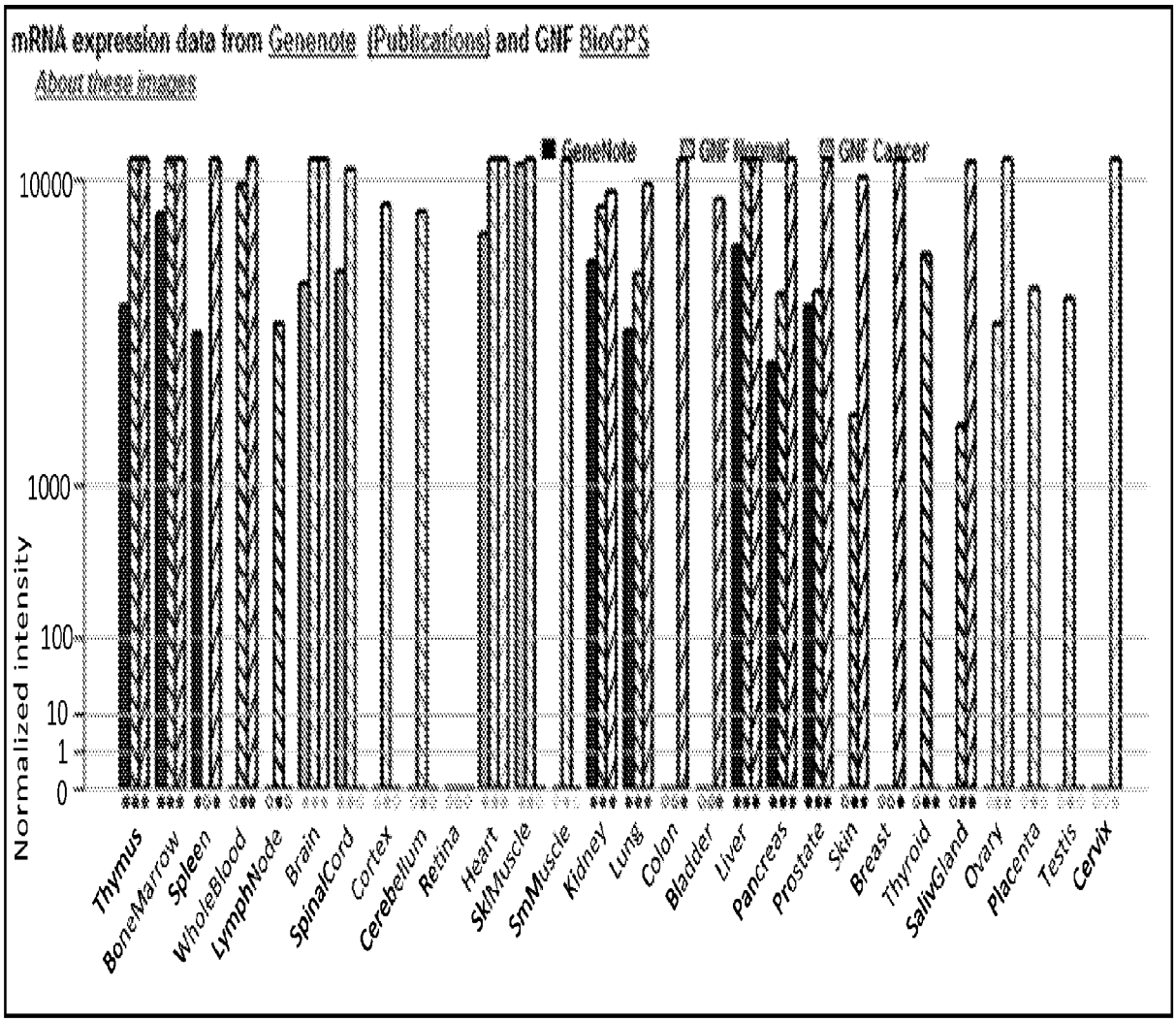
mRNA expression data from Genenote (Publications) and GNF BioGPS
About these images
Genenote
GNF Normal
GNF Cancer
10000
1000
100
10
1
0
Normalized intensity
Thymus
BoneMarrow
Spleen
WholeBlood
LymphNode
Brain
SpinalCord
Cortex
Cerebellum
Retina
Heart
SkinMuscle
SmMuscle
Kidney
Lung
Colon
Bladder
Liver
Pancreas
Prostate
Skin
Breast
Thyroid
SalivGland
Ovary
Placenta
Testis
Cervix

Figure 5

Assay details:

Use Universal ProbeLibrary probe: #72, cat.no. 04688953001

Primer	Length	Position	Tm	ASC	Sequence
Left Primer	20	302-321	60	55	cactactgggctcagggaaa
Right Primer	20	353-372	59	50	tcacagtccttcacgaggaa

Amplicon (71 nt)

cactactgggctcagggaaagctgtgctgccagatgtgtgagccaggaacattcctcgtg
aaggactgtga

Download pack insert | PDF report | Text report | Order probes or set

Transcript overview:

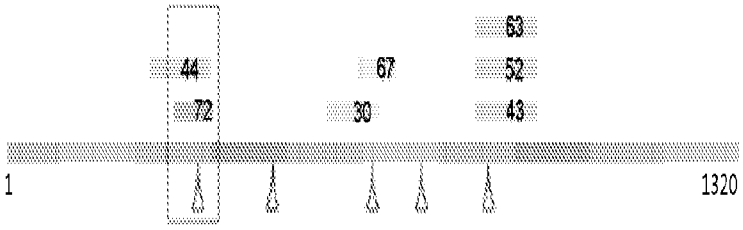

Detailed view:

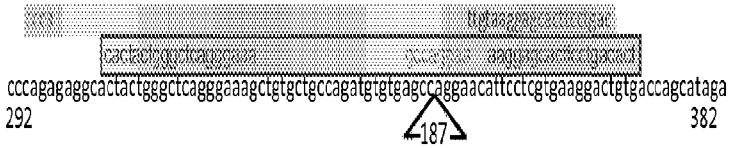

Figure 6

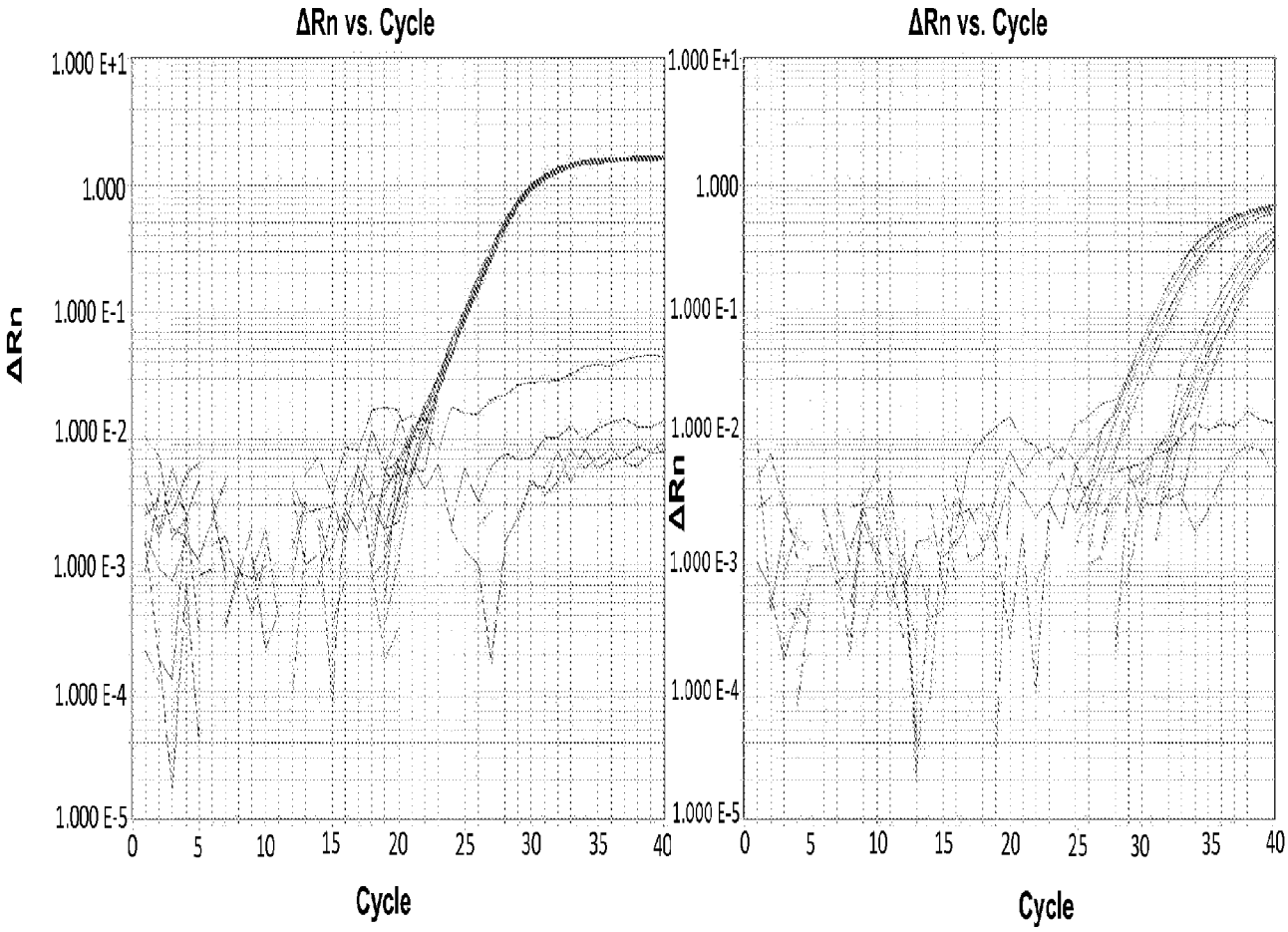
ΔRn vs. Cycle
ΔRn
1.000 E+1
1.000
1.000 E-1
1.000 E-2
1.000 E-3
1.000 E-4
1.000 E-5
0
5
10
15
20
25
30
35
40
Cycle
ΔRn vs. Cycle
ΔRn
1.000 E+1
1.000
1.000 E-1
1.000 E-2
1.000 E-3
1.000 E-4
1.000 E-5
0
5
10
15
20
25
30
35
40
Cycle

INTERNATIONAL SEARCH REPORT

International application No.
PCT/US 12/69561

A. CLASSIFICATION OF SUBJECT MATTER
IPC(8) - C12Q 1/68, G06F 19/24 (2013.01)
USPC - 435/6.12, 702/19
According to International Patent Classification (IPC) or to both national classification and IPC

B. FIELDS SEARCHED

Minimum documentation searched (classification system followed by classification symbols)
IPC(8): C12Q 1/68, G06F 19/24 (2013.01)
USPC: 435/6.12, 702/19

Documentation searched other than minimum documentation to the extent that such documents are included in the fields searched
USPC: 435/6.11, 6.1 (text search)

Electronic data base consulted during the international search (name of data base and, where practicable, search terms used)
Electronic data bases: Google Scholar; PatBase
Search terms: RNA or ribonucleic acid; RNA integrity, degrad*, qPCR or amplir; Ctau or Ct or threshold cycle, expression profiling; system for RNA isolation or extraction or purification, thermocycler. RIN (RNA integrity number); RQI (RNA Quality Indicator)

C. DOCUMENTS CONSIDERED TO BE RELEVANT

Category*	Citation of document, with indication, where appropriate, of the relevant passages	Relevant to claim No.
Y	US 2010/0057371 A1 (DENISOV et al.) 4 March 2010 (04.03.2010). Especially para [0024], [0112], [0118], [0119], [0121], sheet 9 fig 9A, 9C.	1-11. (12-1β)/(1-11)
Y	OPITZ et al.. Impact of RNA degradation on gene expression profiling. BMC Med Genomics, 9 August 2010, Vol 3, No 36, Pages 1-14. Especially pg 3 col 1 para 2, pg 3 table 2, pg 9 fig 4.	1-11, (12-18)/(1-11)
Y	US 2011/0027862 A1 (BATES et al.) 3 February 2011 (03.02.2011). Especially para [0059].	2, (12-18)/2
Y	US 2006/0204989 A1 (KOPRESKI) 14 September 2006 (14.09.2006). Especially para [0011], [0012], [0021].	5-8, (12-18)/(5-8)
Y	US 2005/0095634 A1 (BAKER et al.) 5 May 2005 (05.05.2005). Especially para [0053], [0054], [0073], [0074].	(12-18)/(1-11)
A	US 2006/0063170 A1 (ERLANDER et al.) 23 March 2006 (23.03.2006). Especially [0009-0030].	1-11
A	US 2006/0246577 A1 (SCHROEDER et al.) 2 November 2006 (02.11.2006). Especially [0007-0073]	1-11
A	FLEIGE et al., Comparison of relative mRNA quantification models and the impact of RNA integrity in quantitative real-time RT-PCR. Biotechnol Lett, October 2006 (published online 10 August 2006), Vol 28, No 19, Pages 1601-1613. Especially abstract, pg 1607 fig 1.	1-11

☐ Further documents are listed in the continuation of Box C.

* Special categories of cited documents:
"A" document defining the general state of the art which is not considered to be of particular relevance
"E" earlier application or patent but published on or after the international filing date
"L" document which may throw doubts on priority claim(s) or which is cited to establish the publication date of another citation or other special reason (as specified)
"O" document referring to an oral disclosure, use, exhibition or other means
"P" document published prior to the international filing date but later than the priority date claimed
"T" later document published after the international filing date or priority date and not in conflict with the application but cited to understand the principle or theory underlying the invention
"X" document of particular relevance; the claimed invention cannot be considered novel or cannot be considered to involve an inventive step when the document is taken alone
"Y" document of particular relevance; the claimed invention cannot be considered to involve an inventive step when the document is combined with one or more other such documents, such combination being obvious to a person skilled in the art
"&" document member of the same patent family

Date of the actual completion of the international search	Date of mailing of the international search report
4 March 2013 (04.03.2013)	05 APR 2013

Name and mailing address of the ISA/US	Authorized officer:
Mail Stop PCT, Attn: ISA/US, Commissioner for Patents P.O. Box 1450, Alexandria, Virginia 22313-1450 Facsimile No. 571-273-3201	Lee W. Young PCT Helpdesk: 571-272-4300 PCT OSP: 571-272-7774

Form PCT/ISA/210 (second sheet) (July 2009)